

The Value Chain of Sustainable Dual Carbon Sodium Ion Capacitors

Roman Mysyk,^[a] Daniel Carriazo,^[a, p] Damien Saurel,^[a] Maria Arnaiz,^[a] Olivier Crosnier,^[b, c] Thierry Brousse,^[b, c] Kangkang Ge,^[c, d] Pierre-Louis Taberna,^[c, d] Patrice Simon,^[c, d] Sander Ratso,^[e, f] Einar Karu,^[g] Alberto Varzi,^[h, i] Juan Pablo Badillo,^[j] Andrea Hainthaler,^[k] Akshaya Sidharthan,^[k] Andrea Balducci,^[k] Obinna Egwu Eleri,^[l] Amaia Saenz de Buruaga,^[m] Javier Olarte,^[a, m] Juan Dayron Lopez Cardona,^[n] Fatemeh Bahmei,^[o] Sebastian P. Bautista,^[i, o] Marcel Weil,^[h, i, o] and Jon Ajuria^{*[a]}

Now that fast action is needed to mitigate the effects of climate change, developing new technologies to reduce the worldwide carbon footprint is critical. Sodium ion capacitors can be a key enabler for widespread transport electrification or massive adoption of renewable technologies. However, a years-long journey needs to be made from the first proof-of-concept report to a degree of maturity for technology transfer to the market. To shorten this path, this work gathers all the stakeholders involved in the technical development of the sodium ion capacitor technology, covering the whole value chain from academics (TRL 1–3) and research centers (TRL3–5) to companies and end-users (TRL 6–9). A 360-degree perspective is given

on how to focus the research and technology development of sodium ion capacitors, or related electrochemical energy storage technologies, from understanding underlying operation mechanisms to setting up end-user specifications and industrial requirements for materials and processes. This is done not only in terms of performance metrics, but mainly considering relevant practical parameters, i.e., processability, scalability, and cost, leading up to the final sustainability evaluation of the whole of the technology by Life Cycle Assessment (LCA) and Life Cycle Cost (LCC) analysis, which is of utmost importance for society and policymakers.

1. Introduction

By definition, sustainability refers to the ability to continuously maintain or support a process over time.^[1,2] In 1987, the United

Nations (UN) Brundtland Commission added a social perspective to the term. It defined sustainability as “meeting the needs of the present without compromising the ability of future generations to meet their own needs”.^[3] Sustainability rests on

- [a] R. Mysyk, D. Carriazo, D. Saurel, M. Arnaiz, J. Olarte, J. Ajuria
Centre for Cooperative Research on Alternative Energies (CIC energiGUNE), Basque Research and Technology Alliance (BRTA), Alava Technology Park, Albert Einstein 48, 01510 Vitoria-Gasteiz, Spain
E-mail: jajuria@cicenergigune.com
- [b] O. Crosnier, T. Brousse
Nantes Université, CNRS, Institut des Matériaux de Nantes Jean Rouxel, IMN, F-44000 Nantes, France
- [c] O. Crosnier, T. Brousse, K. Ge, P.-L. Taberna, P. Simon
RS2E, Réseau Français sur le Stockage Electrochimique de l'Energie, FR CNRS, 3459, Amiens Cedex 80039, France
- [d] K. Ge, P.-L. Taberna, P. Simon
CIRIMAT, UMR CNRS 5085, Université Paul Sabatier Toulouse III, Toulouse 31062, France
- [e] S. Ratso
Department of Nuclear Engineering, University of California, Berkeley, 2521 Hearst Ave, Berkeley, CA 94709, USA
- [f] S. Ratso
National Institute of Chemical Physics and Biophysics, Akadeemia tee 23, Tallinn, Estonia
- [g] E. Karu
UP Catalyst OÜ, Akadeemia tee 23, Tallinn, Estonia
- [h] A. Varzi, M. Weil
Helmholtz Institute Ulm (HIU), Helmholtzstrasse 11, 89081, Ulm, Germany
- [i] A. Varzi, S. P. Bautista, M. Weil
Karlsruhe Institute of Technology (KIT), 76021, Karlsruhe, Germany

- [j] J. Pablo Badillo
E-Lyte Innovations GmbH, Mendelstrasse 11, 48149 Münster, Germany
- [k] A. Hainthaler, A. Sidharthan, A. Balducci
Friedrich Schiller University Jena, Institute of Technical Chemistry and Environmental Chemistry (ITUC) and Center for Energy and Environmental Chemistry Jena (CEEC Jena), Philosophenweg 7a, 07743, Jena, Germany
- [l] O. Egwu Eleri
Beyonder AS, Stokkamyrveien 30, 4313 Sandnes, Norway
- [m] A. Saenz de Buruaga, J. Olarte
BCARE, Alava Technology Park, C/Hermanos Elhuyar 4 Pavilion 6 Office 6, building Ada Lovelace, 01510 Miñano, Alava, Spain
- [n] J. Dayron Lopez Cardona
Patentes Talgo S.L.U, Calle Las Norias 92, 28221, Majadahonda, Madrid, Spain
- [o] F. Bahmei, S. P. Bautista, M. Weil
ITAS, Institute for Technology Assessment and Systems Analysis, Karlsruhe Institute of Technology (KIT), Karlsruhe, Germany
- [p] D. Carriazo
Ikerbasque, Basque Foundation for Science, Plaza Euskadi 5, 48009, Bilbao, Spain

 © 2025 The Author(s). *Batteries & Supercaps* published by Wiley-VCH GmbH. This is an open access article under the terms of the Creative Commons Attribution License, which permits use, distribution and reproduction in any medium, provided the original work is properly cited.

three interconnected pillars that must be balanced: environmental, social, and economic. Economic sustainability is perhaps the most straightforward to understand, as any long-term economic activity needs to be profitable to continue. However, achieving this profitability must also respect the other two pillars of sustainability: i) Social sustainability, which involves responsible and ethical treatment of the people and communities where a business operates; and ii) Environmental sustainability, which includes maintaining ecological balance through practices like reducing carbon footprint, managing waste responsibly, and using sustainable supply chains, as well as other practices that protect natural resources. In 2015, the United Nations introduced the Sustainable Development Goals (SDGs) as part of the 2030 Agenda for Sustainable Development, aimed at building a better and more sustainable future. These 17 goals include objectives such as sustainable economic growth, ending poverty, achieving zero hunger, ensuring clean water and sanitation, and providing affordable and clean energy. Today, with the escalating threat of climate change and its severe consequences, many countries are developing strategies to reduce their CO₂ emissions by advancing clean energy production and consumption, transforming industries, and electrifying transportation. For these strategies to succeed, various energy storage systems must be developed. Energy storage systems are essential for building a more sustainable energy future by stabilizing power grids, supporting renewable energy integration, and ensuring consistent electricity access. Among these, electrochemical energy storage systems (EESs) stand out for their high energy density, efficiency, and rapid response times, making them particularly advantageous for large-scale and portable applications. EESs are vital for managing the intermittent nature of renewable energy generation. These systems can store excess energy during periods of high generation and low demand, making it available for use at any time when needed. Moreover, their high energy density – *i.e.*, the ability to store large amounts of charge in a compact space – makes them ideal as portable reservoirs of electricity, enabling the growth of the electric transport sector and the portable electronics market. Fast response times are also critical for applications requiring sudden power bursts, such as emergency backup systems or grid stabilization. Unfortunately, no single technology can cover all applications, as different solutions

excel either in energy storage or in power delivery. The well-known lithium-ion battery (LIB) technology is at the forefront of energy-demanding applications, while electric double-layer capacitors (EDLCs) are the vanguard of power applications. In short, the strength of one technology is the weakness of the other, and *vice versa*. The complementarity offers a promising solution as depicted in Figure 1a. It presents an ideal scenario for developing a novel hybrid technology: lithium-ion capacitors (LICs), which aim to combine the benefits of their ancestors while minimizing their weaknesses (see Figure 1b). However, LICs still have a long way to go to compete with the energy densities of LIBs, even though they are already comparable in power density with EDLCs and exceed them in energy density (see Figure 1c).

Since the first LIBs were first commercialized in 1991, lithium-based technologies have been the driving force of EESS. However, despite lithium being a key enabler of this technology, concerns have arisen regarding its impact on the three pillars of sustainability. In 2023, the lithium market faced unprecedented volatility, driven by global economic uncertainty and geopolitical challenges affecting the worldwide lithium supply chain. This created uncertainty among investors, stakeholders, and the lithium-based industry. Moreover, lithium mining is notorious for its enormous water consumption, often in regions rich in lithium but scarce in water resources, thereby limiting water supplies for agricultural communities and basic human needs. Even worse, lithium extraction contaminates water sources with harmful chemicals devastating thousands of hectares of fertile land indispensable for the survival of local communities. Lithium mining contributes a significant amount of CO₂ emissions. That is the paradox of lithium: while it is used to develop technologies aimed at creating a more sustainable society, its extraction process causes environmental and social harm, undermining those very goals.^[4]

In this context, post-lithium technologies have emerged as a more sustainable alternative, with sodium leading the race toward viable market substitutes. Sodium is the sixth most abundant element in the Earth's crust, and its extraction methods are sustainable, primarily relying on the electrolysis of molten sodium chloride. Although the first sodium-ion batteries (SIB) were demonstrated in the last century, the technology re-emerged during the past decade, and the first sodium-ion



Roman Mysyk earned his degree in Chemical Engineering from Donetsk National Technical University and a PhD in Chemistry from the National Academy of Sciences (Ukraine). He worked as a postdoctoral fellow at Dalhousie University and a Marie Curie Fellow at CNRS before joining the Electrochemical Storage Department at CIC energiGUNE in 2012, where he established a research program focused on supercapacitors. His research interests lie at the intersection of electrochemistry and carbon materials, particularly in the development of next-generation hybrid cells that leverage capacitive and faradaic charge storage mechanisms.



Jon Ajuria is the research line manager for metal-ion capacitors at CIC energiGUNE. He earned a Chemistry degree from the University of the Basque Country and a PhD in 2012, focusing on hybrid organic-inorganic photovoltaic solar cells. His research covers electrochemistry and energy storage materials, from fundamental studies to prototype development. With extensive industrial collaboration experience, he works on advancing hybrid energy storage systems that integrate capacitive and faradaic mechanisms to enhance performance and sustainability.

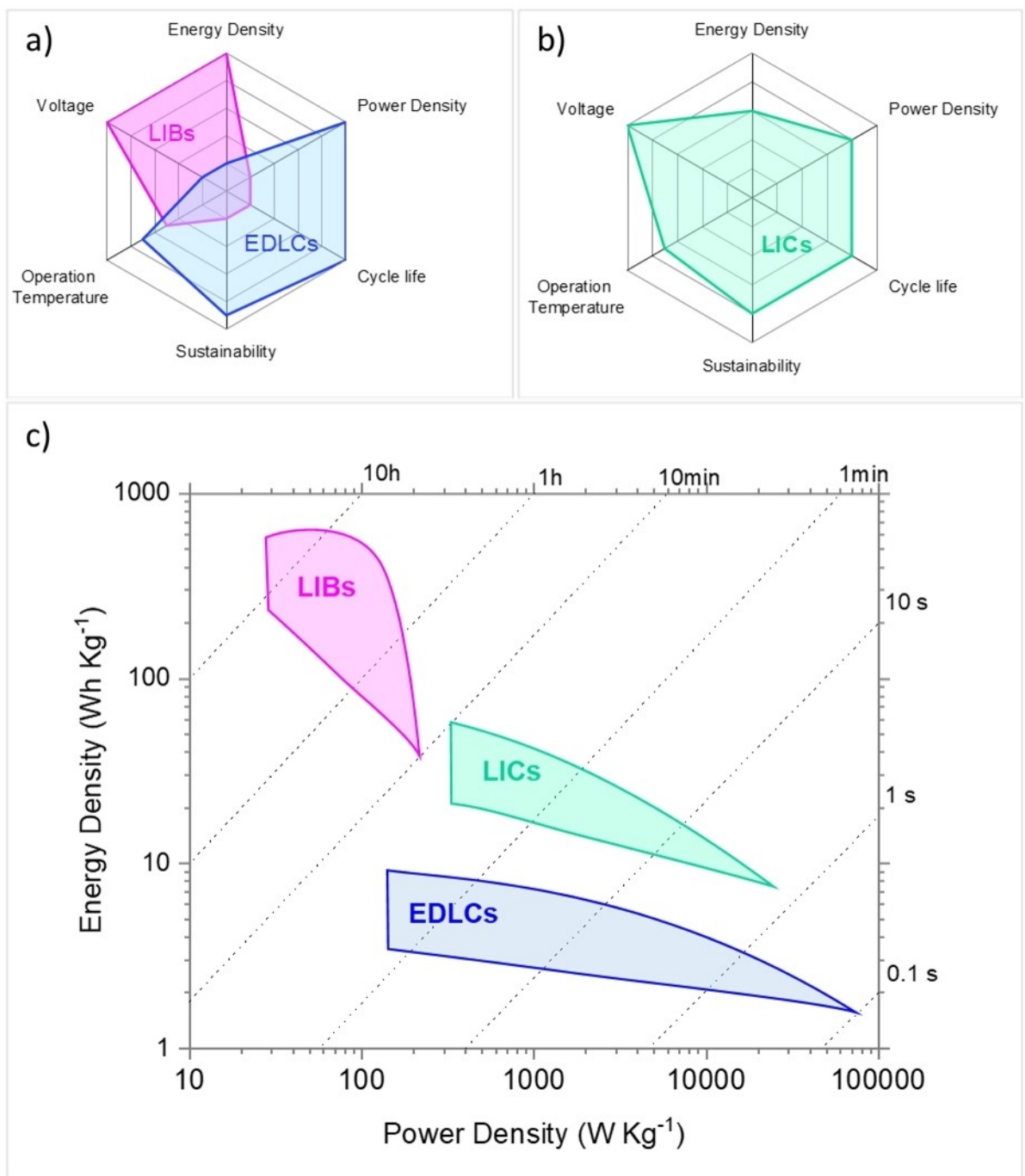


Figure 1. Technology characteristics of a) LIBs and EDLCs and b) LICs. Ragone plot for the different technologies.

batteries are already commercially available from companies such as Faradion, Natron Energy, Altris AB, CATL, and others. Initial tests have even been conducted in electric vehicles (EVs), with the promise of mass production of sodium-ion-based EVs already underway. In parallel with this transition, sodium-ion capacitors (SICs) are also progressing, despite lacking a fully mature market, like EVs, to accelerate their development. According to LIC manufacturers, LICs could be the best cost-of-ownership solution for various applications such as forklifts, grid stability (voltage sag support, peak load shaving), catenary-

free trams, auxiliary power supplies for EVs, automated guided vehicles, and small autonomous vehicles, among others. Equally to lithium, sodium belongs to the first column of elements (*i.e.*, alkali metals), and they both show similar chemical properties. Therefore, it is reasonable to assume that if LICs can perform well, SICs might be able to do the same. However, the reality is more complex. The ionic radius of bare Na^+ is 0.95 nm while that of bare Li^+ is slightly smaller, only 0.76 nm, a tiny difference that opens an abyss in electrochemical performance, for good and for bad. And this is not the only difference. For

instance, energetic instability prevents the formation of sodium graphite intercalation compounds (Na-GICs), making it impossible to use the widely adopted graphite negative electrode material in sodium-ion batteries' negative electrodes. However, this challenge also creates an opportunity to explore more sustainable alternative negative electrode materials, reducing reliance on critical raw materials (CRM) such as graphite.

Since the first SIC was reported in 2012, scientific literature on the topic has surged and technology reviews have skyrocketed, especially after the unproductive COVID-19 period. Materials, mechanisms, technology challenges, and prospects have been extensively revisited, with a focus on outstanding materials performance.^[5] Meanwhile, its sister SIB technology has recently entered the market, although it has yet to conquer it. There are real possibilities for SICs to also achieve market success in the near future, with dual-carbon SICs emerging as one of the most promising and sustainable configurations. These capacitors, which utilize carbon-based materials for both electrodes, offer advantages such as cost-effectiveness, environmental friendliness, and a balance between high power and energy densities, making them strong candidates for large-scale commercialization. Thus, the emphasis of this review is placed on the marketability of SIC technology from a sustainability

perspective, with special attention to the role of dual-carbon systems in meeting critical industry demands. Which materials and processes can meet the sustainability requirements for the scale-up of SIC technology to reach the market? To answer this question, the whole value chain of SIC technology is revisited by relevant academic and industry stakeholders. First, a review of the technology and its operating mechanism is provided, since understanding these aspects is key to proper design and evaluation. Second, both classic and novel materials are analyzed from the sustainability and scalability perspective, assessing their potential for use in real devices. Third, fabrication processes and industrialization requirements are evaluated for mass production. Fourth, the need for innovative management systems for SIC modules and packs is analyzed to ensure the efficient usage of the technology. Fifth, the need for technology assessment in terms of life cycle assessment (LCA) and life cycle costing (LCC) is addressed. Sixth, a perspective on recycling opportunities is discussed in the framework of the circular economy. To conclude, the outlook on future needs is given to ensure that SIC technology is sustainable by design and aligned with the UN chart and code of The Sustainable Development Goals within the 2030 Agenda for Sustainable Development (see Figure 2).



Figure 2. Sodium ion capacitors are a technology born to bridge the energy-power gap between LIB/SIBs and EDLCs. With a smart design through the whole value chain, the technology shows great potential to become sustainable in economic, social, and environmental aspects as represented by some of the 17 UN Sustainable Development Goals.

2. Background

Lithium-ion capacitors were first reported in 2001 by Amatucci et al. when lithium titanium oxide ($\text{Li}_4\text{Ti}_5\text{O}_{12}$ or LTO) was combined with activated carbon (AC) to bridge the energy gap between LIBs and EDLCs.^[6] Shortly thereafter, the substitution of LTO by graphite laid the foundation for the development of dual carbon LICs, which are now commercially available from several manufacturers. Similarly, the first SIC was reported in 2012 using a metal oxide negative electrode ($\text{V}_2\text{O}_5/\text{CNT}$) paired with an AC positive electrode.^[7] However, compared to dual carbon LICs, the high redox potential of V_2O_5 vs. Na/Na^+ limited the operation voltage to 2.8 V. Later that same year, the first dual carbon sodium ion capacitor was introduced, featuring pre-doped carbon microbeads and achieving a high operating voltage of 3.7 V, akin to their LIC counterparts.^[8] This work spurred research into dual carbon SICs, laying the groundwork for the technological advancements seen today, despite the technology not yet being commercially available. This early study already identified several critical challenges for SIC viability, including: i) presodiation of the negative electrode, ii) the capacity ratio of negative-positive electrodes, iii) high rate performance, and iv) cyclability. While not an exhaustive list, these remain the key considerations for successfully designing SICs. Undoubtedly, a thorough understanding of the operation principles and charge storage mechanisms is a *sine qua non* condition. Such knowledge is also essential for designing future smart materials and electrodes, which will be crucial in unlocking the full potential of SICs.

2.1. SIC Technology: Operating Principles of Devices

Metal ion capacitors (MICs) consist of a battery-type negative electrode that stores energy via faradaic reactions, and a capacitor-type positive electrode that utilizes electrostatic adsorption to store charge. This combination enables MICs to achieve both higher energy density than EDLCs and a higher power density than batteries. SICs essentially operate in the

same way as their LICs, sharing both advantages and drawbacks. However, the drawbacks are more pronounced due to sodium's higher reactivity compared to lithium. In transforming an EDLC into a SIC, the capacitive negative electrode is replaced with a faradaic battery-type electrode, fundamentally altering the operation mechanism of the device. This results in two key impacts: i) a significant increase in energy density, and ii) an extra presodiation step and the use of an auxiliary, sacrificial presodiation material.

i) Increase of Capacity and Energy Density

The primary advantage of SIC design is its combination of a capacitive positive electrode and a battery-type negative electrode, which enhances the stored energy compared to conventional EDLCs. Two major factors contribute to this energy improvement:

i) The positive electrode in SICs has a higher capacity due to its extended potential range compared to that in EDLCs; ii) The SIC cell operates at a higher voltage because the battery-type electrode's redox storage occurs below the electrolyte's reduction limit, enabled by the protective barrier of an electrolyte-derived solid electrolyte interphase (SEI). These points can be detailed as follows (Figure 3).

In a standard EDLC (Figure 3, the left-hand side), the operation cell potential window rarely exceeds 2.7 V, which means that each electrode of a full cell operates in a similar potential window $\Delta E_{+EDLC} = \Delta E_{-EDLC} \approx 1.35$ V up and down from OCP, correspondingly, provided the same capacitance under positive and negative polarizations. In a full EDLC cell, the potential-limiting electrode is typically the one that operates reversibly within a narrower stable potential range between its OCP and its oxidation or reduction limits.^[9] Equation (1) shows that a capacitance C of $\approx 100 \text{ F g}^{-1}$ translates into a capacity Q of 135 C g^{-1} (or $\sim 38 \text{ mAh g}^{-1}$ with a potential window of 1.35 V) for a single electrode, be it a negative or positive one.

$$Q = C \times \Delta U \quad (1)$$

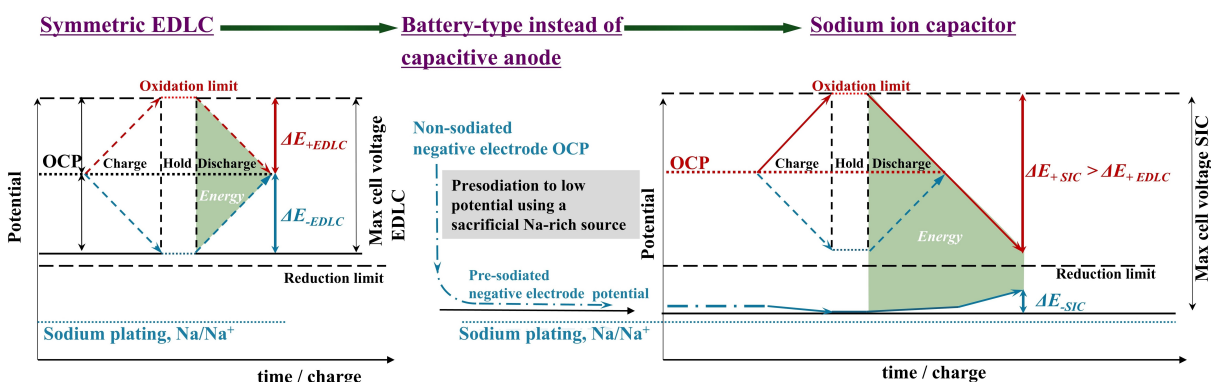


Figure 3. Schematic Operation Principle (Resistance-Related Curve Distortion Neglected): EDLC SIC vs EDLC. Separate Electrode Potential Span in EDLCs (Left-Hand Side) and SICs (Right-Hand Side). Arrows reflect the potential evolution of the positive (red) and negative (blue) in EDLCs (dashed) and SICs (solid). The SIC shows the first cycle, assuming the positive electrode's OCP matches that of EDLCs. Green-shaded areas represent the usable discharge energy for both EDLC and SIC. The negative electrode's potential is reduced in the preliminary presodiation step.

The hybrid device can be schematized via swapping a negative electrosorption electrode with a low-redox-potential faradaic electrode (Figure 3, the right-hand side), with two major effects. First, as the redox activity of the negative electrode approaches the sodium plating potential, the maximum cell voltage can be much higher than that of a symmetric EDLC cell, constituting the first major factor for higher energy density. Second, the positive electrode can now operate in a larger potential window compared to a standard EDLC. The low cut-off potential can now reach 2 V instead of approximately 2.6 V vs Na/Na⁺ (OCP) as in fully discharged symmetric EDLC cells. Specifically, the typical potential window for a single activated carbon-based electrode in such an electrolyte lies between 2 V to 4.3 V vs Na/Na⁺, resulting in $\Delta E_{+ \text{SIC}} \approx 2.3 \text{ V}$ instead of $\Delta E_{+ \text{EDLC}} \approx 1.35 \text{ V}$ in a symmetric EDLC. This consideration allows the capacity of the positive electrode in a SIC to be estimated at 64 mAhg⁻¹ (based on 100 Fg⁻¹ over a 2.3 V range). The working range of activated carbon (AC) electrodes is limited by electrolyte decomposition: oxidation sets the positive limit, and reduction (with or without SEI formation) sets the negative. The high surface area of ACs promotes electrolyte breakdown, leading to pore clogging and loss of cycle reversibility. To maintain effective charge storage, these reactions must be avoided, defining the lowest potential limit for the positive electrode.

The maximum achievable energy density in SICs can be estimated by balancing the full capacities of the hard carbon negative electrode and the activated carbon positive electrode using the specific capacities of each material. Due to the differences in full specific capacity, it is understood that a lower mass of the battery-type negative electrode is needed to balance the charges stored on the positive capacitive electrode, as hard carbon has a higher capacity compared to activated carbon. As a baseline, a symmetric, carbon-based full EDLC cell achieves an energy density of 25 Wh kg⁻¹ when operating at a cell voltage of 2.7 V ($\Delta E_{+ \text{EDLC}} + \Delta E_{- \text{EDLC}}$), given the estimated capacity of 38 mAhg⁻¹ per electrode active material, or 19 mAhg⁻¹ based on the total mass of active materials in both electrodes. This voltage represents the widest potential difference between the two electrodes, i.e., between 1.6 V and 4.3 V vs Na/Na⁺. When shifting from an EDLC to a SIC, 1 g of a hard carbon negative electrode with an average capacity of ~300 mAhg⁻¹ balances the capacity of ~4.7 g of activated carbon as the positive electrode. This is based on the activated carbon's capacity of ~64 mAhg⁻¹, measured within a potential window of [2 V–4.3 V] vs. Na/Na⁺. The overall capacity of this SIC is ~53 mAhg⁻¹ (mass of total active materials in both electrodes, with a 4.7:1 mass ratio of AC:HC) is controlled by the potential window of the positive electrode, $\Delta E_{+ \text{SIC}}$ [2 V–4.3 V] vs Na/Na⁺. Meanwhile, the potential window of the negative electrode, $\Delta E_{- \text{SIC}}$, ranges from ~0.010 to ~0.5 V vs Na/Na⁺. This means that the cell discharges between ~4.29 and ~1.5 V vs Na/Na⁺, translating into an energy density of ~154 Wh kg⁻¹, assuming a mean discharge cell voltage of about 2.9 V. However, the energy density difference between hybrid cells like SICs and EDLCs in real devices is reduced. EDLCs typically offer 6–7 Wh kg⁻¹ whereas SICs' analogue, LICs pro-

vides 15–18 Wh kg⁻¹ at device level, but the improvement is still significant, 2.5–3 times. The smaller-than-expected difference is attributed to two primary factors: i) the presence of inactive components such as binders, additives, current collectors, and casings, which account for 70–80% of the cell's total mass; and ii) the impracticality of achieving perfect capacity balance in SICs, as assumed previously. In practice, the full capacity balance between the electrodes is unachievable because the formation of the solid electrolyte interphase (SEI) and ongoing electrolyte degradation irreversibly consume both sodium and electrolyte during each cycle, limiting the usable capacity of the negative electrode and accelerating capacity fade. Additionally, the slow reaction kinetics of the negative electrode restrict its high-rate capability, distort its potential profile, and compromise both safety and cycle life when operating at full capacity.

Therefore, the practical realization of a long-lasting SIC requires the negative electrode to undergo a separate 'presodiation' step, rather than relying on full charge compensation by the capacitive positive electrode.

ii) Presodiation: A Key Requirement Derived from the Low-Redox-Potential Negative Electrode

Presodiation involves introducing sodium into the negative electrode from an additional sodium source due to its insufficiency in the electrolyte and the positive electrode, to reach a defined capacity. This reduces the electrode potential to a value near Na/Na⁺ and simultaneously facilitates the formation of a solid electrolyte interphase (SEI). The need for presodiation arises due to the sodium-deficient state of typical negative electrodes, which are electrochemically active in charge storage reactions below the electrolyte's reduction limit (see Figure 3). More specifically, a typical hard carbon (HC) electrode has an OCP approximately 300 mV lower than that of activated porous carbons (~2.7 V vs. Na/Na⁺). By enriching HC with sodium, its potential can be pushed down to a few millivolts above Na/Na⁺, with the precise sodium content controlling the lowest achievable potential. However, presodiating HC before its integration into SICs presents significant technological challenges: i) Sodiated HC cannot be synthesized through a simple, isolated chemical process; ii) Sodiated HC is highly reactive, complicating its handling during electrode fabrication and cell assembly; iii) Sodiated HC triggers electrolyte reduction upon contact, leading to spontaneous SEI formation while a stable, uniform, and thin SEI should be aimed for through a carefully regulated process.

These difficulties have driven the development of technologically viable presodiation methods for SICs, which focus on introducing sodium into the battery-type HC negative electrode from an external source. Ideally, presodiation should be performed within the same cell that will be used for energy storage to streamline the process and reduce costs. Although prelithiation from LIC technology can serve as a guideline for presodiation, the latter is more difficult to manage due to sodium's higher chemical reactivity compared to lithium. Nonetheless, the fundamental concept of pre-charging the negative

electrode with sodium ions remains consistent between the two technologies.

Successful presodiation enables a SIC to be prepared for operation with its negative electrode in a partially charged state, containing more sodium than required to fully balance the capacity of the positive electrode. This results in only partial changes to the state of charge of the negative electrode during cycling, offering several key benefits:

- i) Improved control over the negative electrode's minimum potential, its operating potential window, potential profile, and overall cell voltage;
- ii) Enhanced cycle stability of the negative electrode, due to the avoidance of extreme charge/discharge states;
- iii) Improved rate performance, as a significant portion of sodium remains inserted within the HC structure;
- iv) Reduced risk of sodium plating, particularly at high current densities, due to the weaker polarization potential curve distortion at the negative electrode.

Presodiation is also beneficial in terms of better cell tunability: the use of an external source to different presodiation depths allows coupling the negative and positive electrodes in different mass ratios, but always with an excess capacity of the negative electrode. This results in a better degree of control over the energy-to-power spectrum and lifespan, depending on the application's requirements.

The specific methods for presodiation are detailed in a separate section of this review. Despite significant research progress, presodiation remains one of the primary technological barriers to the commercial development of SIC devices, both in terms of process and cost.

2.2. Charge Storage Mechanism in Carbon Materials for SICs

Carbon-based materials have long been considered the most promising electrode materials for both the positive and negative SIC electrodes, due to their low cost, sustainability, non-toxicity, abundant precursors, excellent physical/chemical

stability, and recyclability.^[5] In SICs, the key challenge for carbon-based negative electrodes is to improve their rate capability while maintaining sufficient capacity, which is crucial for enhancing the power density of the device. On the other hand, the main challenge for the capacitive (positive) electrode is to increase its energy density, which is essential for developing high-energy SICs. In this section, we will review the latest advancements in understanding sodium storage mechanisms in conventional carbon-based positive and negative materials for SIC applications.

i) Charge Storage Mechanism in Hard Carbon Negative Electrodes

Hard carbons have demonstrated high theoretical sodium-storage capacity ($\sim 300 \text{ mAh g}^{-1}$), low reaction potential (close to 0 V vs. Na/Na⁺) and excellent cycling stability as promising negative electrodes for sodium storage. In the following section, we will examine the charge storage mechanism of hard carbon negative electrodes with a particular focus on the complexity of the hard carbon structure, the SEI formation mechanism, and the processes of sodium solvation and desolvation (Figure 4). Accordingly, we will underscore how these factors influence the sodium storage performance of hard carbon negative electrodes.

Structure of Hard Carbon. Unlike graphite and soft carbon, hard carbon exhibits an amorphous and heterogeneous micro-crystalline structure characterized by turbostratically disordered carbon segments (Figure 5a). These segments are composed of randomly oriented and interconnected graphene sheets with abundant defects. The graphitic domains that form the main sodium storage active sites can be characterized by three main parameters: the crystal thickness along the c-axis (Lc), the crystal size along the a-axis (La), and the d-spacing between graphene layers (d002).^[11] Figure 5b presents a rich geometric variety, featuring nanoslits, nanopores, and external surfaces of hard carbons. Based on the d-spacing that can be characterized by the X-ray diffraction (XRD) technique, hard carbon always

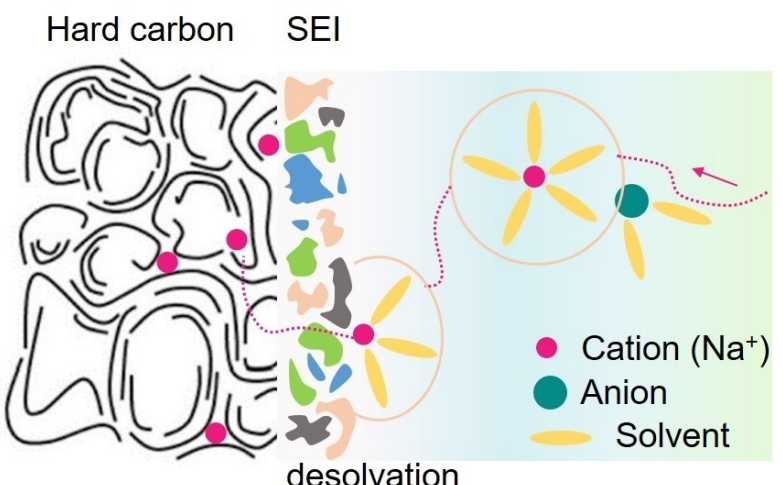


Figure 4. Schematic illustration of SEI formation, Na⁺ desolvation, and sodium storage on hard carbon negative electrodes during the charging process. Adapted with permission from ref. [10] (licensed under CC BY 4.0, Copyright ©, Wiley-VCH GmbH, 2021) and ref. [16].

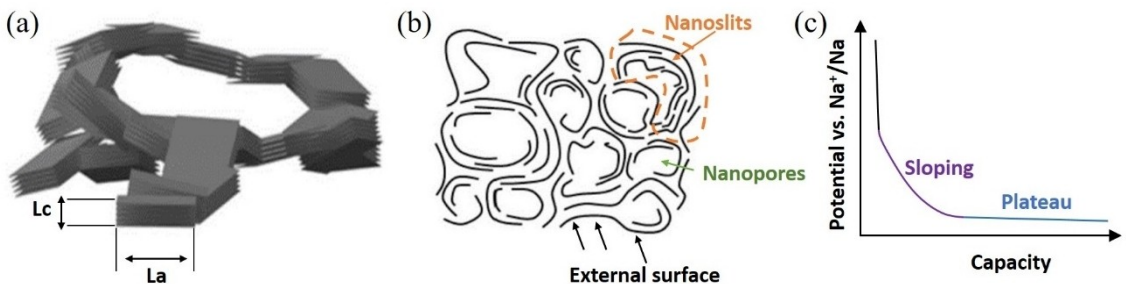


Figure 5. (a–b) Illustration of hard carbon structure: randomly oriented carbon microcrystalline structure and (b) Coexistence of abundant active sites including external surface, nanoslits, and nanopores of hard carbon. Reprinted from ref. [16]. (c) Classical galvanostatic charging (sodiation) plot of hard carbon negative electrode with a sloping region and plateau region present.

contains different types of carbon phases: highly-disordered phase ($d_{002} > 0.4$ nm), pseudo-graphitic phase ($d_{002} = [0.36, 0.40]$ nm), and graphite-like phase ($d_{002} < 0.36$ nm).^[12] This structural inhomogeneity and complexity of hard carbon present substantial challenges in defining multiple energy storage sites and understanding the multistage charge storage processes.^[13]

Hard carbons can be produced from biomass precursors, and various biomass sources have demonstrated potential as precursors of high-performance negative electrode materials.^[14,15] For example, argan shells, kapok fibers, peat moss, banana peels, olive stones, and cork have all been identified as promising green hard carbon precursors due to their wide availability, low cost, and environmental friendliness⁵. However, hard carbons being non-graphitic (disordered) carbons, the various precursors and different preparation conditions lead to important debate regarding the sodium storage process in hard carbons. This poses a challenge in reaching a consensus and developing a universal Na-storage model for hard carbon materials, compounded by the limitations of current characterization techniques.

Debate on two regions. Regarding the galvanostatic discharge/charge profile of hard carbon negative electrodes as presented in Figure 5c, two regions of sodium storage are clearly defined: a sloping and a plateau region.

Different interpretations have emerged about the origins of the high-voltage sloping and low-voltage plateau regions. Currently, theoretical sodium storage models can be classified into four types:^[12] 1) *Insertion-Filling Mechanism*: Na ions insert into the parallel short-range ordered graphene layers during the sloping region and fill the nanopores during the plateau region; 2) *Adsorption-Filling Mechanism*: Na ions adsorb onto defect sites in the sloping region and then fill the nanopores during the plateau region; 3) *Adsorption-Insertion Mechanism*: Na ions adsorb onto the surface and defect sites in the sloping region and are inserted into the carbon layers during the plateau region; 4) *Multi-Stage Mechanism*: more than two mechanisms, e.g., *Adsorption-Insertion-Filling Mechanism*, working together to produce the observed charge/discharge curves due to the dimensional complexity of hard carbons.

The **sloping region**, which takes place in the high potential range of $[0.1, 2.5]$ V (vs. Na/Na^+), is usually explained as an adsorption or intercalation mechanism by most previous

reports.^[17,18] As an early Na-storage model, the sloping region shown in Figure 2 is ascribed to the insertion of Na ions into the carbon layers, which ignores defects and heteroatoms, and deserves further clarification.^[19–22] Hard carbons are usually prepared by pyrolysis of carbon-containing precursors at different temperatures, where the lower temperature leads to abundant defects and smaller carbon fragments. *Temperature-programmed Desorption Mass Spectrometry* (TPDMS) has proved to confirm the presence of a fair amount of defects, such as oxygen surface functional groups and active sites in hard carbons.^[23] In situ *Raman spectroscopy*, often used to assess the graphitization degree and defects of carbon materials,^[24] revealed that there is no peak splitting of the D or G band, and no new peaks appear during the sodiation process,^[25] indicating that Na^+ does not intercalate the layers of the graphitic domains in hard carbons in this potential region.^[26,27] Additionally, a strong correlation has been found between the sodium storage capacity in the sloping region and the defect concentration, identified by the intensity ratio of D band to G band (I_D/I_G) in a hard carbon negative electrode, indicating that the defect sites are highly likely responsible for the Na-storage capacity in the sloping region.^[28] Furthermore, the shallow active sites, including defects, external surfaces, and interlayer galleries (not the d-spacing sites) are also accessible for simultaneous and continuous sodium adsorption.^[29] Several experimental results have further justified a strong correlation between the sloping region and the capacitive-like sodium adsorption process along the sloping region.^[28,30] As shown in Figure 6a (Stage 1), a fast surface-like “pseudo” sodium adsorption process takes place within large interlayer distances (> 0.40 nm) at a low pyrolysis temperature (600°C). This mechanism corresponds to the sloping region observed in the charge/discharge profiles and seems to have reached a consensus in the field.

The **plateau region**, occurring at relatively low potentials ($[0, 0.1]$ V vs. Na/Na^+), is highly desired for achieving reversible high-capacity sodium storage in hard carbon negative electrode materials. The “insertion/intercalation” model has gained credibility because it aligns well with many current scientific findings. Sodium intercalation during the sodiation process can be evidenced by the noticeable shift of the 002 diffraction peak to a lower angle in *in-situ XRD*^[31] and by volume expansion observed in real-time with *in-situ Transmission Electron Micro-*

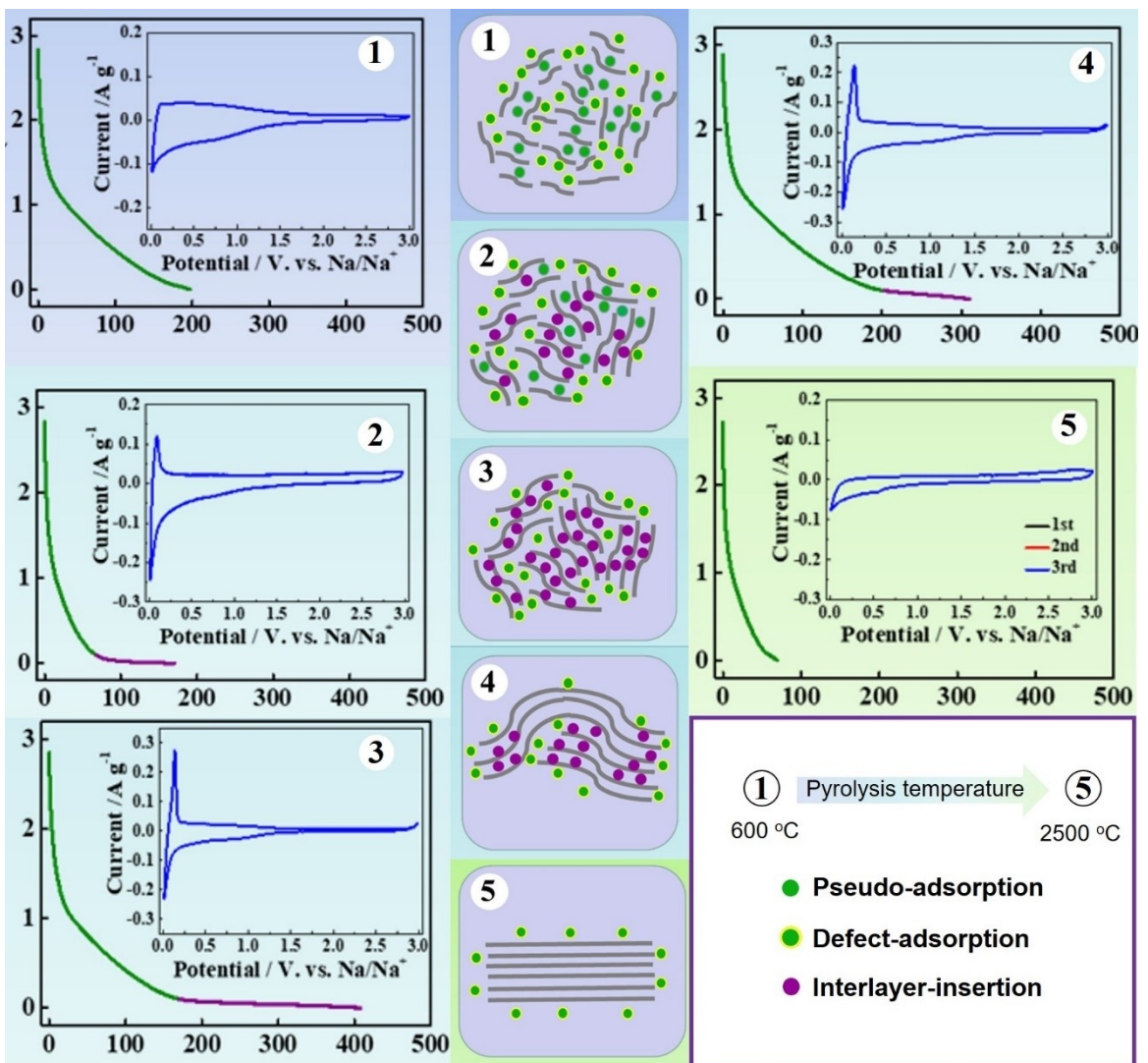


Figure 6. Evolution of sodium storage mechanism and the microstructure with the pyrolysis temperature of hard carbons. Reprinted with permission from ref. [12]. Copyright © Wiley-VCH GmbH, 2021

scopy (TEM).^[32] Based on combined experiment results, Xu et al. proposed a model combining adsorption and insertion of sodium storage mechanisms based on a thorough study of the sodium storage behavior with carbon microstructure evolution^[33] (Figure 6). The coexistence of various microstructures in hard carbons, confirmed by HRTEM and XRD, demonstrates distinct sodium storage mechanisms depending on the pyrolysis temperature.^[33] Different from low pyrolysis temperature in Stage 1 (600 °C), the pyrolysis temperature increases to 800–1700 °C (Stage 3), pre-adsorbed Na-ions insert into pseudo-graphitic domains (d -spacing = [0.36, 0.40] nm), corresponding to the low-voltage plateau region. Higher temperatures (> 2000 °C, Stage 5) create graphite-like carbon with a d -spacing < 0.36 nm, which is inaccessible for Na storage. Transition states occur at Stages 2 and 4. Importantly, the plateau region capacity and the proportion of pseudo-graphitic carbon domains are positively correlated. This linear relationship predicts a maximum plateau region capacity of 277 mAh g⁻¹

assuming all the hard carbon consisted of pseudo-graphitic carbon domains, closely matching the theoretical capacity of 279 mAh g⁻¹ for NaC₈, which is the likely sodium-graphene intercalation compound in hard carbon.

The surface-controlled sodium storage at the high-voltage sloping region exhibits fast kinetics without significant diffusion limitations, whereas the intercalation process at the plateau region is diffusion-controlled.^[34] Thus, balancing the contributions of the insertion and adsorption mechanisms is crucial for optimizing the sodium storage performance of hard carbons, aiming to enhance capacity, cycle stability, and rate capability. This balance ensures that both fast surface reactions and stable intercalation processes are effectively utilized.

Confinement in Carbon Negative electrode. Some studies attribute the low-voltage plateau region to the *micropore-filling* process, with differing views on whether open or closed pores are involved.^[35–38] *Gas sorption* experiments can measure the specific surface area, pore size, and distribution of open pores,

while *Small Angle X-ray Scattering* (SAXS) is effective for identifying the closed pores.^[18] From the latest research on the *micropore-filling* model, the closed pore filling mechanism that occurs at the end of the plateau region seems to be the predominant opinion.^[39–41] Closed micropores are more confined spaces and less accessible than the external surface, defects, and interlayer of graphene sheets, rationalizing this model. Despite diverse theoretical models for sodium storage in hard carbons have been proposed,^[12] they share a common sequence: Na-ions first occupy shallow active sites (surface defects or interlayer spaces) before moving to (relatively) more confined active sites (graphene interlayers or nanopores). This universal principle rationalized the various sodium storage behaviors induced by geometrical differences and tortuous and inhomogeneous structures, especially in hard carbons. As reported previously, a transition from capacitive to pseudocapacitive to faradaic charge storage processes could be mediated by a specific confined local environment.^[42] More confined active sites store charges more efficiently,^[43] aligning well with our observations in hard carbon negative electrodes. Accordingly, both Na intercalation in 2D confined interlayers and Na filling in 3D confined nanopores contribute to the low voltage plateau capacity. Moreover, the formation of the solid electrolyte interphase (SEI) at the local scale is crucial, as it significantly affects Na⁺ desolvation and facilitates charge storage under confinement. Therefore, the following section will focus on the significance of SEI and Na⁺ desolvation in the sodium storage performance of hard carbons.

SEI and Na⁺ desolvation. The SEI formation on the negative electrode material surface greatly affects its electrochemical performance, such as rate capability, and Initial Coulombic Efficiency (ICE), which are far from being satisfactory.^[44] A SEI layer is formed by the reduction of electrolyte components at low potentials, preventing further reduction and co-insertion of electrolyte solvent and insulating electron transfer.^[45] Although the SEI formation has been extensively studied in lithium-ion batteries, it remains less understood in the context of sodium storage. When compared to Li, the higher reactivity of Na leads to a less controlled formation of the Na SEI, often resulting in a thicker, more porous, and less stable layer. This instability and porosity typically cause lower coulombic efficiency, rapid capacity fade, and shorter cycle life.^[46] These issues highlight the need for further research into SEI formation in sodium storage. An *operando electrochemical quartz crystal microbalance* (EQCM) technique has been employed to detect the SEI formation and dissolution processes of sodium negative electrodes. Results found the distribution of organics and inorganics of SEI components having high solubility and instability.^[47] In this section, we will demonstrate how to improve sodium storage performance by controlling the SEI and optimizing the desolvation process of porous carbon negative electrodes.^[48]

Sieving carbons (SC), prepared by controlled chemical vapor deposition (CVD) of methane on commercial porous carbons (PC) with open porosity, present reduced pore entrance size (< 0.4 nm) while maintaining similar pore body size and pore surface areas (insert of Figure 7a and b). SAXS was used to detect nanopores inaccessible to N₂ adsorption due to geo-

metrical constraints. Similar SAXS signals in the intermediate Q range indicate that the pore size control offered by the CVD method does not significantly change carbon porosity.^[49] However, sodium storage performance showed sharp differences: pristine PC exhibited a sloping charge/discharge profile with an extremely low ICE of 15% and a reversible specific capacity of only 39 mAh g⁻¹ (Figure 7c). In contrast, SC had a high ICE of 77% and a reversible capacity of 328 mAh g⁻¹, primarily originating from the long low potential plateau (Figure 7d). The disappearance of the broad peak in the intermediate Q range implies that SEI filled the nanopores, destroying porosity after cycling for the pristine PC sample, while the SEI was mainly formed at the orifice and on the outer surface of the SC nanopores.

Ex-situ^[30] Na *solid-state nuclear magnetic resonance* (ssNMR) spectroscopy revealed the formation of quasi-metallic sodium clusters within 2.4 nm carbon nanopores, which aligns well with other reports.^[35,50,51] Figure 7e shows the evolution of the carbon environment during sodiation, revealing the structural and chemical characteristics of sodium atoms based on Löwdin charges and carbon environments. Sodium ions in groups 1 and 2 carry charges close to 1 (per Na) when adsorbed into sp² and sp³ sites. Group 3 includes clustered sodium ions with partially delocalized electrons, the charge numbers are between 0.4 and 0.8. Group 4 consists of quasi-metallic sodium atoms in more confined sites, with charge numbers between 0.2 and 0.4 and more delocalized electrons. The stronger the confinement of electrolyte ions, the more efficient the charge storage.^[43,52,53] Similarly, the effective nanoscale structural confinement proposed here drives reversible sodium clustering formation in this work.

Another key issue affecting capacity, rate capability, and long-term cycling performance in SIC negative electrodes is sodium ion desolvation. Figure 8 shows an example of regulating the desolvation process through size effect and SEI. A stable, thin, robust SEI film is essential for efficient sodium storage. Figures 8a and b present a step-by-step desolvation strategy to reduce the activation energy, via an artificial SEI film made with zeolite molecular sieves (3.2 Å nanopores). The desolvation activation energy (E_{a1}) decreased to 10.87 kJ mol⁻¹, much lower than 21.87 kJ mol⁻¹ for pristine 1 M NaPF₆-Diglyme (G2) electrolytes (Figure 8c). In addition, the activation energy for Na⁺ transport through SEIs (E_{a2}) also dropped from 22.76 kJ mol⁻¹ to 16.36 kJ mol⁻¹, due to a thinner SEI which results in a higher Na⁺ conductivity. This led to significantly improved rate performance and long-term cycling stability (Figures 8d and e).

In summary, we reviewed several sodium storage mechanisms on hard carbon negative electrode materials. Although there is ongoing debate due to the inhomogeneous local carbon structure of hard carbon (e.g., co-existence of defects, disorder, and graphitic domains), the main processes can be described as follows: (i) sodium adsorption on shallow active sites, including the external surface, defects, and gallery domains and graphene interlayers (normally with d-spacing > 0.4 nm), corresponds to the high voltage ([0.1, 2.5] V vs Na/Na⁺) sloping capacity; (ii) while sodium storage in confined

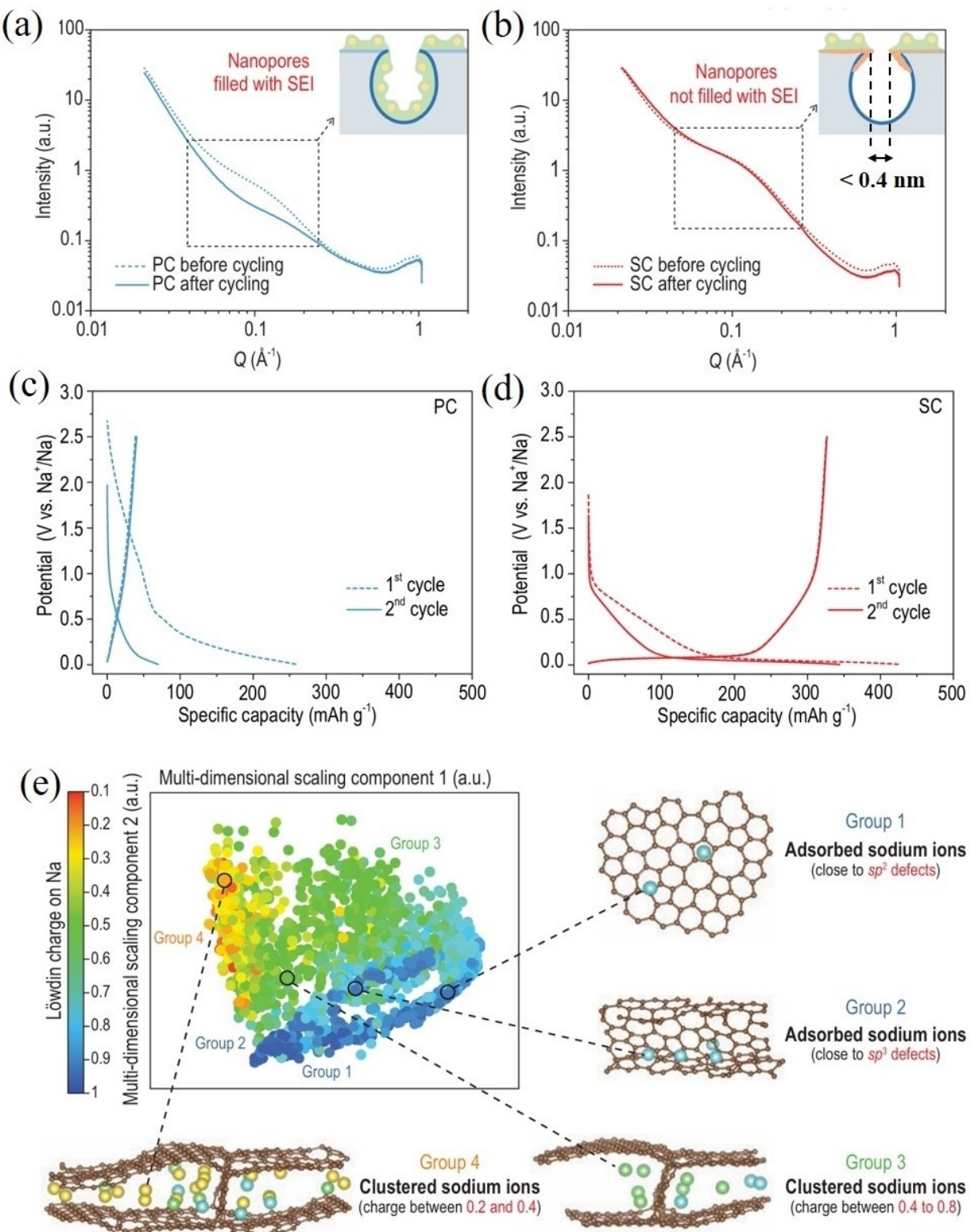


Figure 7. (a-b) SAXS patterns of (a) pristine porous carbon and (b) sieving carbon negative electrodes (with tightened pore size) before and after (dashed line) five full cycles at 50 mA g^{-1} . Inset: schematic illustration of the SEI location inside or outside the nanopores. The SEI is shown in a green irregular shape with yellow solid circles representing sodium ions. (c-d) Charge/discharge curves for the first two cycles at a current density of 50 mA g^{-1} for (c) pristine porous carbon and (d) sieving carbon negative electrodes. (e) Local environment and arrangement of stored sodium in SC, using a smooth overlap of atomic positions (SOAP) kernel, originally developed for Gaussian approximation potential fitting. The map, obtained by multidimensional scaling based on structural distances (representing disimilarity), shows the most similar points aggregated together with similar colors. Reproduced from ref. [48] under the CC BY license. Copyright © Oxford University Press, 2022

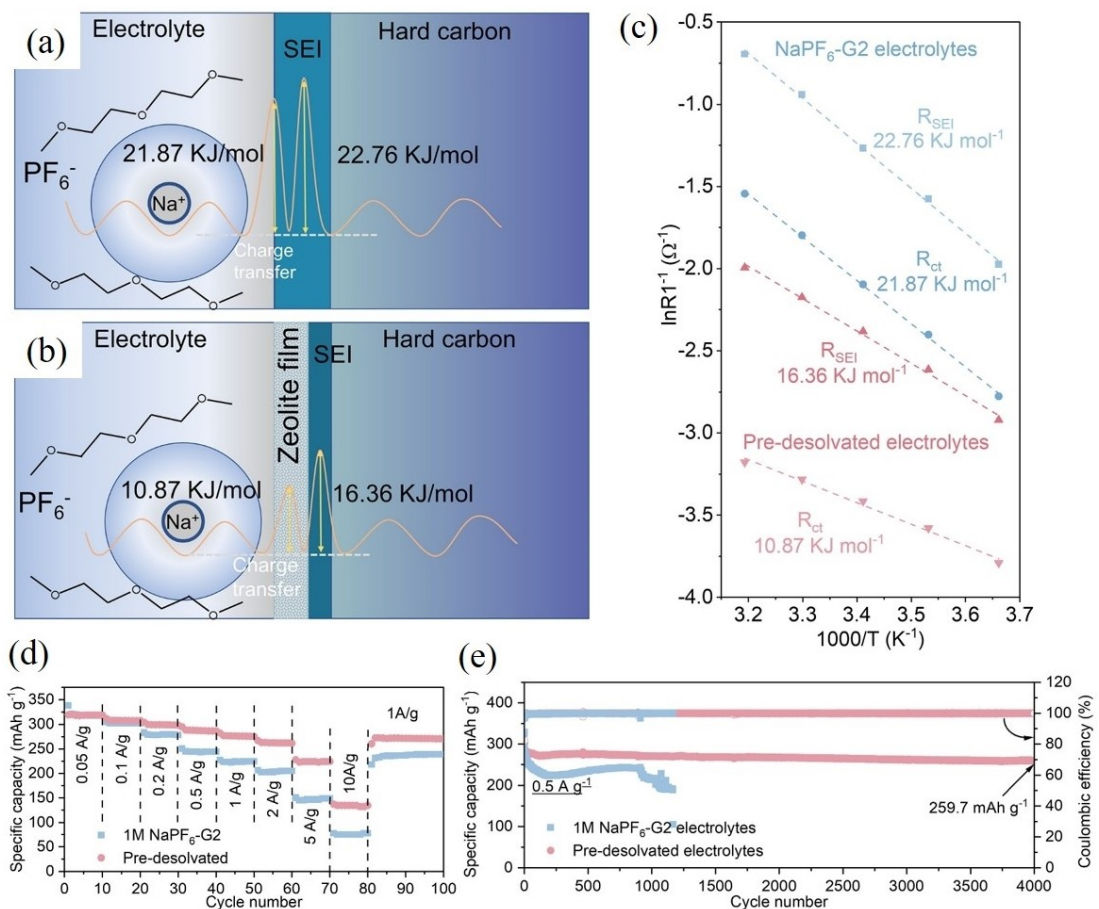


Figure 8. (a-b) Comparison of the kinetics of desolvation and Na⁺ transport through the SEI in (a) pristine ether electrolytes and (b) predesolvated electrolytes with activation energy calculated from (c) the Arrhenius plots. (d) Rate capability at various current densities from 0.05 to 10 Ag⁻¹ and (e) long-term cycling performance at 0.5 Ag⁻¹ in pristine 1 M NaPF₆-G2 and predesolvated electrolytes. Negligible capacity decay was observed with increasing current density from 0.05 to 2 Ag⁻¹. A high capacity retention of 82.3% was obtained at 2 Ag⁻¹, and a specific capacity of 224.0 mAh g⁻¹ is still present at a high current density of 5 Ag⁻¹, corresponding to a capacity retention of 70.3%. For cycling data, a high capacity of 260.4 mAh g⁻¹ still remains after 4000 cycles, with a capacity retention rate of 94.1%. Reproduced from ref. [54] under the CC BY-NC-ND license. Copyright © National Academy of Sciences, 2022

regions, such as graphene interlayers with smaller d-spacing (for example, 0.36–0.40 nm) and micropores, accounts for the low voltage (<0.1 V vs Na/Na⁺) plateau capacity.

Additionally, the manipulation of SEI helps in Na ion desolvation, which is also key to improving capacity, rate performance, and long-term cycle stability.

ii) Charge Storage Mechanism in Porous Carbon Positive Electrodes

Porous carbon materials are the preferred positive electrode materials for SICs. These materials store charges through reversible electrostatic ion adsorption/desorption, forming an electric double layer (EDL) at the electrode/electrolyte interface (Figure 9). The porosity of these materials distinguishes EDL-type supercapacitors from low-energy density conventional dielectric capacitors. Nanopores, particularly those with pore sizes below 1 nm, are crucial for enhancing the capacitance.^[55] Additionally, non-electrostatic ion-electrode interactions also promote ion desolvation and facilitate efficient charge storage under confinement.^[56] This section will explore several key

factors that contribute to enhancing the energy density of porous carbon positive electrodes in SIC cells

Specific Surface Area (SSA). Activated carbons with high electric conductivity^[57] (0.01–1 Scm⁻¹), large specific surface area (SSA, > 1000 m² g⁻¹), and cost-effective are the first choice for SICs positive electrode material; they are currently the only EDL-type materials that have been commercialized.^[58]

Under the EDL-type charge storage mechanism, the porosity enables more charges stored at the interface of porous carbon electrode/electrolyte interface, as the specific capacitance (C) is defined as^[48]:

$$C = \frac{\varepsilon \cdot S}{d}$$

Where C, ε, S, and d, are the specific capacitance, the permittivity of the electrolyte, the surface area of the electrode/electrolyte interface, and the charge separation distance, respectively.

Activation by KOH has long been recognized as an efficient method to enhance carbon porosity.^[59,60] Generally, increasing

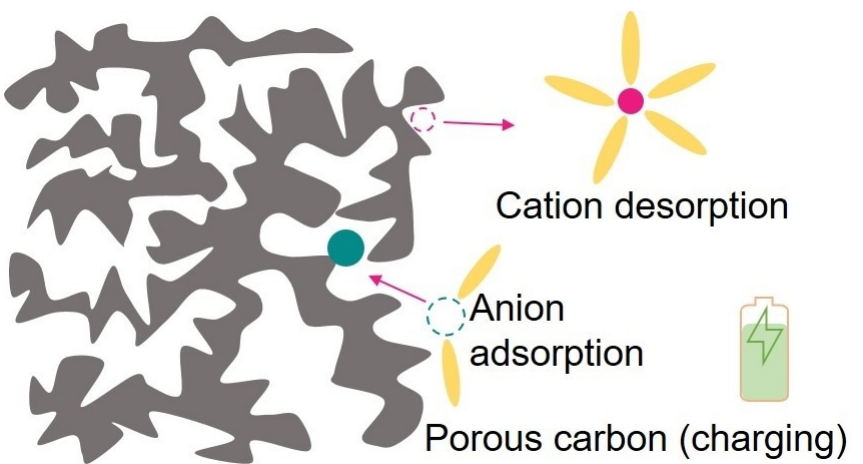


Figure 9. The charge storage mechanism of porous carbon as a positive electrode involves anion adsorption, cation desorption, or ion exchange processes while charging the hybrid SIC.

the activation temperature and the mass ratio of KOH to carbon can enlarge the SSA and widen micropores. KOH activation also dramatically increases the interconnected pore networks and porosity while maintaining the original textural properties (morphology, pore size, etc.), which improves the rate capability as well.^[59]

Local Carbon Structure. Beyond SSA, pore size – particularly subnanopores ($< 1 \text{ nm}$) – plays a critical role in carbon capacitance, with a notable increase observed at pore sizes below 1 nm .^[55] Intensive research has focused on Na^+ solvation/desolvation at the negative electrode-electrode interface, as summarized in Figures 3 and 4. However, anion desolvation energy is equally important for porous carbon positive electrodes. The pore size matching theory has provided key design principles for efficient charge storage in nanopores.^[62] Figure 10a illustrates the solvation structure of ClO_4^- anions in EC/DMC mixed solvents.^[63] A series of heteroatom-doped porous carbon materials were prepared with average pore sizes ranging from 1.20 to 1.68 nm (Figure 10b). The specific capacitance and normalized capacitance (normalized to SSA), shown in Figure 10c, indicate that the highest capacitance is achieved when the pore size matches the solvated anion size (1.48 nm). However, anion desolvation does not take place in this work as expected in smaller pore sizes of carbide-derived

carbon materials. This is because of additional heteroatom (O, N, and S) doping and varying anion desolvation energy barriers, as calculated from the Arrhenius plots. Further research into electrolyte solvation/desolvation engineering is needed to enhance the charge storage capacity of carbon positive electrode materials in Na^+ -containing non-aqueous electrolytes. Additionally, the importance of electrode-electrolyte interaction (without polarization) has recently been recognized as crucial for driving charge storage behavior and improving capacity.^[56] This interaction can be modulated by both the heteroatom doping^[64] and local carbon disorder.^[65,66]

Potential Window. The specific capacitance of porous carbons is theoretically independent of the potential window ($C=Q/\Delta U$). However, when these materials are used as positive electrodes and coupled with negative electrode materials, the cell voltage window becomes a limiting factor and must be taken into account. Figure 11 presents strategies to maximize the specific capacity (in mAh g^{-1}) by fully utilizing the stable electrochemical operating potential window.^[67] In Figure 11a, the capacity is limited by the positive potential limit, restricting the cell voltage to 3 V . Increasing the mass of the positive electrode makes the cell voltage extend to 4.5 V ; but the specific cell capacity remains unaffected and still short. In contrast, Figure 11b shows that by regulating the electrode

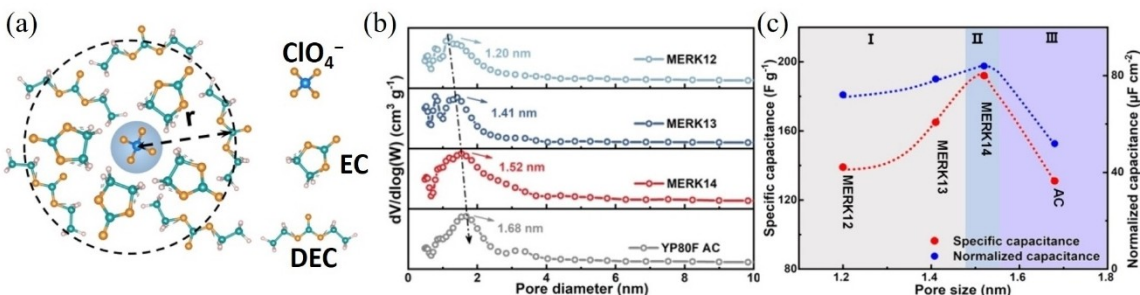


Figure 10. (a) Schematic of solvated ClO_4^- anion in EC/EDC non-aqueous electrolyte. (b) Pore size distributions calculated from the quenched-solid density functional theory (QSDFT) method. (c) Dependence of the specific and normalized capacitance on the pore size. Reproduced with permission from ref. [63]. Copyright © Elsevier, 2022.

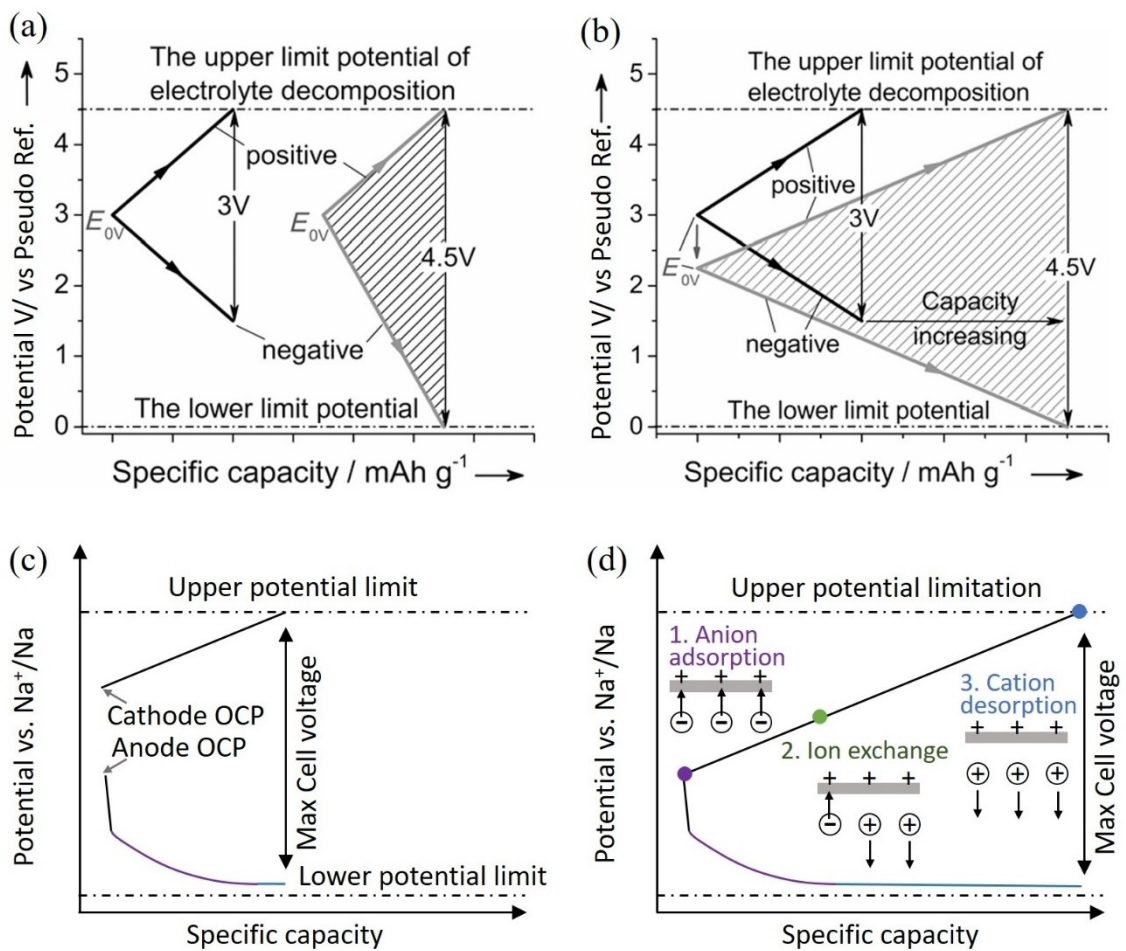


Figure 11. Positive and negative electrochemical potential window (EPW) in a two-electrode device during the charge storage process. (a). Limited EPW (left) and optimized EPW (right) by increasing the mass of the positive electrode, but the specific capacity remains the same. (b) Optimized EPW by tuning surface charge (E_{0V}) to simultaneously increase the specific capacity and working voltage. The shadowed area is proportional to the energy density. Reproduced from ref. [67] Copyright © Wiley-VCH GmbH, 2021. (c-d) Galvanostatic charging plot of SIC cells with porous carbon serving as the positive electrode and hard carbon as the negative electrode. The specific capacity is different when employing (c) higher OCP and (d) lower OCP. The inserts in (d) demonstrate different electrolyte ion behavior, governed by the location of PZC at low (purple), medium (green), or high (blue) potential.

surface charge through charge injection, the E_{0V} can be shifted to a lower potential (vs. pseudo reference electrode) at OCP. This shift enabled the cell voltage window to reach up to 4.5 V, and the specific capacity improved as well.^[67] For applicable SICs the negative electrode plateau (hard carbon) is almost fixed at ~0.1 V vs. Na/Na⁺. However, the potential window of the porous carbon positive electrode can be carefully regulated to maximize the cell-level charge storage performance, as described in Figure 11c-d.

Figure 11c presents a limited specific capacity and energy density due to the relatively high OCP of the positive electrode. In contrast, Figure 11d demonstrates an optimized scenario: lowering the positive electrode OCP maximizes the negative electrode capacity and overall cell capacity within the same electrolyte stability window. It is worth noting that the location of the *potential of zero charge* (PZC), indicated by colored dots on the positive potential path in Figure 11d, plays a crucial role in determining the direction of ion flux. If the PZC is located at or below, Case 1 (pzc = purple dot), the positive electrode

charging corresponds to anion adsorption all along the way. In contrast, in Case 3 (pzc = blue dot), where the PZC is high or above, cation (Na⁺) desorption occurs. If the PZC is situated in between these cases (green dot), ion exchange happens, which is generally less efficient for power performance.^[68] Therefore, careful modulation of the PZC is essential for controlling which electrolyte ions are involved in the positive electrode charging/discharging process. This is important because cations (Na⁺) and anions have distinct solvation energies and effective ion sizes, which directly influence the positive electrode's charge storage performances. It is worth noting that a higher PZC ensures purely Na⁺ based charge compensation, without anions playing a role, which may improve the sodium storage. Additionally, the PZC also significantly impacts the SEI formation and dendrite growth on the negative electrode side.^[69]

Overall, this section presents several effective strategies for improving the charge storage performance of porous carbon materials used as SIC positive electrodes. Designing low-cost, mild, and efficient synthesis methods for producing highly

porous carbons with high SSA is a practical approach to enhancing capacitance. The local carbon structure affects ion-electrode interactions and can further improve capacitance by facilitating ion desolvation. Additionally, regulating the surface charge of the carbon positive electrode can fully utilize the stable electrochemical potential window, maximizing cell-level capacity and energy density. Moreover, carefully controlling the positive electrode PZC has been proposed as a practical method for driving the ion flux, which needs further investigation.

In summary, we have presented the charge storage mechanisms for both the negative electrode and positive electrode carbon materials for SIC applications. For the negative electrode material, although the state-of-the-art understanding of the sodiation process in hard carbons is still under debate, we proposed a general confinement concept to guide the structure-performance relationship: shallow active sites correspond to the high voltage ([0.1, 2.5 V] vs Na/Na⁺) sloping capacity; while confined active sites (e.g. graphene interlayers with smaller d-spacing: [0.36, 0.40] nm) and micropores, which are less accessible and account for the low voltage (<0.1 V) plateau capacity. Confined geometries are expected to store charges more efficiently.

Additionally, the solid electrolyte interface (SEI) also plays a crucial role in facilitating Na⁺ desolvation, which in turn improves the overall performance including rate capability, cycling stability, and charge storage capacity of SICs with hard carbon negative electrodes.

For the positive electrode porous carbon material, specific surface area (SSA), local carbon structure (including pore size and local ion-electrode interaction), and a potential window optimization strategy at the cell level are crucial for achieving high-performance hybrid devices. Besides, the location of the potential of zero charge (PZC) is crucial for enhancing the performance of both positive electrode and negative electrode materials. As a matter of fact, the activated carbons' PZC determines which ions are involved in the charge/discharge process, and which of those are prominent. On the negative electrode side, the PZC influences the formation of SEI and the growth of dendrites. Finally, in-situ and ex-situ characterization techniques such as high-resolution transmission electron microscopy (HRTEM), in-situ Raman spectroscopy, in-situ X-ray diffraction (XRD), and solid-state nuclear magnetic resonance (ssNMR) are essential for elucidating local charge storage mechanisms. Moreover, *operando* techniques such as electrochemical quartz crystal microbalance (EQCM) and electrochemical dilatometry (ECD) are promising characterization tools. These methods enable high-resolution and real-time monitoring of electrode mass and volume changes during electrochemical processes. Employing these advanced techniques provides valuable insights that guide the design of high-performance sodium-ion capacitors (SICs).

3. Materials: Scalability, Sustainability, and Trade-Offs with Performance

3.1. Carbon Electrode Materials

Carbon materials have always been essential to human life, serving various purposes throughout history, from charcoal adsorbents known from prehistoric times to more ordered carbon forms such as graphite, which have become indispensable in numerous industries, particularly those based on electrochemical properties such as, for example, primary and secondary batteries based on graphite fluoride and lithium graphite intercalation compounds, correspondingly.

From the sustainability and scalability standpoint, carbon materials often present one of the best options due to plentiful natural resources as well as established production methods. However, tuning carbon materials (porosity, surface chemistry, purity, doping, etc...) to specific applications and/or maximizing their efficiency can render the derived product prohibitively costly.

Given that the main rationale behind SICs hinges on their sustainability, this section focuses on the production methods, structures, and textures of carbon materials with an emphasis on their scalability for use in SICs. We provide a detailed view of both non-porous non-graphitizable hard carbons and nano-scale-porous carbons in terms of their synthesis methods and maximum electrochemical output, always considering the trade-offs between performance and scalability.

Requisites for Scalable Carbon Synthesis

Despite the wide history and use of hard carbon and activated carbon and thousands of publications reporting different production methods, only a selected number of companies capable of producing high quality battery-grade hard carbons and supercapacitor-grade activated carbons. Numerous available methods report remarkable results, in the case of activated carbon, with surface areas up to 3000 m²g⁻¹ and capacitance values above 100 Fg⁻¹ per single electrode.^[70] Regarding hard carbon, low surface areas of 5–10 m²g⁻¹ and reversible capacities over 400 mAh g⁻¹ have been reported. However, several considerations during R&D on HC and AC production must be satisfied to ensure that the synthesis procedures can be upscaled successfully. These will be discussed according to the subheadings: Performance, Raw materials supply chain (precursors and activation agents), Process (process efficiency, consistency, and material/equipment interactions), Economic viability, and Regulations.

Performance. The performance of the synthesized carbon is the primary criterion beside the cost. For optimum performance, activated carbons for the positive electrodes of hybrid capacitors must possess well-developed and interconnected micropore structures.^[71] The most suitable SSA is about 1500–2000 m²g⁻¹. Further increase in SSA and pore volume leads to a leveling-off of gravimetric storage metrics^[72] and a decrease in volumetric performance.^[73] Avoiding excessive activation is crucial since it can affect yields, and handling, and pose

challenges such as drying before cell assembly and electrolyte degradation during operation. Additionally, factors like purity, oxygen content, ash, metal content, and residual activation agents must be controlled or reduced to appropriate levels to prevent unwanted interactions with the electrolyte and minimize the parasitic self-discharge of the final cells. In the case of the hard carbon for negative electrodes, the activation step is not needed, and the requirement should be rather opposite: SSA must be reduced to minimize the irreversibility and excessive electrolyte consumption during the SEI formation. Additional post-treatment may be warranted to fine-tune texture and surface chemistry. Other additional requirements should mostly replicate those for AC.

Raw materials supply chain. Several precursors have been utilized to produce HC and AC.^[74–76] The precursors typically considered are naturally abundant carbon-rich materials, which must be readily available for successful upscaling. Mass production facilities typically target a 10 –100 kg precursor-processing capacity to facilitate economies of scale while maximizing the profit from large-scale sales and synthesis. In this regard, the precursors used must be consistent in terms of carbon content, purity level, and moisture content. These factors will influence the efficacy of the activation agents and potentially cause product non-uniformity during mass-scale production. Among various biomass precursors tested, coconut shell is the most sustainable due to the year-long supply in East and Southeast Asia. The chosen activation agent must also be readily available, inexpensive, and capable of being recovered to reduce associated costs. Additionally, interactions between the activation agent and the process equipment must be considered.

Economic viability. An eventual cost vs benefit analysis must be considered during upscaling. While high-quality hard carbon can be synthesized in a temperature range from 800 to 1500 °C with a yield below 50%, AC requires an additional step using intensive activation, further reducing the yield, which makes upscaling unfavorable. The current cost of battery grade HC ranges from 30–45 USD·kg⁻¹ while the capacitor-grade activated carbon ranges from 40 – 60 USD·kg⁻¹ (kuraray.com). Any process that incorporates multiple fabrication and post-treatment steps, and expensive activation agents will be reflected in the final cost of the carbons, rendering it unattractive for upscaling. This is especially true for high-performance carbons produced on a lab scale, which have little to no prospects of reaching the market due to the prohibitively high cost of their synthesis routes.

Regulatory compliance. All manufacturing processes must adhere to various regulatory standards concerning safety, health, environmental, and quality requirements. The developed process must ensure that the occupational health and safety standards, such as exposure to unsafe conditions (heat, gases, and chemical environments), are minimized and appropriate personal protective equipment can be used to prevent accidents and health hazards. This can pose challenges for upscaling, especially for AC when dealing with activation agents like ZnCl or post-treatment methods involving hydrogen fluoride. Environmental regulations, including compliance with

local emissions standards, waste management practices, water usage, air quality standards, and emissions limits, must also be considered. The accompanying equipment and costs associated with wastewater treatment, emissions control, monitoring systems, and pollution control measurements will affect the scalability of the process. Hence, these must all be factored in during the initial development phases.

Activation process. The activation process applies only to AC, to increase the specific surface area and porosity of the carbon. Typical activation processes used in lab-scale experiments include physical activation (using CO₂ or water steam) and chemical activation (using KOH, NaOH, ZnCl₂, etc.), often combining both methods. When scaling up from lab-scale to large-scale industrial processes, it is essential to consider the interactions between the activation agent and the process equipment. In the pursuit of intensive activation, specifically using chemical activation, highly corrosive chemicals are used, such as high-concentration strong bases that pose compatibility issues with the metal-based equipment commonly used in large-scale activation processes. Consequently, upscaling becomes challenging due to the risk of product contamination from metal dusting and leaching into the final product. Moreover, certain activation agents also affect material flowability during heat treatment, leading to plasticization behavior where the precursor and the activation agent fuse or form solid aggregates that may adhere to reactor walls. Thus, the interaction between the activation agent and the process equipment is crucial. From both cost and sustainability perspectives, prioritizing physical over chemical activation is advisable.

3.1.1. Carbon Negative Electrode Materials for SICs

Beyond sustainability and scalability requirements, suitable negative electrode materials for Sodium-ion Capacitors (SICs) should enable optimum electrochemical performance as defined by the following electrochemical prerequisites:

- i) **High-Capacity Reversible Low-Potential Redox Processes:** These should ideally approach but not reach sodium-plating potentials, with a maximally flatter discharge profile to maximize not only capacity but also overall energy thanks to optimum potential evolution.
- ii) **High-Rate Capability:** The materials should exhibit high-rate capability with a low-polarization resistance voltage drop to approach the rate response of a capacitive electrode. Although perfect harmony is difficult due to the inherently slower charge storage in redox-based negative electrodes, minimizing this discrepancy is crucial.
- iii) **Maximized Initial Coulombic Efficiency (ICE):** While this requirement should be less stringent for SICs compared to SIBs due to the unavoidable use of a presodiation agent whose amount can be adjusted to mitigate a margin of irreversibility in the initial cycles, ICE remains important from the technology standpoint to minimize side effects such as gas generation and irreversible electrolyte consumption.

Among potential SIC negative electrode materials, hard and soft amorphous carbons stand out since they combine multiple electrochemical advantages with scalability prospects. Electrochemically, they offer sufficiently high capacity, low-potential redox storage reactions favorable for energy, and a superior high-rate response compared to other negative electrode materials based on alloying or conversion reactions.

From a scalability and sustainability perspective, amorphous carbons can be derived from various biomass-forming natural polymers, many of which are lignocellulosic materials or by-products of their industrial processing. Lignocellulosic waste biomass typically contains about 50% carbon, making it an inexpensive, renewable, and environmentally friendly carbon source.^[77] These materials should be considered as primary sources for amorphous carbons designed for SICs, aligning with the rationale behind Na⁺ technologies: the use of non-critical raw materials. The cost advantage of amorphous carbon synthesis lies in its simplicity, involving heat treatment and optional pre- and/or post-treatment, without the need for additional activation processes required for porous materials used in SIC positive electrodes.

Below, we examine various types of amorphous carbons, their synthesis methods, properties, and the resulting electrochemical response relevant to SICs.

Soft vs hard carbon: definition, chemical-physical characteristics, synthesis, and performance. Non-graphitic soft carbons (SC in this chapter) and hard carbons (HC) are typically synthesized through the pyrolysis of organic precursors within a temperature range of 500 to 1500 °C. The classification of the final product as either HC or SC relates to the structure and

microstructure of the carbons. The terms "soft" and "hard carbon" refer to the mechanical properties of the resulting material, which, along with their ability to undergo graphitization, are influenced by the plasticity of their layered structure.^[18,78,79] Graphitization involves the conversion of the original turbostratic structure of disorderedly arranged non-graphitic carbon layers into the ABAB or ABCABC layer stacking arrangement, the process requiring the sliding and rotation of layers.^[79,80] Similarly to graphite, the structure of SC exhibits this plasticity, providing flexibility under stress and the potential to undergo graphitization at temperatures exceeding 2200 °C (graphitizable carbons). In contrast, the fine structure of HC lacks this plasticity, resulting in mechanical hardness and an inability to undergo graphitization even at temperatures exceeding 3000 °C ("non-graphitizable carbon").^[79] This is due to the presence of layer curvature (related to sp³ partial hybridization) and micropores, forbidding the layer gliding required to form the ordered graphitic stacking.^[79]

While both SC and HC display a sloping voltage-composition curve below 1 V, HCs showcase an additional low-voltage plateau below 100 mV (Figure 12). Not only does this feature enhance the capacity, with multiple reports of capacities up to 300–350 mAh/g, but also lowers the average working voltage to be below 0.4 V vs Na/Na⁺, with the initial Coulombic efficiencies exceeding 80% according to the most notable studies (see e.g.,^[82,83]). Through high-temperature treatment and expert micropore optimization, specific capacities can be further enhanced to be beyond 400 mAh g⁻¹.^[84,85] By contrast, SCs exhibit specific capacities at best up to 200–250 mAh g⁻¹, with working voltages of about 0.5–0.6 V vs Na/Na⁺ and the

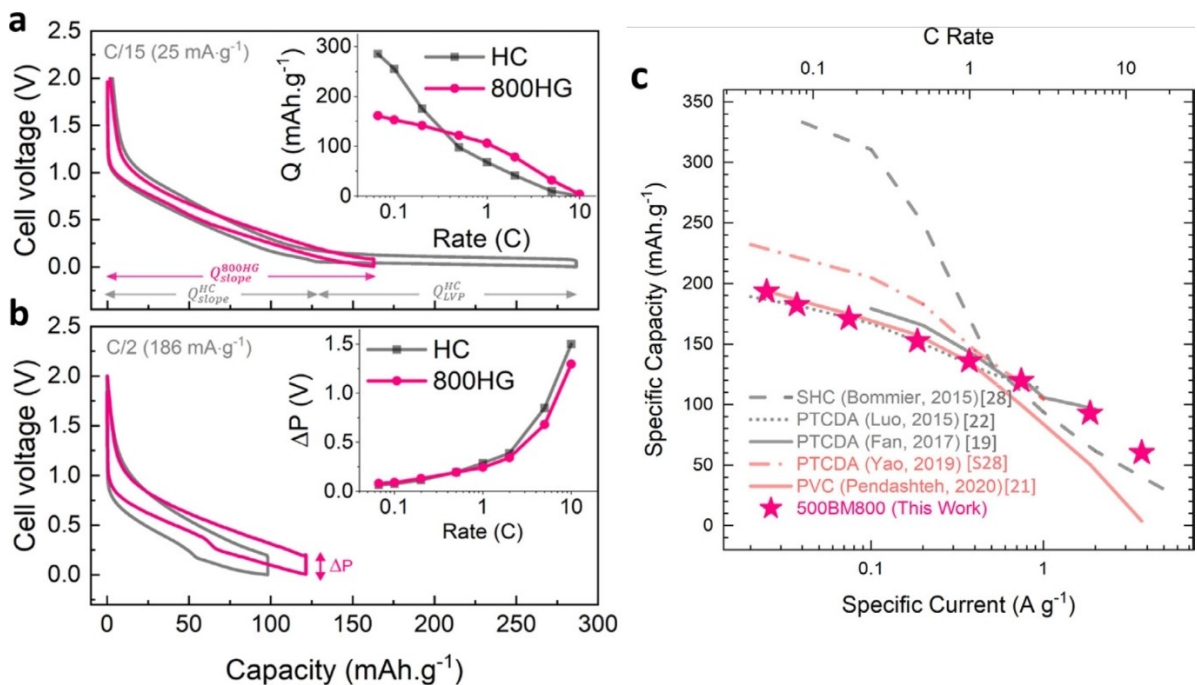


Figure 12. Voltage-capacity profiles (vs Na/Na⁺) of a hard carbon (HC, gray line) and a soft carbon (800HG, pink line) with similar micron-sized particles, cycled galvanostatically at rates of C/15 (a) and C/2 (b); 1 C = 372 mA·g⁻¹. Inset of (a): reversible capacity as a function of C-rate. Inset of (b): cell polarization (estimated as the voltage jump between the end of discharge and beginning of charge) as a function of rate. c) rate capability of some of the best reported soft carbons along with one of the best reported hard carbon ("SHC"). Reprinted from [81] under the CC BY-NC-ND 4.0 license. Copyright © Elsevier, 2022

best ICE falling between 70% and 80%.^[86] However, the significantly lower energy density of SCs is counterbalanced by their superior rate capability, making them an interesting option for the negative electrode of all-carbon metal ion capacitors such as SICs, even in comparison to LICs where graphite is used as the negative electrode.^[87,88] SCs are also considered to offer a safer alternative since HC provide over half their capacity at very low voltages (≤ 0.1 V vs. Na/Na⁺), where even a slight potential drift can pose significant risks of Na plating and derived dendrite formation, which is of relevance to high-rate storage required from SICs.^[28,86,89] With respect to the hybrid cells such as MICs in general and SICs in particular, maximizing the first Coulombic efficiency can be less of a concern since presodiation is an unavoidable formation step in preconditioning SIC cells for stable operation. Therefore, moderate differences in the ICE can be mitigated within the formation step by tuning the amount of presodiation agents.

The properties of the final product, either HC or SC, depend largely on the nature of the precursor material, and, in a minor way, the synthesis conditions. Thermosetting precursors, which remain solid upon carbonization, typically lead to hard carbon, while thermoplastic polymers, which melt at the early stage of carbonization, typically lead to soft carbon.^[49] HC precursors are hence commonly derived from the carbonization of oxygen-rich organic precursors such as carbohydrates (sucrose, glucose, cellulose) and lignin.^[49] For this reason, the use of plant-derived biomass consisting of a mixture of cellulose and lignin, either raw or processing waste by-products, has become very common. HC may also be prepared from thermosetting polymer and resins. Conversely, SC is predominantly derived from hydrogen-rich sources like hydrocarbons and aromatic compounds. SCs are hence more commonly synthesized from synthetic hydrogen-rich polymers such as polyvinyls, PAN, etc..., synthetic aromatic dies, and side products from the coal and oil industry (coke, pitch, etc...). A comprehensive survey of precursors used for SCs and HCs can be found in other informative review articles.^[18,90]

Besides the nature of the precursor, many synthesis parameters can affect the properties of the final carbon. First, the flow of inert gas is of prime importance for effectively clearing the reaction zone from evolved gases to prevent their interaction with the carbon residue. This can lead to its excessive burn-off and self-activation through partial self-combustion.^[91] Effective gas removal is crucial for maximizing the degree of closure of the buried micropores while simultaneously minimizing the development of external surface area and thus its posterior reactivity when the HC is employed as an electrode active material. Temperature is also critical. Higher temperature tends to reduce surface area and surface reactivity, leading to lower capacity loss during the formation of the SEI. However, the extension of the sloping contribution to the capacity, common for both SCs and HCs, also tends to decrease with increasing temperature. In the case of HC, this is partially alleviated by a lengthier low-voltage plateau. However, the improvement through the higher plateau capacity may be less relevant to SICs than SIBs since the plateau region is more prone to Na-plating risk under high-rate conditions required

from SICs. Therefore, HCs tend to be prepared at higher temperatures than SCs. The optimum temperature needs to be determined for the best balance among reversible capacity, rate capability (related to sloping capacity), and Coulombic efficiency. The optimum temperature will hence differ depending on the target performance and will be highly dependent on the nature of the precursor.

To some extent, the precursor's chemical nature can also be altered to tune the properties of the resultant carbon. For HCs, pre-carbonization strategies such as acid leaching, oxidation by heating in air, or hydrothermal treatment allow controlling crystallinity, micropore size, and volume, as well as their degree of pore closure. For SC precursors, oxidation may prevent fusion during pyrolysis, leading to a stabilization of the morphology of the final SC. This is particularly interesting when the plasticity of the precursor is used to form high aspect ratio morphologies such as microfibers, which may be beneficial for power capability by favoring electrical interconnection and short diffusion paths. Oxidation of SC precursors may even lead to an HC in some cases (oxidized pitch). Low-cost and abundant precursors such as coke and pitch, typically leading to SC, can hence be also used to produce HC.

Morphology control in amorphous carbons and related electrochemical response. Decreasing particle size via ball milling is a widely recognized and effective method for enhancing the rate capability of active materials by reducing ion diffusion pathways. Smaller particles amplify energy storage properties by increasing surface-related capacity, expediting reaction kinetics, and unlocking bulk capacity.^[92] This principle underpins the use of nanostructured materials in both supercapacitors and batteries. However, for negative electrodes operating at low voltages beyond the lowest unoccupied molecular orbital (LUMO) of the electrolyte (e.g., potential below 1 V vs. Na/Na⁺), such as those based on carbonaceous materials, reducing particle size can lead to increased coulombic losses associated with electrolyte decomposition, such as SEI formation.^[93–98]

Numerous strategies have been proposed in the literature to ensure short ion diffusion lengths without compromising the coulombic efficiency of carbon materials, such as passivation after milling (e.g., coating) or inducing a desired morphology prior to carbonization, as seen in mesophase pitch,^[93,95] spherical HC,^[31,99] carbon fibers,^[98] etc. Pre-carbonization morphology control is straightforward in HCs, where typical solid-state carbonization preserves precursor morphology up to the final carbon product.^[100] However, this is not feasible for SCs, where carbonization typically occurs in a molten state through pitch formation. To maintain pre-carbonization morphology in SCs, oxidation before pyrolysis is necessary to prevent further melting through cross-linking. This is observed in samples derived from mesophase pitch,^[101] or electrospun fibers from thermoplastic polymers like PVC, polyacrylonitrile, or polyethylene.^[102,103] However, carbon obtained through this route can differ significantly from direct pyrolysis, as oxidation alters the chemistry and microstructure of the precursor, sometimes resulting in behavior akin to hard carbon.^[104] Thus, achieving soft carbon with appropriate particle size (approx-

imately 1–10 μm), ensuring high specific charge, easy processability, and good power capability, while maintaining a high ICE, remains a significant challenge. This underscores the need for innovative strategies and solutions to develop soft carbons with competitive performance.

CO₂ Capture: A Novel Sustainable Route to Synthesize Carbon Nanotubes

While less relevant to charge storage than amorphous carbon, mainly due to prohibitive cost and low density, carbon nanomaterials may need to be considered as possible alternatives for SICs due to several advantages with respect to the electrochemical response. First, they offer numerous active sites for sodium ion storage in a relatively open carbon nanotube (CNT) structure. Moreover, their excellent electrical conductivity and more open pore structure facilitate efficient electron and ion transport, enabling rapid charge/discharge. Finally, CNTs can offer improved cycle life due to the ability of the open structure to accommodate the volume changes during sodium insertion and extraction, thereby reducing mechanical degradation over cycles.

On the other hand, CNTs show some technical drawbacks that hinder their use as negative electrode materials for Na storage. CNTs exhibit low to moderate initial coulombic efficiency in the range of 50–80%. However, again as is the case of amorphous carbons, the use of a presodiation agent enables one to mitigate the irreversibility of the initial cycles, and the material should not be discarded solely based on disadvantageous ICE. Another main issue of CNTs is related to processability since they tend to agglomerate by van der Waals forces, reducing the effective surface area and hindering the uniform distribution of sodium ions.

However, major concerns arise from the sustainability and scalability perspective. The production of high-quality CNTs can be prohibitively expensive and involves complex synthesis processes, making large-scale applications very challenging. Moreover, the synthesis and disposal of CNTs raise environmental and safety concerns due to potential toxicity and challenges in handling nanomaterials. For the economic

viability of CNTs, it should first be mentioned that facilities capable of producing $>100 \text{ t yr}^{-1}$ of CNTs via CVD are now functional.^[105] However, the price of CNTs remains prohibitively high, at 25–250 € t^{-1} . Obviously, CVD requires a large infrastructural investment with complicated equipment, especially on a large scale. The CVD approach requires catalysts to be mostly absent upon synthesis, which can be achieved by the acid leaching – oxidation method, however with added cost. The catalysts themselves are produced by either CVD or RF magnetron sputtering and comprise a large part of the running costs of CVD synthesis. The second largest economic impact comes from the use of large volumes of carrier gas (Ar or N₂) which cannot be recycled due to impurities.^[106]

More than anything else, however, CNT synthesis by CVD poses an enormous environmental impact. A comparison done between LCA studies of CVD synthesis technologies of CNT revealed that the CO₂ equivalent of these methods ranges from 0.48 to 200.44 kg per gram of CNT depending on the use of substrate, choice of catalyst, and carrier gas.^[106] Even considering the lowest number, which considers the use of pure N₂ as a carrier gas, something that has not been demonstrated on the industrial scale, this means that for every gram of CNTs produced 480 grams of CO₂ will be exhausted into the atmosphere. Clearly, this is not acceptable in the long term as there is an enormous need and political pressure to limit rather than increase CO₂ emissions.

Alternatively, the MSCC-ET (molten salt carbon capture and electrochemical transformation) technology bypasses this problem entirely by using, rather than emitting, CO₂ to produce CNTs. The MSCC-ET process is based on concurrent chemical and electrochemical processes, where a carbonate salt is electrochemically split into solid carbon and oxide, with the oxide then reacting with a CO₂-containing gas bubbled through the electrolyte (Figure 13).

This process allows for the efficient production of CNTs and other carbon nanomaterials, with a carbon budget analysis showing that when coupled with renewable electricity, up to 0.890–0.971 kg of CO₂ can be captured of per kg of carbon produced depending on the energy source.^[108] The MSCC-ET

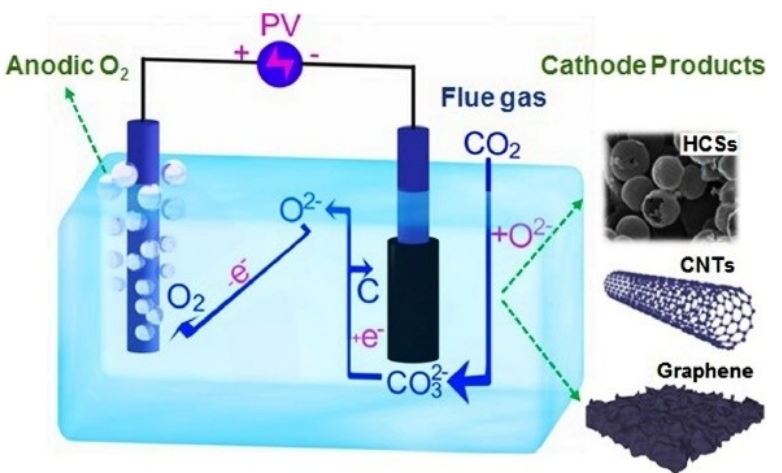


Figure 13. Schematic representation of the CO₂ electrolytic splitting process. Reproduced with permission from [107]. Copyright © Elsevier, 2019.

has shown to be a versatile method for CNT synthesis, yielding a wide variety of MWCNTs from long, straight MWCNTs^[109–111] to short, tangled webs^[112] and even carbon nanocoils.^[113] The primary descriptors for efficient MWCNT synthesis have been shown to be the presence of a catalyst (with Fe and Ni catalysts demonstrated to yield straight MWCNTs),^[112,114] an electrolyte that allows for fast transfer of oxide from the positive electrode to the negative electrode,^[115] a negative electrode with a high oxygen evolution reaction activity^[114] and the use of a pre-electrolysis step or pulsed current to increase nucleation sites for MWCNT formation.^[116] Even though the synthesis of CNTs and other carbon nanomaterials via the MSCC-ET has seen significant attention in the last decade, and many of the studies highlighting batteries as a potential field of application, studies utilizing CO₂-derived materials in batteries, especially Na-ion batteries, remain few. After the first study by Licht et al. using tangled CO₂-derived CNTs as a Na-ion battery negative electrode with a reversible capacity of 130 mAh g⁻¹, the focus has mostly been on Li-ion batteries.^[110] However, the development of a CO₂-neutral, cost-effective synthesis method for CNTs can trigger their use in SICs, either as negative electrode, as composite, or as additive.

3.1.2. Carbon Positive Electrode Materials for SICs

Apart from sustainability/scalability, performance-dictated requirements should be fulfilled for a realistic implementation of nanoscale-porous positive electrode materials in SICs. Based on the common character of electrosorption mechanisms in both SICs and traditional supercapacitors' positive electrodes, the following requirements for positive electrodes can be stipulated:

- i) Ion-adapted pore networks, high electronic conductivity, and good chemical stability within the voltage and temperature range of operation.
- ii) Surface chemical groups or carbon-lattice heteroatoms enhancing capacitance and not deteriorating electrolyte stability.
- iii) A good balance between pore volume and material density to maximize both gravimetric and volumetric energy density.
- iv) The last requirement also aligns with the above-defined economic viability and excludes the highest-SSA low-density carbons prepared under excessive low-yield activation conditions.

The performance-based considerations should go hand-in-hand with the other requisites for scalable AC synthesis elaborated above. Therefore, finding an optimum combination of technical and non-technical requirements in a single material is not straightforward. This complexity explains why few materials on the market are suitable for implementation in SICs at the production level despite the variety of proven academic approaches to porosity generation and optimization to the maximum electrochemical capacitive performance required by SICs. The following paragraphs summarize the most representative R&D strategies and assess their upscaling viability.

Activation-based strategy. Without a doubt, the most common process for the generation of porosity and increasing the specific surface area of carbons in large amounts is the carbonization/activation of different precursors. In this regard, biomass precursors such as coconut shell, fruit pits, rice husk, and many others have been explored since they are often inexpensive waste by-products matching perfectly the suitability and scalability purpose. However, less attention has been paid to other elements of activation processes such as activation agents, yield, corrosiveness, and wastewater treatment, often having a decisive impact on cost and likely canceling out the benefits of abundant renewable precursors. This gap is still to be addressed in the context of sustainability-centered technologies such as SICs to ensure the material synthesis is economically viable and does not represent a stumbling block to the value chain of technology. Below we consider the technical peculiarities of various activation processes, the performance of derived materials in SICs, and their scalability prospects. According to the activating agent used for pore generation, activation processes can be broken down into physical and chemical activation.

Physical activation involves a two-stage treatment: the carbonization of a carbon precursor in an inert atmosphere, followed by its activation with a suitable oxidizing agent (CO₂, air, and steam) to induce porosity, typically between 600 and 1250 °C. Active oxygen species first open part of closed pores by burning resin compounds, then make further micropores through partial gasification of the carbon skeleton. When air (or oxygen) is utilized as the activating agent, a highly exothermic gasification reaction makes the process energy-efficient and cost-effective due to the lower activation energy compared to using steam or CO₂, but activation is poorly controllable and goes along with excessive burn-off and a reduced yield of activated carbon. Between CO₂ and steam, the latter is more reactive and therefore can be efficiently used at lower temperatures. The maximum SSA of carbons produced via physical activation depends on various factors such as the type of precursor used and the activation conditions, attaining *ca.* 1200–1400 m² g⁻¹ as can be demonstrated, *e.g.*, with a steam activation of graphene aerogels^[117] or with a CO₂ activation of scalable biochar derived from olive pits.^[118] Overall, while physical activation is relatively cost-efficient, it does not reach the pore network tunability of chemical activation producing a developed microporosity, with a Brunauer, Emmett, and Teller (BET) SSA tunable from below 1000 up to 2500–3000 m² g⁻¹. It is also noteworthy that bibliographical research does not allow discovering literature sources on physically activated carbons applied to SICs, but neither for mature technologies such as EDLCs. This is likely due to intellectual property (IP) rights concerning the peculiarities of activation processes or the insufficiency of the pore texture for maximizing electrosorption-driven storage in SIC positive electrodes, as distinct from chemical activation being extensively documented, at least in academic literature.

Chemical activation is achieved by blending carbonaceous materials or pre-pyrolyzed non-porous amorphous carbons with chemical activating agents (KOH, ZnCl₂, H₃PO₄, etc.) and

subjecting them to pyrolysis at 500–900 °C. Those methods result in the formation of porous carbons characterized by SSAs often over 2000 m² g⁻¹ and a significant pore volume, mainly formed by micropores and narrow mesopores. There are numerous examples of porous carbons starting from different abundant bio precursors (olive pits, coconut shells, cork, wood, brewery wastes, etc.) or synthetic polymers, which are then chemically activated using KOH, NaOH, KHCO₃, etc. Recently, a cesium (Cs) salt-based new strategy^[119] has been proposed for synthesizing porous carbons with high SSAs (>3000 m² g⁻¹) and pore volume approaching 2 cm³ g⁻¹. This method allows for controllable pore size, is less corrosive, and operates at a lower temperature than the KOH activation method. Figure 14a illustrates a bottom-up preparation of porous carbons through the direct thermal treatment of cesium acetate (CsAc).^[119] Cs species efficiently promote the condensation of organics by accelerating dehydration; after Cs reduction, they donate electrons and intercalate into graphitic layers to form slit nanopores. Cs is almost completely evaporated at the final stage. N₂ sorption measurements at 77 K (Figure 14b) indicate the existence of large volumes of micropores. BET SSAs gradually increase with increasing temperature, reaching up to 2936 m² g⁻¹ at 800 °C. A porous carbon (MC800) prepared by Cs salt-assisted pyrolysis,^[120] demonstrated higher capacity than conventional activated carbon (YP 50 F) as SIC positive

electrode material (Figure 14c). These studies underscore the importance of developing simple, mild, and efficient synthesis/activation methods to produce highly porous carbons with enhanced SSA and charge storage capacity.

Some representative examples and the most significant specifications of successful conversion of biomass into activated carbons for SICs can be exemplified (Table 1) with olive pits (produced at 1 million tons worldwide yearly),^[123] garlic,^[124] and cork biowastes,^[125] with the performance of the maximum energy of materials in a full cell up to 125 Wh kg⁻¹ (Table 2) and a good capacity/capacitance retention at the high current rate (Figure 15). Additional surface treatments (e.g., plasma NH₃^[126]) can enhance carbon performance through surface redox reactions, but the energy gain must be evaluated in the context of the associated manufacturing implications. Biomass revalorization can be additionally highlighted by the fact that both negative electrodes and positive electrodes can be derived from the same precursor, making the whole process simpler, more affordable, and scalable.

Although none of these studies contain specific information about process performance, precursors availability, cost, etc, most of them are based on biowaste precursors, which are susceptible to upscaling under similar conditions to those synthesized, for instance, by Kuraray, whose carbons are also obtained from lignocellulosic coconut shell wastes.

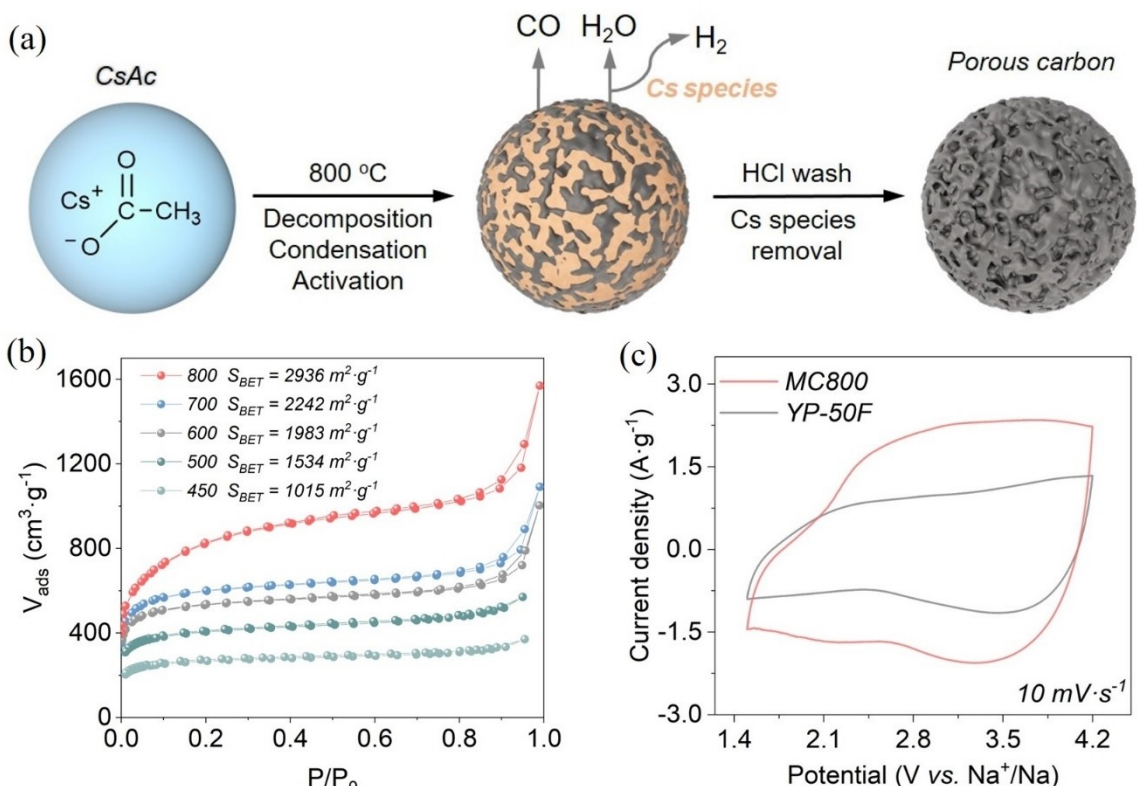


Figure 14. (a) Schematic illustration of porous carbon formation during pyrolysis of cesium acetate (CsAc). (b) N₂ adsorption/desorption isotherms at 77 K with Brunauer-Emmett-Teller (BET) specific surface areas. (c) Cyclic voltammetry (CV) of SIC full cell at a scan rate of 10 mV·s⁻¹, using 1 M sodium hexafluorophosphate (NaPF₆) in vinyl carbonate: dimethyl carbonate (50:50 vol%) with 5 wt% fluoroethylene carbonate as electrolyte. Porous carbon (MC800) prepared from pyrolysis of Cs salt serves as the positive electrode and metal Na serves as the negative electrode. The larger CV area suggests improved capacity when using as prepared porous carbon (MC800) than conventional activated YP-50 F carbon. Reproduced with permission from ref [121,122]. Copyright © Wiley-VCH GmbH, 2023, 2024.

Table 1. Representative examples of activated and template-based carbons and their electrochemical performance in SiC positive electrodes and derived full cells.

Bio-waste derived synthesis	Activation method	Positive electrode: capacity, current density, potential range	Electrochemical performance SiC// Coupled negative electrode	Reference
Olive pits/carbonization @ 800 °C	KOH activation @700 °C 1:6 ratio alkali:precursor	65 mAh g ⁻¹ , 2 A g ⁻¹ , 2 V	70 Wh kg ⁻¹ @ 2 kW/kg ⁻¹ // Olive-pit derived hard carbon	[123]
Garlic/soaking with KOH solution	KOH activation @900 °C (2 M KOH impregnation)	80 mAh g ⁻¹ , 2 A g ⁻¹ , 2.8 V	100 Wh kg ⁻¹ @ 2 kW/kg ⁻¹ // Garlic derived carbon	[124]
Cork biowastes pre-carbonized @ 600°C	KOH/NaOH (1:1) mixture the 3:1 ratio mixture:precursor	92 mAh g ⁻¹ , 2 A g ⁻¹ , 2.2 V	125 Wh kg ⁻¹ @ 2–5 kW/kg ⁻¹ // S-doped cork derived hard carbon	[125]
Bambu carbonization @900°C	CO ₂ activation/NH ₃ Plasma	30 mAh g ⁻¹ , 2 A g ⁻¹ , 2 V	125 Wh kg ⁻¹ @ 2–5 kW/kg ⁻¹ // Bamboo derived hard carbon	[126]
Polypprole	KHCO ₃ KHCO ₃ /PPy 1:6 ratio salt:precursor	80 mAh g ⁻¹ , 5 A g ⁻¹ , 2 V	100 Wh kg ⁻¹ @5 kW/kg ⁻¹ // Carbonized polypprole	[127]
Template-based synthesis	Precursor/treatment	Positive electrode: capacity, current density, potential range	Electrochemical performance SiC// Coupled negative electrode	
KIT-6 silica powder hard template	furfuryl alcohol impregnation/pyrolysis	30 mAh g ⁻¹ 1 A g ⁻¹ 1.3 V	25 Wh kg ⁻¹ @ 2 kW/kg ⁻¹ // Na ₃ V ₂ (PO ₄) ₃	[128]
SBA-15 silica hard template	Pyrolysis @750 °C	~50 mAh g ⁻¹ 2.5 A g ⁻¹ ~1.5 V	50 Wh kg ⁻¹ @2 kW/kg ⁻¹ // reduced graphene oxide	[129]
NaY zeolite hard template	furfuryl alcohol impregnation, acetonitrile CVD, pyrolysis @750 °C	90 mAh g ⁻¹ 2 A g ⁻¹ 1.3 V	Zn _{0.25} V ₂ O ₅ .nH ₂ O 65 Wh kg ⁻¹ @2 kW/kg ⁻¹ // ordered microporous carbon	[130]
ZnCl ₂ Salt template	Sucrose/salt-assisted pyrolysis	40 mAh g ⁻¹ 2 A g ⁻¹ 1.3 V	55 Wh kg ⁻¹ @2 kW/kg ⁻¹ // Microporous nitrogen-rich carbon fibers	[131]
KCl Salt template	Gluconic acid/K ₂ CO ₃ activation	ca. 65 mAh g ⁻¹ 2 A g ⁻¹ 2.2 V	100 Wh kg ⁻¹ @ 2 kW/kg ⁻¹ // Sodium carbonate d-(+)-Gluconic acid δ-lactone derived hard carbon	[132]
ZIF-8 (a Zn-containing zeolitic imidazolate metal-organic framework	pyrolysis @750 °C/acid washing	ca. 121 mAh g ⁻¹ 2 A g ⁻¹ 2.5 V	125 Wh kg ⁻¹ @ 2 kW/kg ⁻¹ // TiO ₂ /Carbon Nanocomposites	[133]

Table 2. Electrolytes employed in lab-scale SICs. The viscosity and conductivity values were measured at RT (20 or 25 °C). The used abbreviations are NaTFSI = sodium bis(trifluoromethanesulfonyl)imide, NaFSI = sodium bis(fluorosulfonyl)imide, EC = ethylene carbonate, PC = propylene carbonate, DEC = diethylcarbonate, DMC = dimethylcarbonate, GPE = gel polymer electrolyte, EMC = ethylmethylcarbonate, TEG = tetraethoxyethane, C₃mpyrFSI = N-propyl-N-methyl pyrrolidinium bis(fluorosulfonyl) imide, FEC = fluoroethylenecarbonate.

SALT	SOLVENTS	ADD.	REF. FOR SIC APPLICATION	η [mPa s]	σ [mS cm ⁻¹]
ORGANIC SOLVENTS	NaPF ₆	EC:PC	[123,157]	6.69 ^[158]	7.39 ^[158]
		EC:DEC	[8,159,160]		5 ^[161]
		EC:DMC	[162]		6 ^[161]
		Diglyme	[163–165]		
		GPE	[166]		
	NaClO ₄	PC	[167]	6.9 ^[168]	6.3 ^[168]
		EC:PC	[169]	5.2 ^[168]	8.1 ^[168]
		EC:PC	[170,171]		
		EC:DMC	[172,173]	10.1 ^[168]	2.3 ^[168]
		EC:DMC	[174,175]		
INORGANIC SOLVENTS	NaTFSI	EC:DEC	[176–180]	2.9 ^[168]	6.1 ^[168]
		EC:DEC	[124,181]		
		DMC:PC	[182]		
		EC:EMC:DMC	[183]		
		GPE	[184]		
	NaFSI	TEG:PC	[185]	8.7 ^[185]	3.1 ^[185]
		C ₃ mpyrFSI	[186]		
		Na ₂ SO ₄	H ₂ O	[187]	1.27 ^[188]
					80 ^[189]

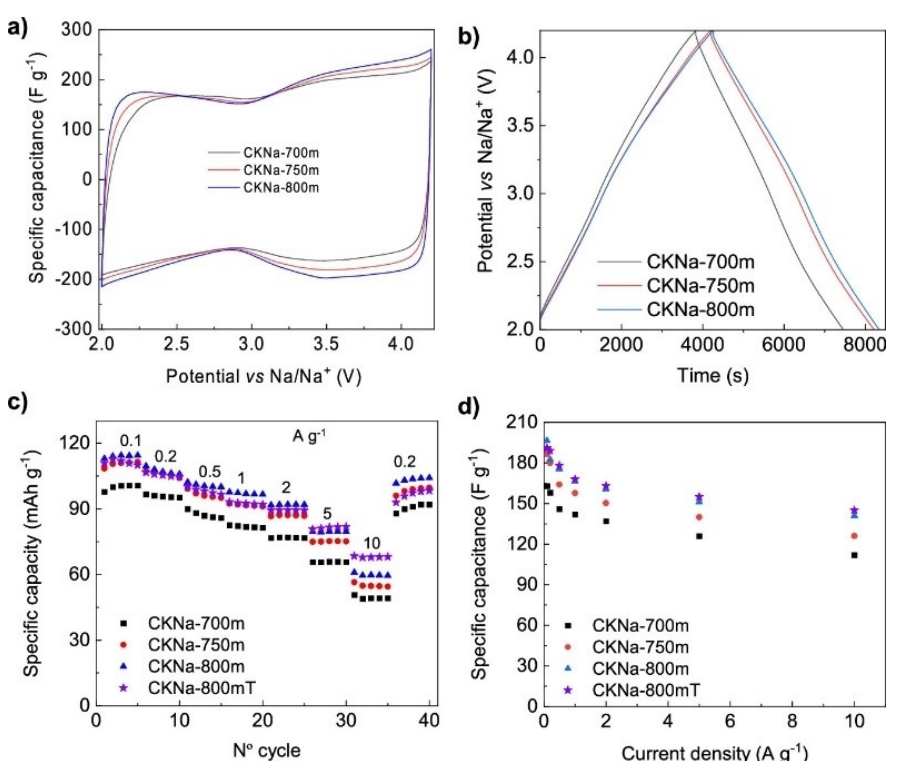


Figure 15. Electrochemical performance of indicated porous carbons depending on the synthesis temperature. Reproduced from [125] under the CC BY 4.0 license. Copyright © American Chemical Society, 2023.

Alternative to bio-waste-derived carbons, carbons from synthetic polymers can offer better control over particle

morphology and sizes, which could benefit pore accessibility for the electrolyte, thus enhancing power capability. Thus, Diez

et al. reported the preparation of performing high specific surface area carbon as positive electrode for SICs starting from the polypyrrole synthetic precursor and yielding carbon nanospheres with a narrow particle size distribution centered at 92 nm, a large specific surface area of $2970 \text{ m}^2 \text{ g}^{-1}$ and appropriate pore size distribution within 1–2 nm, finally resulting in a high-performance SIC (Figure 16).^[127] However, despite enabling a design on demand of carbon structures, the use of synthetic polymers as precursors increases the total cost of the final carbon, hindering its market entry.

Overall, chemical activation offers several advantages, including lower activation temperatures, higher carbon yields, reduced activation time, and increased specific surface areas and pore volumes. However, it also features important drawbacks: i) the corrosive nature of chemical activation agents; ii) the need for additional washing and wastewater generation; and iii) the cost associated with large amounts of reagents.

Even though activation methods can have a potential for upscaling in terms of precursors and process flow (the latter applies to physical activation), the limited control over the properties of resultant porous carbons does not allow for maximizing the electrochemical storage in SIC positive electrodes. It is therefore pertinent to explore electrolyte-optimized porous carbons enabling maximum performance, even though their synthesis methods cannot yet be considered cost-efficient, at least in the current state of development, but can have an opportunity in the future, as demonstrated below with the templating strategy.

Template-based strategy. The templating approach is one of the most advanced methods for preparing porous carbons with well-defined pore structures and narrow pore size

distributions. It can be divided into hard templating and soft templating, depending on the porogen being a solid/rigid structure or a labile compound. This approach can tune the pore size from micropores to macropores but is most often suitable to tailor mesopores (2 to 50 nm). While there is a plethora of carbons synthesized from hard templates, mainly using silica structures, few have been specifically investigated in SICs (Table 1), for instance, ordered mesoporous carbons with a pore size between 4 and 5 nm and BET specific surface areas of around $1000 \text{ m}^2 \text{ g}^{-1}$,^[128,129] as well as microporous carbons with a BET SSA of around $2700 \text{ m}^2 \text{ g}^{-1}$ outperforming the standard YP-50 F carbon (Figure 17).^[130]

An alternative and more straightforward approach to obtaining nanoporous carbons with a high SSA suitable as capacitive electrodes involves salts as the template agent. This strategy does not yield carbons with an ordered and narrow pore size distribution within the structure, but in contrast, salts can be easily leached out, being advantageous in terms of simplicity and scalability.^[134] Salt-templated carbons with an SSA of up to ca. $2300 \text{ m}^2 \text{ g}^{-1}$ can be prepared by this method and show a comparable^[131] or even far superior performance^[132] to other template synthesis methods (see Table 2 for details).

Finally, another approach consists of the pyrolysis of nanoporous materials such as covalent organic frameworks or metal-organic frameworks which exhibit well-defined pore structures, giving one of the best energy and power performances, exceeding 100 Wh kg^{-1} at 5 kW kg^{-1} .^[133]

To summarize, the most important highlights from template-based developments can be drawn up as follows:

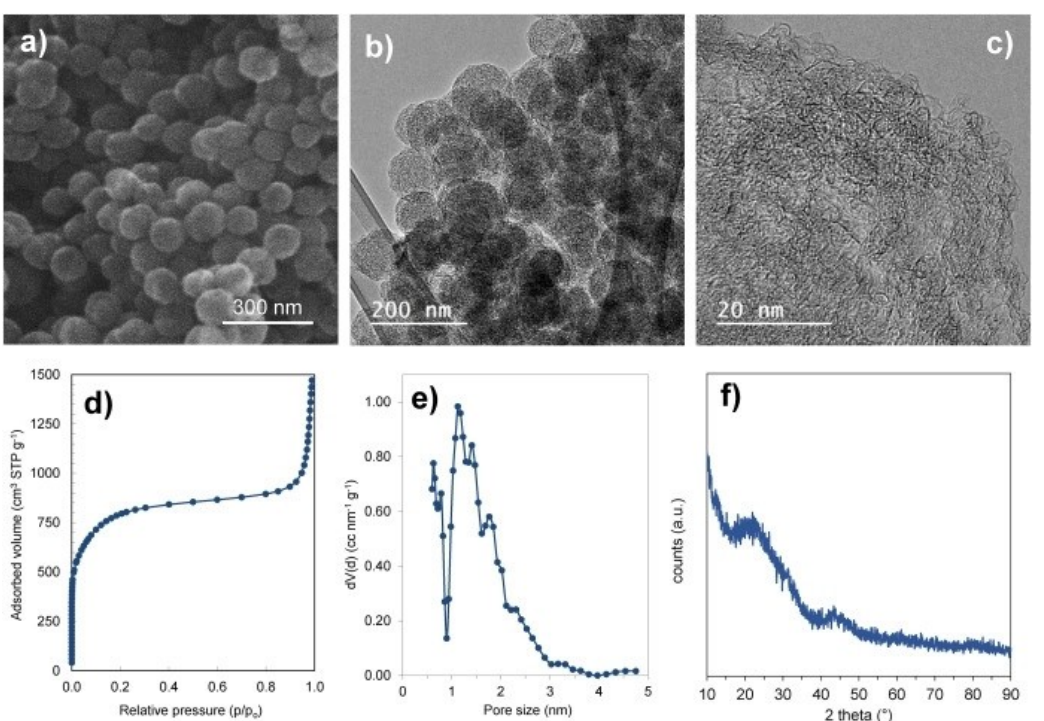


Figure 16. Reproduced from [127] with permission. Copyright © Elsevier, 2023

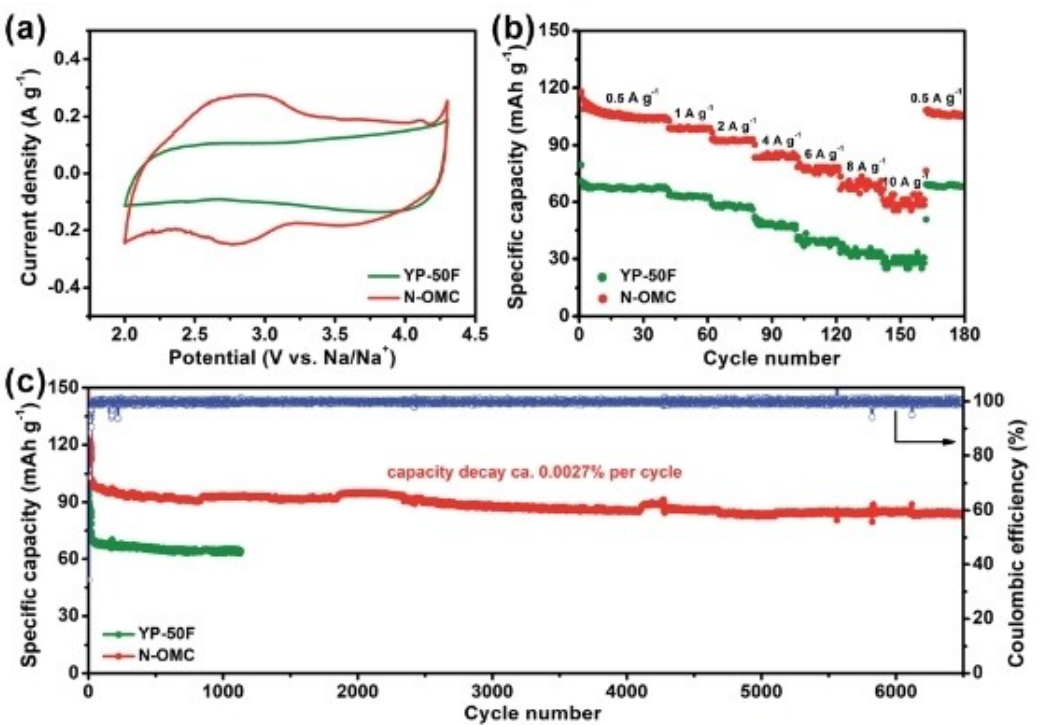


Figure 17. (a) CV curves of N-OMC and YP-50 F at a scan rate of 1.0 mV s^{-1} . (b) Rate capability of N-OMC and YP-50 F. (c) Cycling stability of N-OMC and YP-50 F at a current density of 1.0 A g^{-1} . Reproduced from [130] with permission from The Royal Society of Chemistry.

- i) Ordered porous templated carbons are characterized by low pore tortuosity, thus enhancing electrolyte transport and the rate/power response for a large variety of electrolytes;
- ii) Most studies on templated-based approaches do not supply volume-normalized performance metrics. However, template-derived carbons usually have an above-average pore volume and, therefore, a limited material density, which is a disadvantage for volumetric energy storage. Using templates requires complex multistep synthetic routes toward porous carbons, thus adding to the production cost and limiting viability for large-scale production.

Unfortunately, the existing scientific literature does not focus on the cost-benefit analysis of using template carbons, especially for emerging cost-rationalized technologies such as SICs.

Outlook of synthesis methods: scalability vs. performance in SICs. In summary, there are different approaches to the preparation of carbon materials from non-critical raw materials with optimum textural and chemical features. All of them show capacity values within the range that varies from $60\text{--}120 \text{ mAh g}^{-1}$ depending on the applied current density and the potential range, with the lower limit related to the higher rates. When combined with a negative carbon electrode, the best examples of full cells reach specific energy values of slightly above 100 Wh per kg of active material at a power density of 5 kW kg^{-1} .

Finally, practical industrial interest will be driven by cost, which is a sum of factors such as precursor availability, processing steps, yields, etc. As mentioned above, the best

performance-adapted properties are provided using chemical activation, but its industrial feasibility is hindered by sustainability and cost issues, especially in environmentally savvy jurisdictions. Mixed chemical /physical activation methods may be a viable trade-off between cost/sustainability and performance. Concerning already marketed materials, the best choice for the large-scale production of SICs can be AC previously developed for capacitive ion storage in EDLCs such as YP-50 F from Kuraray Co., Ltd, which offers the optimum cost /performance market-proven trade-off.

3.2. Binders

The binder is a minor electrode component that has, however, a major impact on the properties of the whole electrochemical device. While such inert polymer does not (typically) participate in the charge storage processes occurring at the electrodes and only accounts for a few wt% of the overall electrode mass, it can largely impact the energy, power, and cycle life of an SIC. Not less importantly, though, it does determine the solvent used for electrode manufacturing – and eventually recycling – thus, largely impacting the cost and sustainability of the overall process.

Binder requirements and state-of-the-art fluoropolymers

The polymeric binder should possess properties that favor both the production process and enable exceptional electro-

chemical performance as well. Just to name a few, the binder should, ideally:

- i) Provide homogeneous and stable slurries with appropriate viscosity to enable uniform coating on current collectors;
- ii) Allow fast electrode drying at reasonably low temperature without degrading;
- iii) Provide mechanical stability and flexibility to the electrode, with strong adhesion to the current collector (no easy delamination) and cohesion of the active material particles;
- iv) Be electrochemically stable and should not negatively interfere with the charge storage processes (e.g. by blocking pores, reducing electronic and ionic conductivity, etc.).^[135]

The current SoA binders for SIC do not differ substantially from those employed already in LIB, SIB, or EDLC electrodes.^[136–138] These are thermoplastic fluoropolymers such as polyvinylidene fluoride (PVDF) and polytetrafluoroethylene (PTFE) which, although they fulfill the above-mentioned requirements, present some environmental challenges. PVDF requires N-Methyl-2-pyrrolidone (NMP) for slurry preparation, a teratogenic and irritating organic solvent that must be handled under controlled conditions. PVDF itself is also mutagenic and teratogenic. On the other hand, PTFE could be dry-processed, promising substantial advantages. Nevertheless, being both PFAS (Per- and Polyfluorinated Substances), the use of such substances should preferentially be avoided in the future to enhance the sustainability of SIC.^[139]

Transition to aqueous processable fluorine-free binders

Replacing conventional fluoropolymers with F-free binders that can be processed in water offers the opportunity to substantially reduce the environmental impact of SIC by influencing multiple aspects:

Safety and costs. Water is a largely available and harmless solvent. As a result, the electrode manufacturing process is substantially simplified. In fact, the complex (condensation/distillation) solvent recovery system required to avoid dispersion of NMP in the environment is no longer needed in the case of water-based slurries (see Figure 18a). This naturally leads to reduced costs, both in terms of initial investments as well as maintenance.^[136]

CO₂ footprint. Electrode manufacturing is a very energy-intensive process. For example, during the production of lithium-ion batteries, the energy consumed upon drying the electrodes and recovering the solvent can account for about 50% of the total battery manufacturing process.^[140] To reduce the CO₂ footprint of overall production, less energy-hungry and more sustainable processes are needed. Water dries much faster compared to NMP, thus allowing for reduced drying time/temperature. Less energy means also lower costs.

Sustainability. The most common water-soluble binders belong to the family of polysaccharides and are natural products, or their derivatives (e.g., carboxymethyl cellulose, CMC). Therefore, contrary to synthetic fluorinated polyolefines, these can be obtained from renewable sources and will help reduce the dependency on oil-derived products. Once again,

costs can be potentially cut as well. The market price of cellulose derivatives is, on average, half that of PVDF.

Recyclability. Fluoropolymers are difficult to dispose of at the end of the device's life and largely complicate the recycling process. Binder removal occurs either via thermal decomposition at 400–600 °C or using solvents.^[139] While the latter approach is less energy-intensive, it requires the appropriate solvent. In the case of PVDF, the choice is restricted once again to harmful organic compounds such as NMP, N,N-dimethylformamide (DMF), N,N-dimethylacetamide (DMAc), dimethyl sulfoxide (DMSO), etc.^[141] Deposition of electrodes fabricated with F-free water-soluble binders could be simply performed in water, without any further environmental concern related to the treatment and disposal of the residual wastewater.

Green binders for SIC

Detailed studies on binders for SIC are very scarce compared to those focusing on active materials. Nevertheless, abundant literature is available on sustainable binders for their "parental" devices, i.e. SIB and EDLCs.^[136–138,142] We do not aim here to provide a comprehensive technical review (which can be found elsewhere), but rather to summarize the main classes of polymeric binders (see also Figure 18b) and analyze the specific aspects that are relevant for their application in SIC.

Classes of F-free binders for SIC. As already mentioned in the previous section, the most employed aqueous binder is CMC, a bio-derived polymer obtained from a simple chemical treatment (alkalization and etherification) of natural cellulose. Further examples from the family of natural polysaccharides are Alginate, Starch, Xanthan and Guar Gum. Among the synthetic polymers, polyacrylic acid (PAA) and sodium-polyacrylate (Na-PAA) are the most popular choices, but reports on polyvinyl alcohol (PVA) and polyvinyl butyral (PVB) can be also found.^[136] While all these polymers can be processed in an aqueous environment, each one has its peculiar features that may affect the choice of the right binder for a negative or positive electrode.

Binders for SIC negative electrodes. Hard Carbon (HC) is the SoA negative electrode material in both SIB and SIC. It was extensively proven that CMC can largely overperform PVDF as a binder in HC-based negative electrodes. Firstly, because CMC is not affected by defluorination which results in the formation of NaF and loss of electrode integrity.^[143] Additionally, owing to its capability to form a thin coating layer on the HC particles, CMC reduces the amount of electrolyte consumed to form the SEI.^[144] For both these reasons, CMC enables enhanced coulombic efficiency and capacity retention compared to PVDF. When further active materials are introduced in the negative electrode, such as alloying compounds (e.g., Sn,Sb) that undergo large volume changes during cycling, the reduced flexibility of CMC becomes limiting. In such cases, polymers like PAA are preferred.^[144] CMC is a linear polymer with abundant -OH groups that can form intra-molecular H-bonds, resulting in higher rigidity. On the contrary, PAA and alginate possess carboxylic moieties that can effectively graft on the surface of both the active material particles and the Al current collector, thus conferring improved mechanical stability and adhesion.

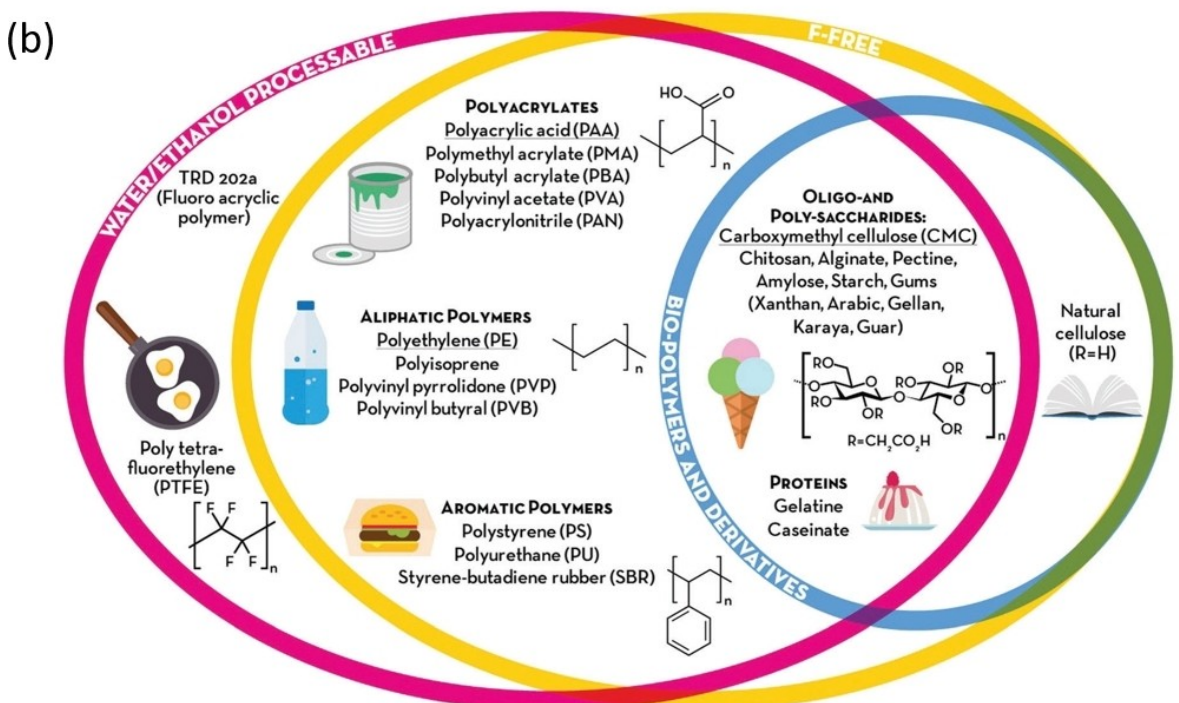
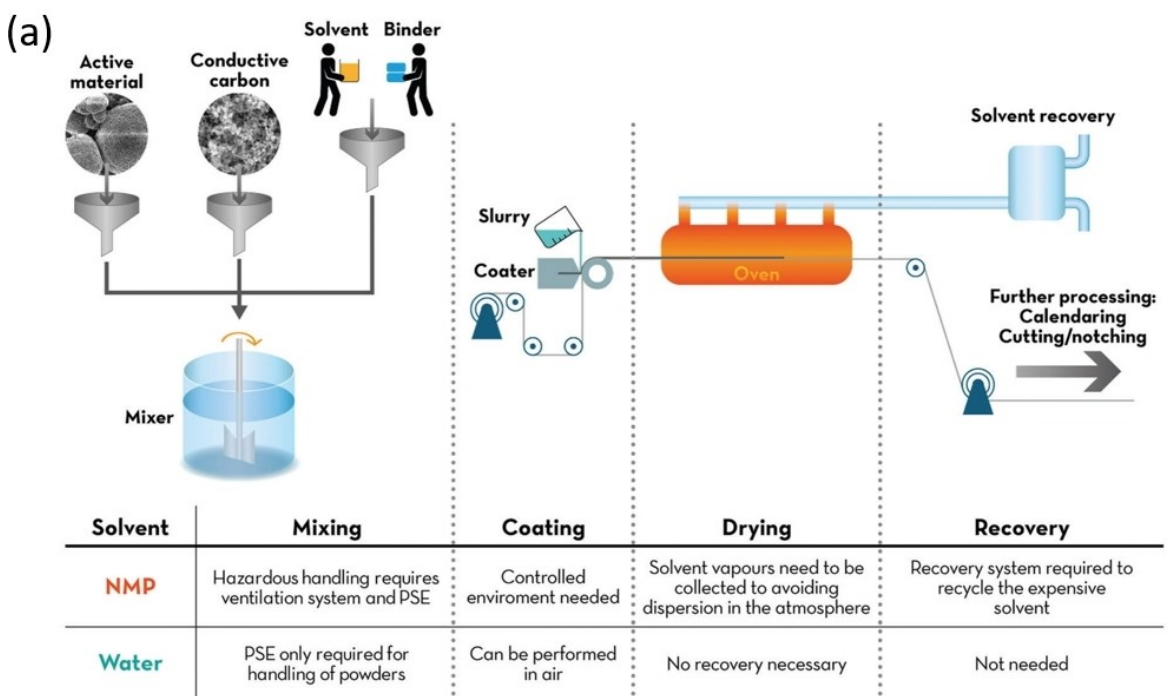


Figure 18. (a) Simplified schematic description of a generic battery/EDLC electrode manufacturing process. From left to right, the main advantages of water over NMP are highlighted for each step, from the initial mixing of the slurry, its coating on the current collector, the drying of the electrode layer, and, finally, the solvent recovery. (b) Overview of different classes of binders. The polymers are divided into three main categories according to their processability (water and/or ethanol processable), chemical composition (F-free), and natural availability (bio-polymers and derivatives). Reproduced from ref. [136] with permission from the Royal Society of Chemistry.

Interestingly, further synergistic effects can be unlocked by mixing the above-mentioned binders. In fact, CMC-Alg and CMC-PAA were found to give rise to an extended cross-linked 3D binder network thanks to the condensation reaction

(esterification) between the -OH groups of CMC and the carboxyl units of Alg/PAA.^[145] Such a matrix could help accommodate the volume changes of alloying materials and mitigate the mechanical stress generated by it.

Binders for SIC positive electrodes. Binder requirements differ substantially for the capacitive positive electrode. Here the charge storage occurs typically on high surface area carbons, such as activated carbon (AC). While in the negative electrode, it is considered beneficial to have large material coverage to modulate SEI formation, here any type of pore-clogging by the binder should be avoided in order not to affect the electrode capacitance. PAA and PVA were found to be particularly prone to infiltrate into the electrode porosity, thus reducing pore volume and available surface area.^[146,147] To avoid excessive pore clogging, the hydrophilic/hydrophobic character of both binder and AC should be carefully considered. For hydrophobic AC, hydrophilic binders such as CMC, PVP, etc. should be preferred. Conversely, hydrophobic resins such as PVB may better avoid excessive binder spreading in the pores of hydrophilic AC.^[148]

A further challenge to overcome in the positive electrode is the difficulty of achieving high active material areal loading. This aspect is often overlooked but is extremely important, in general, to increase the active material/current collector mass ratio, consequently improving the specific energy of the device. Furthermore, in SIC, this is needed to balance the larger capacity of the HC negative electrode compared to the AC positive electrode. The poor flexibility of CMC-based electrodes typically limits the maximum electrode loading achievable without losing mechanical integrity. To overcome this issue, the addition of rubberizing agents (e.g. SBR, styrene-butadiene rubber) or highly branched polysaccharides (such as starch or xanthan/guar gum) is necessary to avoid excessive shrinking and cracking of the layer upon drying.^[135,149]

Last, but not least, aqueous processing can severely complicate the inclusion of sacrificial compounds in the positive electrode. These are fundamental in SIC for the presodiation of the negative electrode without depleting the electrolyte. Unfortunately, most of the Na-based compounds proposed so far are highly reactive/soluble in water (e.g., NaNO_3 , $\text{Na}_2\text{C}_x\text{O}_y$, NaN_3 , etc.).^[150] Substantial efforts will be required in the future to identify alternative presodiation additives and stabilize them in aqueous slurry.

3.3. Electrolytes

The industrial productions of lithium- and sodium-based technologies do not differ too much from each other (drop in technology), minimizing the industrialization costs since both elements share similar characteristics (alkaline elements).^[151] The electrolyte production is no exception: only different alkaline starting components and production parameters need to be considered. Analogous to the lithium-ion technology, organic electrolytes composed of a sodium salt (mostly NaPF_6), linear carbonates, cyclic carbonates, and additives are used in sodium-ion technologies. Since the current backbone of the electrolyte (carbonate solvent components) does not differ from lithium technologies, the electrolyte costs will be determined by the price of the primary components (salt and additives).

Owing to lower costs of extraction and production of sodium components, it is expected that the production of sodium-containing electrolytes should be lower compared to the cost of lithium electrolytes (242 € T^{-1} for Na_2CO_3 ,^[152] 14000 € T^{-1} for Li_2CO_3 ^[153]). Despite the lower prices of sodium raw materials, the demand for sodium-ion technologies is negligible compared to lithium-ion due to the earlier development and commercialization stage. Therefore, the prices for sodium-containing electrolytes are around two times higher compared to lithium-containing electrolytes.^[154] The electrolyte accounts for around 12–15% of the total price of the sodium-ion cell production. This value is almost double the electrolyte's cost in lithium-ion technologies. It is expected that with an increasing demand for sodium-ion technologies, the costs for sodium-containing electrolytes could drop to similar prices as for lithium electrolytes. A more sustainable and environmentally friendly sodium production can be achieved compared to lithium electrolyte production. Due to the abundance of sodium in the crust of the earth, less sensitive geopolitical deposits, and an easier extraction process with a lower environmental footprint, the development of a stable raw material chain value production is very realistic.

Another important factor that needs to be considered with increasing sodium-technology demand is electrolyte recycling. The recycling process for electrolyte recovery is expected to be less complicated compared to lithium-ion technologies which should help reuse different electrolyte components in further production. Environmental and sustainable aspects of sodium-ion electrolyte production need to be improved in the coming years with continued research and development efforts to realize the up-scaling of SIC electrolytes.

Finally, moving past carbonate components, innovative solvents (e.g. ionic liquids) will increase the electrolyte production costs, due to the higher cost involved in the production of these components. Furthermore, the related new electrolyte production parameters will become a challenging consideration, thus, they are still far from being considered a widespread solution.

After the overview of the industrialization status and perspectives of SIC electrolytes, the scientific requirements for them and the state of research in terms of components and analytical tools will be discussed.

Electrolyte Design Requirements

Electrolytes for SICs must fulfill a variety of different requirements (Figure 19). As for all electrochemical energy storage devices (EES) the electrolyte should display a large electrochemical stability window and high thermal stability. Also, it must be as economically affordable and safe as possible. Furthermore, as discussed above, the sustainability of the production process plays a very important role in its upscaling.

Due to the electrode combination present in SICs, three aspects are especially important for the electrolyte design:

- i) High ionic conductivity. SICs are high-power devices and are therefore charged/discharged in a fast way.^[155] To guarantee high performance and effective cycling under

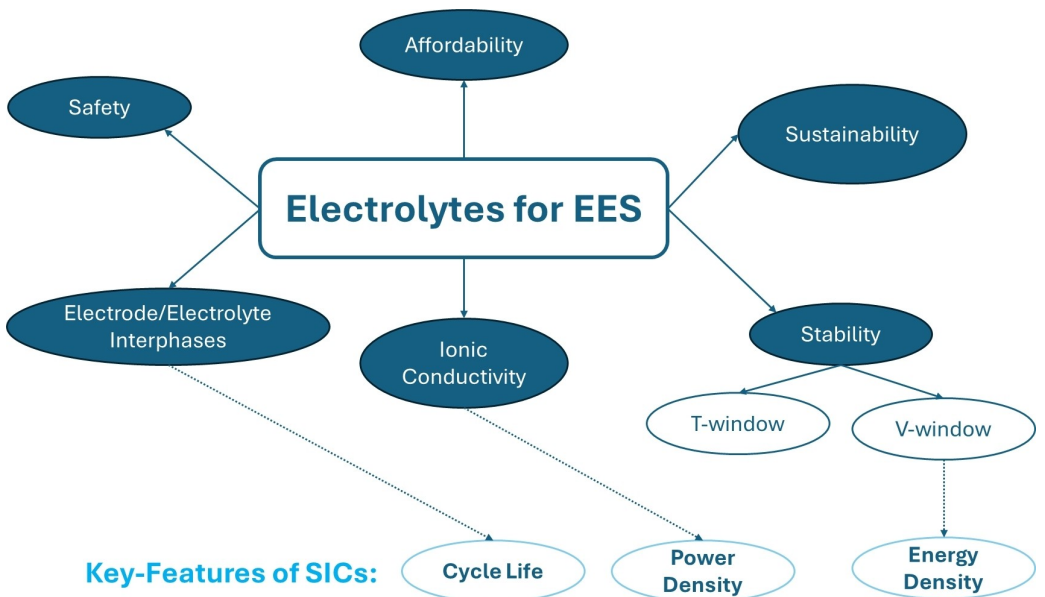


Figure 19. Overview of electrolytes features relevant for EES application. Especially highlighted are the attributes which directly contribute to the key features of SICs. High ionic conductivity, stable electrode/electrolyte interphases, and a large ESW facilitate high power density, high cycle life, and high energy density.

the demanded high current densities, high ionic mobility within the electrolyte is needed.

- ii) Large electrochemical stability window (ESW). To achieve high energy densities, the realization of high-voltage devices is required.^[155] Thus, the electrolyte needs to display a large ESW.
- iii) Ability to stabilize electrode/electrolyte interphases. SICs normally consist of a battery-type negative electrode and a capacitive positive electrode. To realize the key feature of high cycle life for SICs, both electrode/electrolyte interphases need to be stable.^[156] For the negative electrode, the formation of SEI is thus necessary. On the positive electrode side, high potential degradation mechanisms, such as anodic dissolution of the Al current collector, should be prevented by the electrolyte.

The features of an electrolyte are naturally determined by its composition. As mentioned before, electrolytes normally consist of three components: the conducting salt, the solvents and (optionally) additives. The most common electrolyte configurations for SICs in lab-scale research are listed below (Table 2) and discussed afterward.

Solvents

Electrolytes for SICs can be categorized into the most commonly used: organic, aqueous (Aq.) and ionic liquid (IL).^[190] Among them, the most utilized are organic electrolytes. As in SIBs, the electrolyte typically contains a cyclic carbonate (e.g. propylene carbonate PC) combined with a linear carbonate (e.g. dimethyl carbonate DMC). With this combination it is possible to realize a compromise between high conductivity and low viscosity. Most used in SIC systems is a mixture of ethylene carbonate (EC) and diethyl carbonate (DEC) (cf. Table 2).

Ponrouch et al. investigated how the choice of solvents influences different electrolyte properties.^[168] Figure 20a displays the electrochemical and thermal stability window of NaClO₄ electrolytes with varying solvents. Within the investigated electrolyte matrix, the broadest stability windows (~5 V and ~300 °C) are obtained for NaClO₄ in PC and NaClO₄ in EC:PC. Figure 20b shows how those NaClO₄ electrolytes perform in a hard carbon half-cell. The highest capacity retention is obtained for NaClO₄ in EC:PC.

Park et al. investigated the effect of carbonate-based (EC: DEC (1:1 by volume), EC:PC (1:1 by volume) and PC) and ether-based (DME, DEGDME, and TEGDME) electrolytes on the electrochemical performance of SICs with a negative activated carbon electrode and a positive Na₃V₂(PO₄)₃.^[191] The dissociation behavior of NaClO₄ in different solvents was investigated using Attenuated Total Reflectance-Fourier Transform Infrared (ATR-FTIR) spectroscopy, to understand the influence of the dielectric constant of the solvents on the number of free ions in the respective electrolytes (Figure 21i). The spectra were resolved by assigning a peak at 623 cm⁻¹ to the dissociated ClO₄⁻ anion and 635 cm⁻¹ to the contact ion pairs of ClO₄⁻ anions. NaClO₄ in EC:PC due to its high dielectric constant exhibited the highest degree of dissociation and a large number of free ions, resulting in its high specific capacitance. Whereas the DME-based electrolyte exhibited a low degree of dissociation. In conclusion, the carbonate-based electrolytes are reported to exhibit better cycling performance in SIC.^[191]

Organic electrolytes have also been used for the realization of gel polymer electrolytes (GPEs). Implementing GPEs leads to quasi-solid-state SICs which naturally enhances the safety of the systems. Furthermore, GPEs display high ionic conductivity and high mechanical stability.^[192]

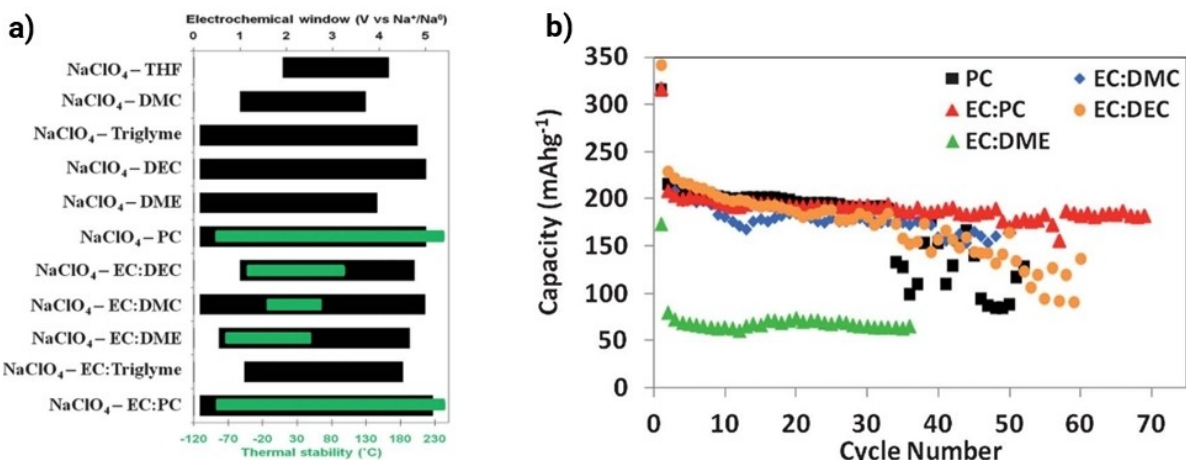


Figure 20. Influences of solvents on electrolyte properties. *a)* Electrochemical potential window stability (black bars and upper y-axis) and thermal range (green bars and lower y-axis) values of electrolytes based on 1 M NaClO₄ dissolved in various solvents and solvent mixtures. *b)* Discharge capacity (at C/20) of hard carbon electrodes using 1 M NaClO₄ in various solvent mixtures versus cycle number for the corresponding cells. Reproduced from [168] with permission from the Royal Society of Chemistry.

Table 2 also indicates the less used electrolyte configurations, namely aqueous and ionic liquids. Aqueous electrolytes are very sustainable, very safe, and show high conductivity values. However, their application is limited since their narrow ESW leads to low energy density values. ILs display rather high viscosity and low conductivity values but due to their non-volatility and non-flammability also enhance the safety of the device.^[193]

Salts

The most used salt in SIC lab-scale research is sodium perchlorate (NaClO₄). Its broad use is due to its good performance, affordability, and historical reasons.^[145] However, a large-scale application of any kind is unrealistic as the dry salt is highly explosive and thus, entails vast safety risks.^[49] An alternative is sodium hexafluorophosphate (NaPF₆). This salt is very common in the SIB field and can also be considered the emerging standard for SICs.^[194,50] Its usage allows for good performance, but a critical point of discussion is its high fluorine content. Fluorine-containing salts normally entail the danger of forming Lewis acids. E.g. LiPF₆ is known to form PF₅, LiF, and possibly HF which can all catalyze parasitic side reactions.^[195] However, NaPF₆ is thermally more stable and thus does not form Lewis acids under the same conditions as its lithium equivalent.^[194] Furthermore, fluorine is often considered necessary to form a stable SEI layer.^[196,197] Nevertheless, salts containing less weight percentage fluorine are being investigated. Examples thereof are imide-based salts like sodium bis(trifluoromethanesulfonyl)imide (NaTFSI) or sodium bis(fluorosulfonyl)imide (NaFSI). Ponroux et al. demonstrated the different electrochemical stability windows for electrolytes containing the same solvent (PC) and different sodium salts (Figure 22a). The imide-based electrolyte NaTFSI in PC shows the narrowest ESW due to the occurrence of anodic dissolution.^[168] Additives like e.g. FEC or in this case, NaPF₆

enable the formation of a passivation layer on the aluminum surface and thus, enlarge the potential window.

Dahbi et al. showed that the use of different salts in PC-based electrolytes significantly influences the electrochemical performance of hard carbon electrodes.^[198] Figure 22b displays stable cycling for NaPF₆ in PC and NaTFSI in PC whereas the NaClO₄ in PC system already lost 50% of its initial capacity after 50 cycles.

Additives

As already mentioned, the electrolyte's film-forming ability is of utmost importance for SIC application. On the one hand, a stable SEI should be formed on the negative (battery type) electrode to ensure high cycle life. On the other hand, a passivation layer on the positive (capacitive) electrode ought to be formed, as well. Since (aluminum) current collector corrosion is a known issue, a passivation layer is needed to inhibit the anodic dissolution and realize a larger operating voltage window which leads to higher energy density values. The most common additive is fluoroethylene carbonate (FEC) (cf. Table 2). In comparison to various additives that work well for negative electrodes in lithium systems, FEC is by far the most promising one for sodium-based devices.^[199]

As an example of the paramount influence additives can have on the stability of a system, Komaba et al.'s results are shown^[199] (Figure 23). In this study, hard carbon half-cells were cycled with NaClO₄ in PC with and without different concentrations of FEC. It is evident that the addition of FEC leads to a significant increase in cycle life.

Monitoring the formation of the SEI is critical for the improvement of these energy storage devices. Various analytical tools such as FTIR, XPS, and Raman spectroscopies are used to probe the composition and formation of the SEI layer.^[200,201] Recently, Hainthaler et al. conducted post-mortem XPS of the electrodes to explain the difference in floating stabilities of the SICs with an HC negative electrode and an AC positive

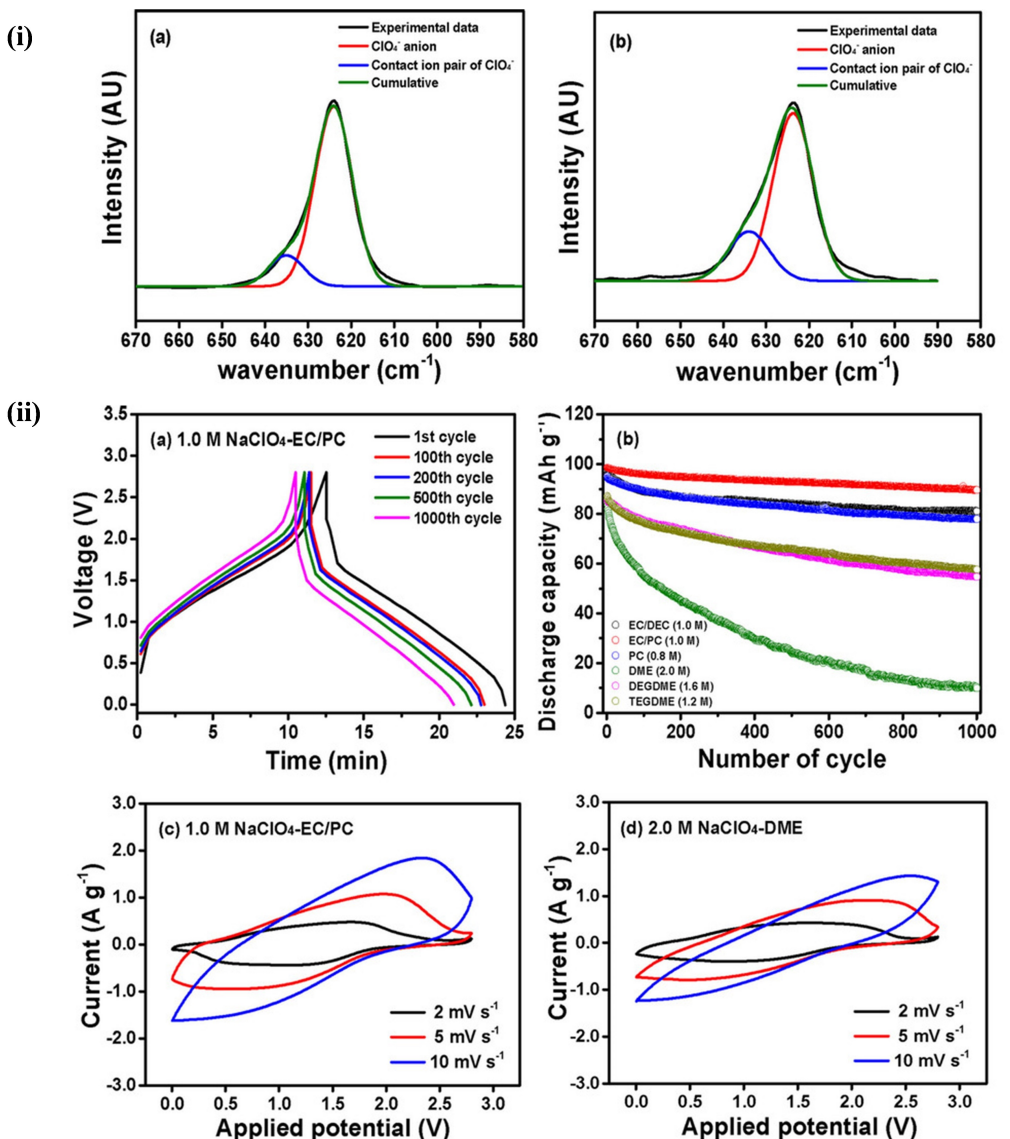


Figure 21. (i) ATR-FTIR spectra of: a) 1.0 M NaClO₄-EC/PC and b) 1.0 M NaClO₄-DME in the wavenumber range: 580–670 cm⁻¹. (ii) a) Charge and discharge curves of the SIC employing 1.0 M NaClO₄-EC:PC at a current density of 500 mA g⁻¹, b) cycling performance of SICs assembled with different liquid electrolytes at a current density of 500 mA g⁻¹, and cyclic voltammograms of SICs with various electrolytes at different scan rates: c) EC:PC and d) DME. Reproduced with permission from [191]. Copyright © John Wiley & Sons, Inc, 2018

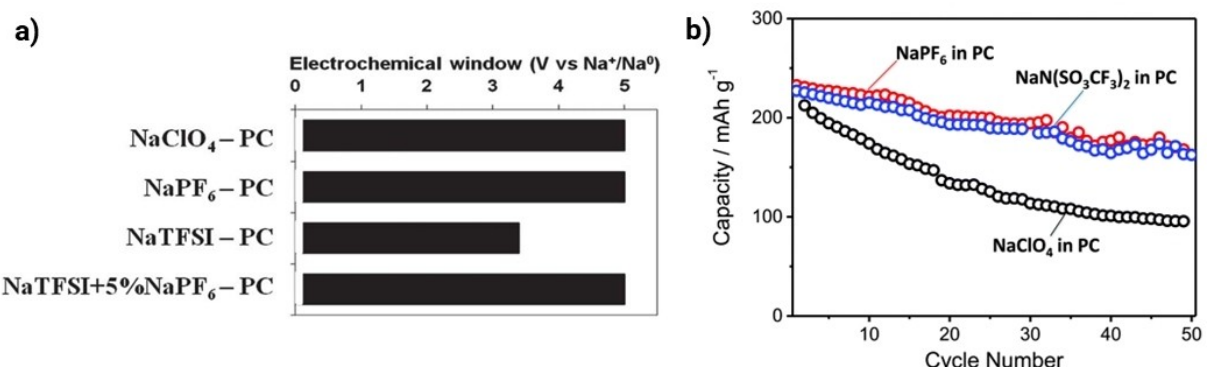


Figure 22. Influences of salts on electrolyte properties. a) Electrochemical potential window stability of PC-based electrolytes with 1 M of various Na salts.^[23] b) Capacity retention for hard carbon electrodes with PC-based electrolyte containing different Na salts at a rate of 25 mA g⁻¹.^[198] Reproduced with permission from the Royal Society of Chemistry.

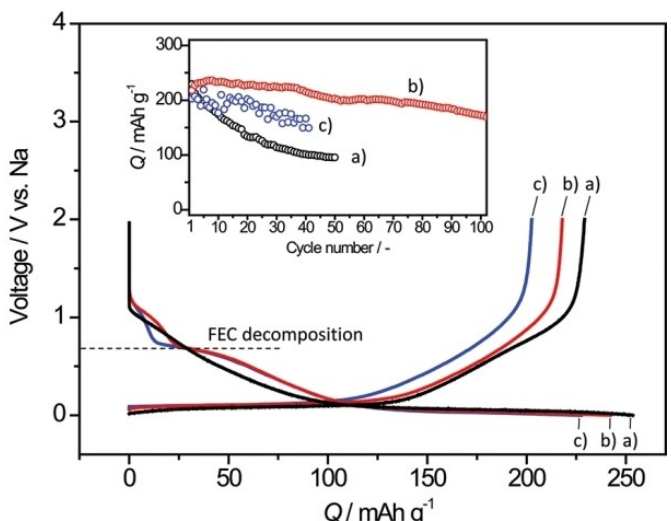


Figure 23. Influence of additives on the electrochemical performance. Hard carbon half-cells with NaClO_4 in PC (a) without and with (b) 2 vol% and (c) 10 vol% FEC.^[199] Reproduced with permission from the Royal Society of Chemistry.

electrode while employing different electrolyte compositions.^[157] The high amount of Na-containing compounds, which are predominantly formed at the HC surface while using the NaPF_6 in EC:PC points to the faster degradation of the system compared to that of systems with NaTFSI in TEG:PC electrolyte.

Prospects for Electrolytes

Overall, there is an infinite number of possible SIC electrolyte configurations. Depending on the target device the electrolyte configuration needs to be adjusted. The optimization of a SIC electrolyte must occur in careful consideration of the interactions with the electrode materials, possible sacrificial agents, and processing steps (e.g. presodiation). To optimize the electrolyte, advanced analytical techniques are necessary to understand the degradation mechanisms, electrolyte decomposition products, etc. High temperatures, voltages, and prolonged cycling can lead to the decomposition of electrolytes, resulting in the formation of various degradation products that can form a passivation layer on the surface of the electrode materials or clog their pores, affecting the overall performance of the system.^[202,203] The anodic dissolution of current collectors upon exposure to these electrolytes is also an important research direction that has to be underlined.^[204] So far, only a few studies have investigated in detail the degradation processes taking place in SICs.

Although a great number of research directions are progressing in the field of SICs that focus on the development of electrode materials, research on electrolytes for SICs is still in its infancy. Advanced *in situ/operando* techniques and post-mortem methods need to be exploited to get a better understanding of the interaction between the electrode and electrolytes, corrosion of the current collectors, and other degradation mechanisms.^[205–215]

3.4. Presodiation

A simple, low-cost, time-efficient, environmentally friendly, and stable/reproducible presodiation of the negative electrode in SICs is the last and major barrier towards the upscaling of the technology. As described before, the lack of a sodium source in a dual carbon SIC requires the presence of a presodiation agent that enables SEI formation and ensures proper electrochemical performance. An evident assumption that lithium- and sodium-based technologies do not differ too much from each other cannot be applied to this key step. Commercially available LICs rely on the use of a sacrificial metallic lithium electrode to pre-lithiate the system, a solution that cannot be transferred to SICs, owing to the higher reactivity of sodium, which makes the solution unaffordable in terms of safety. Therefore, the search for alternative solutions that are technically and economically viable is needed. In general terms, a presodiation strategy should fulfill the following requirements:

- Eliminate the use of metallic sodium. Its high reactivity might hinder any process in terms of safety, even under oxygen and moisture-free environments.
- Provide sufficient sodium ions to complete presodiation on the negative electrode.
- Avoid leaving any dead mass behind the solution to maximize energy and power output. If side products are generated, they should be exhausted.
- To ideally be an air-stable solution that does not require the use of an oxygen-free environment.
- To be environmentally friendly, sustainable, and cost-effective.

Research undergoing in the field is not as abundant as in active materials or electrolytes. As for SIBs, the advantage of SIC technology is that it has gained major attention after an advanced development of its lithium-ion counterpart, *i.e.*, LICs. Thus, many pre-lithiation strategies from LICs,^[216] and presodiation strategies from SIBs^[217] have been transferred to SIC technology. In SIBs, the sodium-based positive electrode is responsible for providing the required Na^+ to the negative electrode, which normally requires to be oversized to compensate for the irreversibility of initial cycles at the negative electrode. Other strategies have also been employed, in particular: i) the use of Na-rich positive electrodes,^[218–220] ii) the introduction of a presodiation agent (also called sacrificial salt or additive) such as Na_3N ,^[221] NaCrO_2 ,^[222] $\text{Na}_2\text{C}_4\text{O}_4$,^[223] Na_2S ,^[224] and Na_2O ,^[225] iii) chemical presodiation of negative electrodes coated with sodium metal powder (NaMP),^[226] immersed into a Na-naphthalene^[227] or Na-biphenyl^[228] in 1,2 dimethoxyethane (DME) solution, or even sprayed by Na-naphthalene dissolved in tetrahydrofuran.^[229] Among them, the most promising solution fulfilling the abovementioned requirements for technical and economic viability is the use of sacrificial salts in the positive electrode.

Sacrificial Salts

Beyond the general requirements identified for presodiation, the use of sacrificial salts requires specific requirements to guarantee its viability:

- i) To be highly reversible to minimize the presence of salt and reduce mechanical and chemical impact in the positive electrode.
- ii) The oxidation potential of the salt needs to be in the operation potential window of the positive electrode.

In 2012 Kuratani *et al.* first studied the presodiation of an HC to be employed as a negative electrode in SICs.^[8] Those first experiments used an electrochemical presodiation technique whose setup consisted of an auxiliary sodium metal electrode as the counter/reference electrode, and HC as the working electrode. The suitability of this strategy was confirmed by the appropriate performance of the final device. Since then, the approach of Kuratani *et al.* has guided most of the researchers in their quest for novel materials or electrolytes in full lab-scale devices while the development of a sustainable presodiation method has often been sidelined.^[87,230] However, scalable presodiation is of paramount importance for upscaling the SIC technology, and in recent years, many alternatives such as Na₂S,^[231] Na₂C₄O_{4r},^[232,233] NaNH₂,^[234] NaBH_{4r},^[235] Na₂CO_{3r},^[236] Na₂C₃O_{4r},^[237] NaCN^[238] have been investigated as sacrificial components incorporated in the formulation of the positive electrode. The main characteristics of these salts are summarized in Table 3, to foster discussion on their appropriateness while some of the details of these works are more in-depth reviewed below, focusing on the salt itself rather than device performance and cyclability, which in these works is conditioned by many factors, such as the selected voltage window, the mass balance, the quality of the electrodes or the cell configuration (coin cell, Swagelok cell).

Starting in 2019, Pan *et al.* proposed a positive electrode with a 40% wt. of sodium sulfide (Na₂S) to be part of the electrode composition for pre-sodiating a Sn₄P₃ negative electrode in the 1 M NaClO₄ (EC:PC) electrolyte.^[231] Na₂S shows a theoretical irreversible capacity of 687 mAh g⁻¹ within two oxidation stages attributed to sulfide anion oxidation and sodium extraction at ca. 2.2 and 3.7–3.8 V vs. Na/Na⁺, respectively (see Figure 24a). The release of Na⁺ during the first charge of the SIC at C/20 (being C the theoretical capacity of Na₂S), allows the proper presodiation of Sn₄P₃ (see Figure 24b) while releasing polysulfides and sulfur gas.

Arnaiz *et al.* reported the use of disodium squareate (Na₂C₄O₄) in a SIC for the first time.^[232] The theoretical capacity of Na₂C₄O₄ (339 mAh g⁻¹) requires a salt content of 40 wt.% in the AC positive electrode (*i.e.*, AC 50 wt.%) for successfully presodiating the negative electrode in 1 M NaClO₄ (EC:PC) electrolyte. Na₂C₄O₄ irreversibly oxidizes at 3.7–3.8 V vs. Na/Na⁺ + Na₂C₄O₄, operating at the same potential range as the AC (see Figure 24c), and releasing CO and CO₂ gases as by-products.

Jezowski *et al.* reported the use of sodium amide (NaNH₂) on one side and sodium borohydride (NaBH₄) on the other side, together with an AC as a positive electrode for SICs in 1 M NaClO₄ (EC:PC).^[234,235] NaNH₂ is shown to irreversibly oxidize at 3.8 V vs. Na/Na⁺ (see Figure 24i), with a high theoretical capacity of 680 mAh g⁻¹ enabling a positive electrode with only 25 wt.% of presodiation agent, but releasing hydrazine species and N₂ and H₂ gaseous byproducts. NaBH₄, which shows a higher theoretical capacity of 710 mAh g⁻¹ and an oxidation potential between 2.4 – 2.7 V vs. Na/Na⁺ was also used in the positive electrode in a 25% amount, releasing H₂ (g) as a byproduct. Both compounds were able to successfully presodiate their corresponding negative electrode.

Sun *et al.* claimed that some of the reported strategies are hazardous (toxic, flammable, and explosive) (*e.g.*, Na₂S and NaNH₂) and sensitive to ambient air conditions, whereas others show too low irreversible capacity output (*e.g.*, Na₂C₄O₄). Thus, they reported the use of sodium carbonate (Na₂CO₃) and sodium oxalate (Na₂C₂O₄) as a presodiation agent, which shows a theoretical and practical capacity of 505 mAh g⁻¹ and 417.1 mAh g⁻¹ (82.6%, with a slopping oxidation potential profile between 3.8–4.4 V vs. Na/Na⁺).^[236] The by-products generated are mainly CO₂ (71.3%) and O₂ (4.5%). For Na₂CO₃, it was experimentally determined that introducing the salt in an amount of 40 wt.% in the positive electrode composition was the most appropriate for a safe potential window operation of the negative electrode, even at fast discharge (*i.e.*, 30 s). With regard to Na₂C₂O₄, it oxidizes irreversibly between 3.7 and 4.0 V vs. Na/Na⁺ (see Figure 25c) with a theoretical capacity of 400 mAh g⁻¹ and CO₂ as the unique by-product, which is easy to remove with a typical degassing process. Moreover, the authors claim that not only does the AC serve as an active material, but it also catalyzes the decomposition of Na₂C₂O₄.

Table 3. Summary of different descriptors for different presodiation agents.

	Na ₂ S	NaNH ₂	NaBH ₄	NaCN	Na ₂ C ₄ O ₄	Na ₂ CO ₃	Na ₂ C ₂ O ₄
Irreversible capacity (mAh g ⁻¹)	687	680	710	547	339	505	400
Oxidation potential (V vs. Na/Na ⁺)	2.2 3.7–3.8	3.8	2.4–2.7	2.9	3.7–3.8	3.8–4.4	3.7–4.0
% required in the AC electrode	40	25	25	36	40	40	55
Negative electrode	HC	HC	HC	HC	HC	HC	HC/Sn ₄ P ₃
By-products	(R-S _n) _x , S	NH ₂ -NH ₂ , N ₂ , H ₂	H ₂	C ₂ N ₂	CO, CO ₂	CO ₂ , O ₂	CO, CO ₂
Toxicity	—	—	—	—	+	+	+
Air stable	—	—	—	—	+	+	+

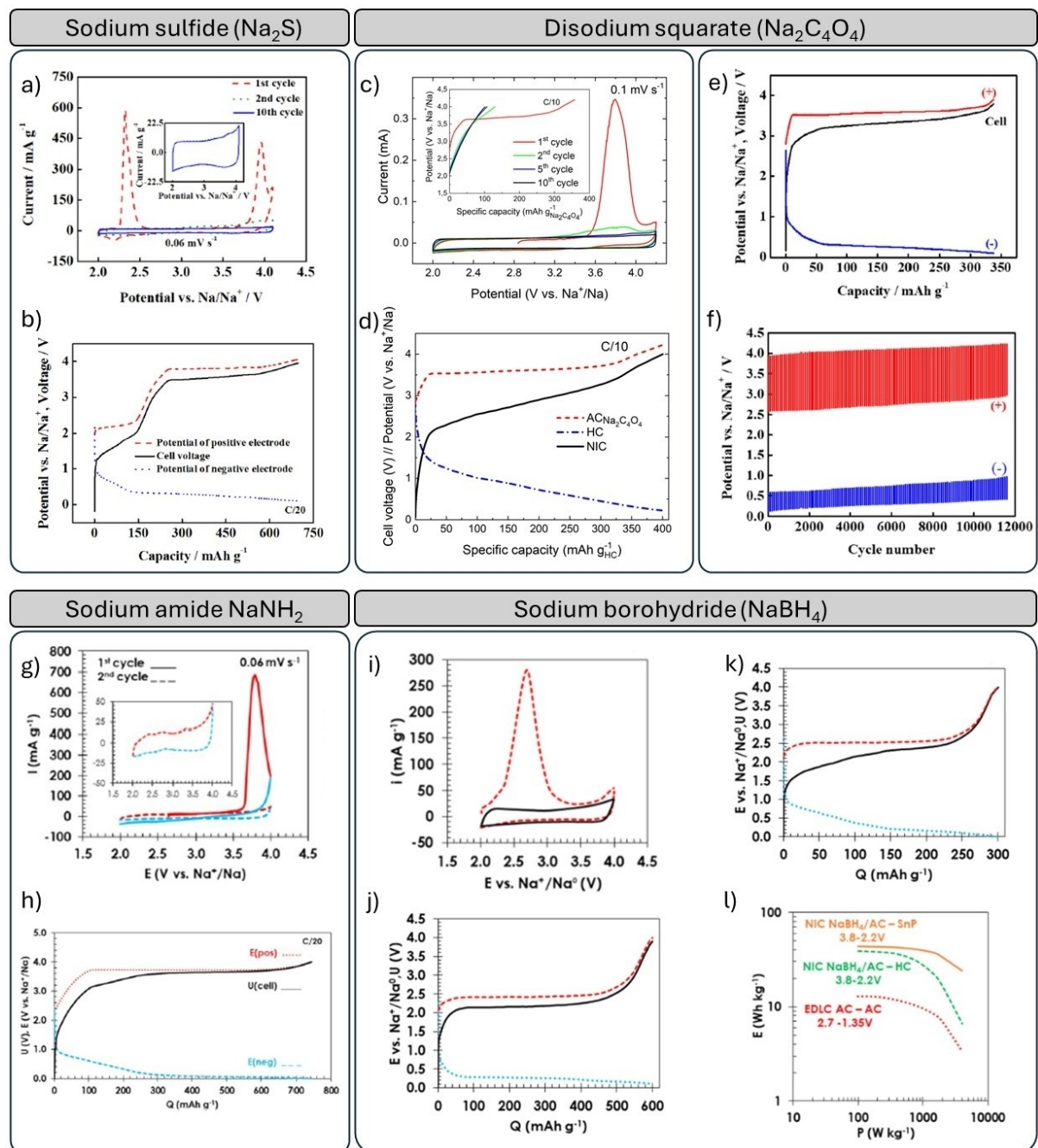


Figure 24. Presodiation components incorporated in the positive electrode such as Na_2S a) CV of AC- Na_2S , b) presodiation of Sn_4P_3 ,^[231] $\text{Na}_2\text{C}_4\text{O}_4$; c) CV of AC- $\text{Na}_2\text{C}_4\text{O}_4$, d) presodiation of HC,^[232] e) presodiation of Sn_4P_3 , f) cyclability test of SIC ($\text{Sn}_4\text{P}_3/\text{AC}$),^[233] NaNH_2 ; g) CV of AC NaNH_2 , h) presodiation of Sn_4P_3 ,^[234] NaBH_4 ; i) CV of AC- NaBH_4 , j) presodiation of Sn_4P_3 , k) presodiation of HC, and, l) Ragone plot of comparing NaBH_4 pre-sodiated SICs.^[235] Reproduced with permission from Elsevier,^[231,233,234] the Royal Society of Chemistry,^[232] and De Gruyter.^[235] e), f), i), j), k), and l) are reproduced under the CC BY 4.0 license.

Again, both compounds show the ability to pre-sodiate the corresponding HC electrode.

Finally, Pan *et al.* reported the use of sodium cyanide (NaCN) as a presodiation agent.^[238] Similarly to previous components, it was also incorporated in the formulation of the positive electrode, in this case, in a 36 wt%. NaCN shows an oxidation potential at 2.9 V vs. Na/Na^+ within a theoretical capacity of 547 mAh g $^{-1}$. The *operando* electrochemical mass spectroscopy of the cell environment and the internal pressure

measurements reveal that the oxidation of this compound does not show any gas evolution. The oxidation of NaCN produces cyanogen C_2N_2 , which is highly soluble in organic solvents, consequently, the subproduct of the oxidation reaction is totally dissolved in the electrolyte. However, the cyanogen is highly toxic as it readily undergoes reduction to cyanide and its large-scale use is questionable with respect to safety concerns.

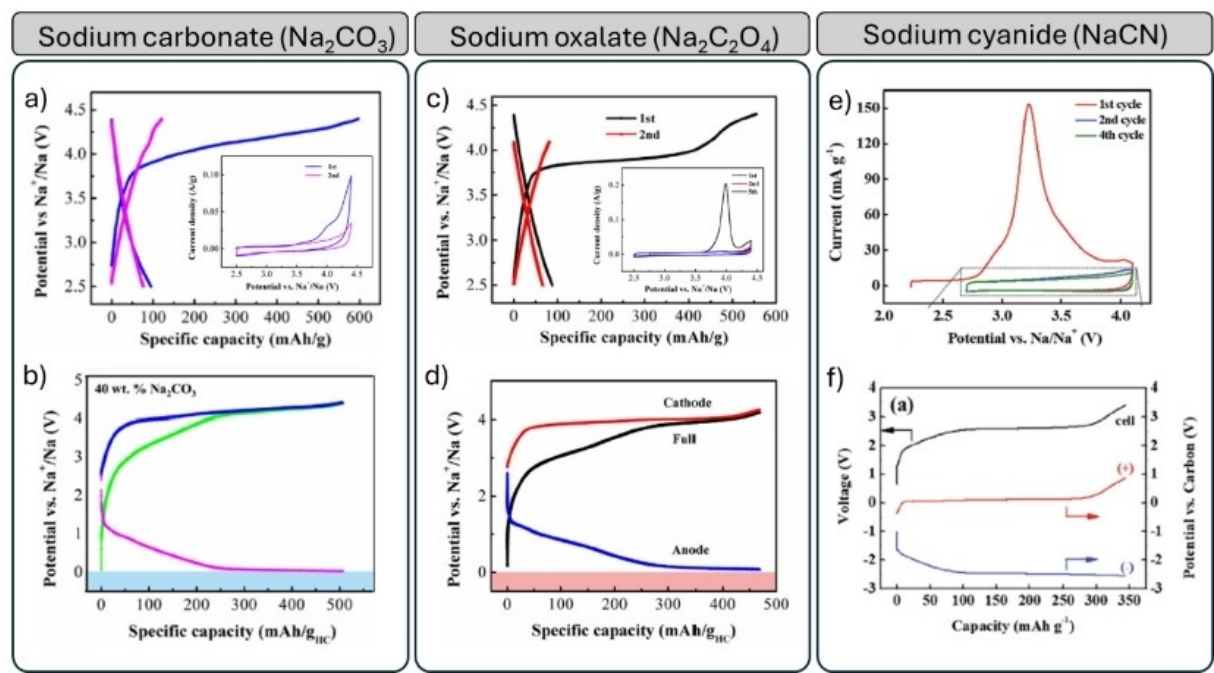


Figure 25. Presodiation components incorporated in the positive electrode such as Na_2CO_3 a) Charge/discharge and inset CV of AC- Na_2CO_3 , and b) presodiation of HC,^[236] $\text{Na}_2\text{C}_2\text{O}_4$; c) Charge/discharge and inset CV of AC- $\text{Na}_2\text{C}_2\text{O}_4$, and d) presodiation of HC,^[237] NaCN; e) CV of ACNaCN, and f) presodiation of $\text{Sn}_4\text{P}_3/\text{HC}$.^[238] Copyright © Elsevier, 2021, 2022, 2023.

Redox-Active Species

Recently, Maćkowiak *et al.* followed a new approach to metal-ion capacitors which is devoted to working with redox-active electrolytes.^[239] The solubility of thiocyanate species in organic and aqueous electrolytes^[240] gave some insights into the possibility of incorporating them into sodium-based electrolytes in order to use SCN^- anions as active species.^[239] This approach is very interesting from the fabrication point of view since it doesn't require the modification of electrode manufacturing, releasing the positive electrode from the mechanical stress that generates the incorporation of a sacrificial salt. However, the possibility of generating cyanides as a subproduct hampers the scalability of this approach.

Future Developments

Table 3 summarizes the main and most important points of all the above described presodiation agents and allows for making an interesting comparison between them. It is worth noting that among the presodiation agents (*i.e.*, Na_2S , NaNH_2 , NaBH_4 , NaCN) incorporated in the formulation of the positive electrode, the highest irreversible capacity pertains to those that generate more prejudicial gases and are hazardous and toxic for the environment. Meanwhile, those with a lower irreversible capacity (*i.e.*, $\text{Na}_2\text{C}_2\text{O}_4$, Na_2CO_3 , $\text{Na}_2\text{C}_2\text{O}_4$) are more environmentally friendly, and the generated gases are shown to influence electrochemical performance, even positively, and can be easily taken out of the cells without any important environmental impact.

In principle, the incorporation of a sodiation agent into the formulation of a positive electrode could be easily implemented in industry without requiring an additional step in the SIC

manufacturing process. Simply adding a new ingredient to the slurry formulation should be sufficient. However, despite the fact that it has already been proven for LICs, targeting water processing might incorporate an extra challenge, since most of the reported sacrificial salts are stable in NMP, but not in water, where they can lose their carbon coatings or even redissolve. Thus, on top of the proper selection of the sacrificial salt, its incorporation in water processing needs to be studied as well.

4. SIC Manufacturing Challenges: Towards Industrialization

The manufacturing process for SICs shares similarities with typical battery manufacturing, and is a key factor in ensuring the sustainability of the technology. Conventional fabrication techniques rely on wet slurry electrode preparation methods using NMP or water-based solutions, as described in various studies.^[140,241,242] Although water-based processing is highly desirable for its environmental and safety benefits, it poses significant challenges, especially for carbon materials in general and AC in particular. As an alternative, the dry electrode fabrication method is gradually gaining traction in the industry. This method offers potential cost reductions by eliminating the solvent and drying steps. However, most manufacturers currently use the conventional wet method because it is a well-established process and is compatible with a wide range of materials.

Manufacturing SICs presents unique challenges due to their hybrid device architecture, which makes the process more

complex compared to conventional batteries. One challenge stems from the high surface area of the AC electrode, which complicates its incorporation into water-based slurries and hampers adhesion to the current collector. Additionally, both AC and HC electrodes lack sodium ions, which necessitates an extra presodiation step to introduce sodium-ion species for charge storage in the battery-type electrode. The manufacturing process typically begins with electrode fabrication, including slurry formulation, electrode coating, drying, and calendaring. This is followed by cell assembly, final quality control, and testing of the produced cells.

Slurry Formulation

In the industry, slurry formulations can be scaled up to batches of 50 L or more, whereas lab-scale testing of initial formulations is typically conducted with only a few millilitres. The sole purpose of these small-scale tests is to evaluate the material's performance. Once the material passes these preliminary tests, its scalability must be assessed by developing slurries at an intermediate scale, typically ranging from 0.1 to 5 L.

The first step in scaling up involves selecting the desired volume, mixing technique, and equipment to ensure a smooth

transition to larger-scale production. Typically, a mixing tank (such as those shown in Figure 26a for up to 1 liter), an impeller, and a cooling jacket are required to maintain a constant temperature during slurry formulation. Additionally, the slurry formulation must be carefully redesigned to ensure that the binder and conductive carbon content during coating is optimal to balance resistance, porosity, electrode adhesion, and cohesion, thereby achieving maximum performance.^[243] To produce high-quality dispersions—essential for high-quality electrodes—several parameters need to be optimized. These include the order in which ingredients are added, the density of materials, the solid content of the slurry, as well as the viscosity and stability of the ink. These parameters should be adjusted based on the electrode coating technique to ensure the proper shear rate of the fluid is maintained consistently from batch to batch (Figure 26b).

During the water-based ink formulation, the active materials (AC and HC) are mixed with binders such as carboxymethyl cellulose and styrene-butadiene rubber, and conducting additives to form a slurry with appropriately controlled viscosity and homogeneity during the coating process (Figure 26c). Compared to NMP processing, it is more challenging to disperse

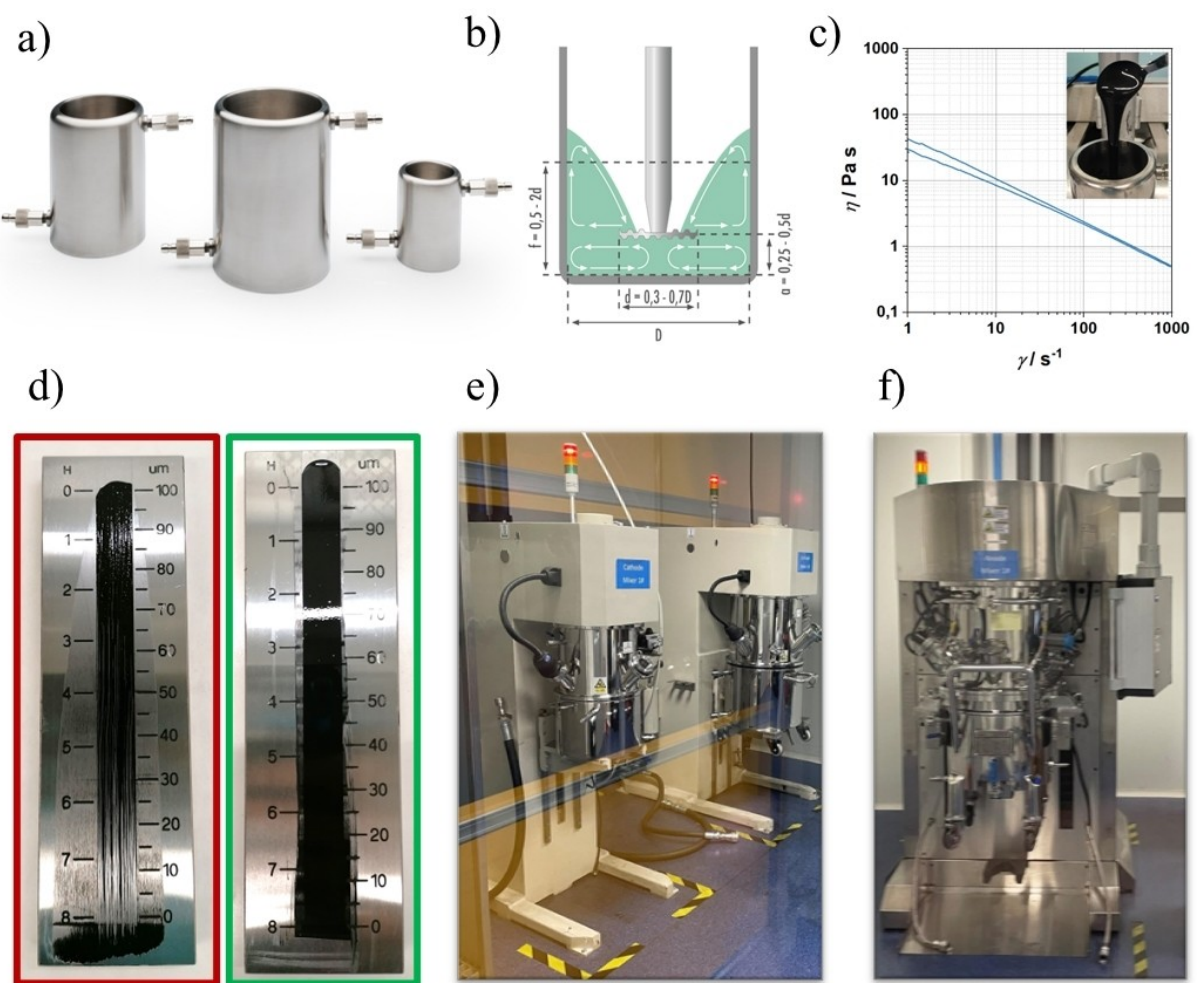


Figure 26. a) tanks of different sizes for slurry formulation b) parameters considered to set disc position c) rheology adjustment of the slurry d) grindometer test e) 5 L tanks f) 50 L tank. Adapted from [245] under the CC BY 4.0 license. © IOP Publishing. Reproduced with permission. All rights reserved.

carbons in water than in NMP-based slurries due to the easier aggregation of conductive carbon black (Figure 26d, red), and special care must be taken in every single step to obtain aggregate-free slurries (Figure 26d, green).^[244] The dispersion quality of both active materials also differs significantly, since the high SSA of AC induces high water uptake. Finally, rheology analysis and quality control are of utmost importance to obtain the required reproducibility for electrode coating when using large tanks of 5 and 50 L shown in Figures 26e and f.

Electrode Coating, Drying, Calendering, and Cutting

The electrode coating process for water-based HC electrodes is well established. However, water-based processing for AC electrodes is significantly more challenging and remains under development. Compared to typical battery-type positive electrodes, the adhesion of AC to the current collector foil is relatively poor due to the high surface area and porosity of the AC particles. As a result, higher binder content is required to ensure sufficient adhesion. Nevertheless, adhesion can be improved by carefully selecting the current collector before electrode coating. For instance, etched aluminum offers higher surface contact, which improves adhesion, but it is considerably more expensive than bare aluminum. A more economically viable option is using a conductive primer-coated foil to aid adhesion, although other properties, such as aluminum corrosion, rate performance, and equivalent series resistance, in which the current collector/electrode interphase plays a critical role, must be investigated to determine the optimal foil.^[246]

Once the formulation is defined and developed, and the current collector selected, the electrode coating process uses a roll-to-roll continuous coater (Figure 27a and c) with a slot die method or comma bar transfer coater attached to multi-staged

combined dryers spanning several meters (Figure 27e). A slot die coater is usually preferred for high throughput and coating speeds. However, much stricter slurry characteristics are required in the slot die coater, which mandates stringent coating tolerance limits regarding agglomerates, fluid pressure, and viscosity instabilities during coating. These aspects must be thoroughly investigated to guarantee successful coatings since they are influenced by particle morphology, binder/active material interactions, and basicity. Generally, higher solid contents in the slurries are desired to increase the energy density and reduce the cost associated with solvent evaporation and recovery in the case of NMP.

Drying is the fundamental parameter of the electrode coating process, which is conditioned by the production rate. Industrial electrode production rate goes beyond 60 meters of electrodes per minute, with 100 meters being a common standard. This production rate conditions the number and length of ovens, the temperatures required, and the techniques used to dry the electrodes while producing them with no cracks, good homogeneity and cohesion as well as good double-sided adhesion. Therefore, usually, the process is optimized in a prototype pilot line before industrial production (Figure 27c). Different drying techniques exist, such as infrared, laser, microwave, or Joule heating technologies, however, still conventional air-drying ovens are mostly utilized in industry. A fixed number of ovens one after each other, with low temperature gradients and contended airflows to avoid turbulence are configured and will determine solvent evaporation rate, which impacts the final structure of the electrode as depicted in Figure 27b.

Upon completing the coating step, electrode compaction (Figure 27f) follows to reduce (and optimize) the electrode's

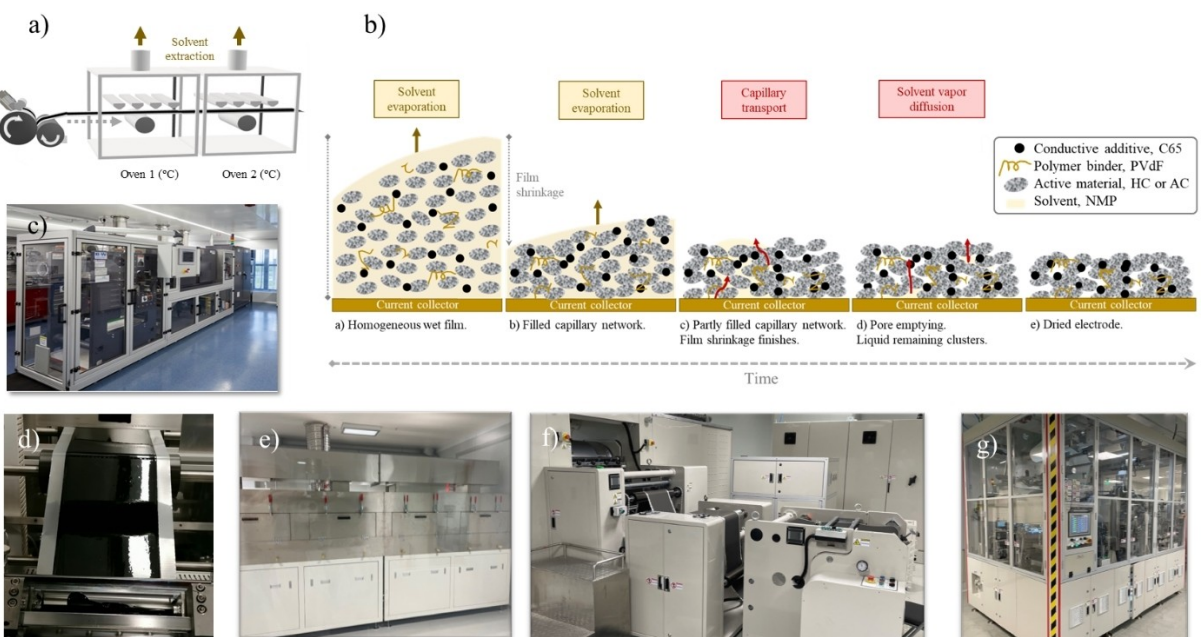


Figure 27. a) Comma bar coating equipment scheme b) drying process c) comma bar d) wet electrode entering the oven e) ovens in a pilot line f) calendering g) semi-automated cell assembly laboratory. Adapted from [245] under the CC BY 4.0 license. © IOP Publishing. Reproduced with permission. All rights reserved.

porosity and improve the volumetric energy density. However, care should be taken to control the compaction degree to avoid over-pressing the electrode, disrupting electrolyte diffusion, and affecting the rate performance. Since activated carbon is porous in nature, compaction can increase the electrode's tortuosity as the void spaces are decreased, also improving the interparticle connectivity. Therefore, careful optimization is required to determine the compaction degree for optimum performance. Finally, electrodes are cut into the desired geometry depending on the cell format selected (Figure 27g).

Cell Assembly

Different formats and form factors of the final cell, including a cylindrical hard case, a prismatic hard case, and a prismatic pouch, can be used to house active materials. The selection of the form factor brings both advantages and drawbacks in terms of device characteristics and production. On the one hand, the selection of the form affects mechanical characteristics, cell capacity, and internal resistance. An example is the additional protection accrued from the hard case formats, which impacts structural rigidity and safety. However, this rigidity, limited internal volume utilization, and additional weight reduce the module and pack density, resulting in lower energy densities compared to the prismatic pouch cell format. The prismatic pouch cell format is a more flexible design option in which the active material layers can be easily increased or decreased at minimal cost. Furthermore, the lightweight and flexible Al-polymer pouch improves both module and pack energy density and efficiency. Nevertheless, the soft packaging of the prismatic pouch does not provide structural rigidity and can easily deform by gas formation during operation. The selection of cell design affects also internal resistance, and consequently, the overall cell capacity. Cylindrical formats present a tightly wound electrode and separator assembly, providing excellent structural stability and uniform current distribution. The consistent internal pressure ensures good contact between the layers, reducing contact resistance and minimizing ESR. In contrast, prismatic and pouch cells require careful attention to electrode stack compression and tab welding quality, as non-uniform contact can increase resistance. On the other hand, the selection of the form factor also affects production rates. For faster throughputs, the cylindrical hard case format is the preferred alternative, but the energy density is lower than using the prismatic hard case format. In contrast, the prismatic hard case format enables much higher energy densities than the cylindrical hard case format, but the manufacturing cost is much higher while the throughput is also lower. Thus, there are several aspects to consider depending on the market strategy. A schematic of the assembly procedure for the different cell formats is presented in Figure 28.

One key point to note in cell assembly is controlling the moisture content of the electrode stack or wound roll by drying it before assembly. This is particularly critical for activated carbon, where the high SSA and porosity make it extremely difficult to reduce the moisture content to very low values (typically less than 250 ppm). Confined moisture and solvent in the pores arise from the mixing process, where solvents such as

NMP and water are used. Despite the much lower boiling point of water compared to NMP, confined moisture trapped in the pores is challenging to remove without very high temperatures and prolonged drying under extreme vacuum. Here, it is once again critical to evaluate the properties of the activated carbon, such as its high surface area and porosity, to ensure that solvent removal can be economically viable before cell assembly. Activated carbons with higher surface area and surface oxygen-rich often require extreme drying conditions to remove the moisture. Prolonged drying, high temperature, and vacuum conditions increase electricity consumption and operating costs when striving to control the moisture and remnant solvent content in the electrode. Failure to remove this solvent can cause issues related to gas formation and visible swelling, depending on the utilized form factor. This can further compromise the safety and performance of the cell, since the organic electrolyte is negatively impacted by the presence of moisture in the cell, especially when using electrolyte salts composed of the PF_6^- anion, which hydrolyses to form HF, POF_3 , and PF_5 in contact with trace moisture in the cell.^[248] Here again, dry electrode fabrication is advantageous since it can eliminate the issues concerning remnant solvent and drying of the electrode. However, the technology is still in its early stages.

Cell Activation

After the cell stacks have been transferred to various housings, the activation step commences with electrolyte injection, as described in Figure 28b. The electrolyte amount and injection process must be carefully controlled to ensure sufficient wetting of the electrode surface and saturation of the total pore volume, including the electrodes and separator, without occupying excess dead space and volumes. Failure to optimize the electrolyte content will result in a decreased energy density, since the weight of the electrolyte is also accounted for when calculating the energy density. Active materials with higher porosity (mesopores and macropores) will necessitate a higher volume of electrolyte and impact the energy density of the produced cell. Separators with too high porosity will also require increased electrolyte amounts to saturate the pores. Hence, unoptimized weights of inactive components will be detrimental to the achievable energy density. The separator porosity, thickness, and ion transport properties must be meticulously optimized to ensure fast charge storage and increased safety with presodiated negative electrodes. Cellulose-based separators provide faster charge transport in capacitors than the industry-used polymers.^[249] However, polymer separators are thinner, have lower porosity, and reduce the contribution of inactive components.

After the injection step, the cell housing is sealed in preparation for the formation step. The formation step is a critical part of the final cell assembly, since it influences the cycle life and performance of the cell in its final application phase. Here, the cells are subjected to specially adapted charging protocols to condition the cell at elevated temperatures. Degradation is accelerated along with the initial side reactions to produce protective passivation films on the electrode surfaces. Gases are produced during this step, and

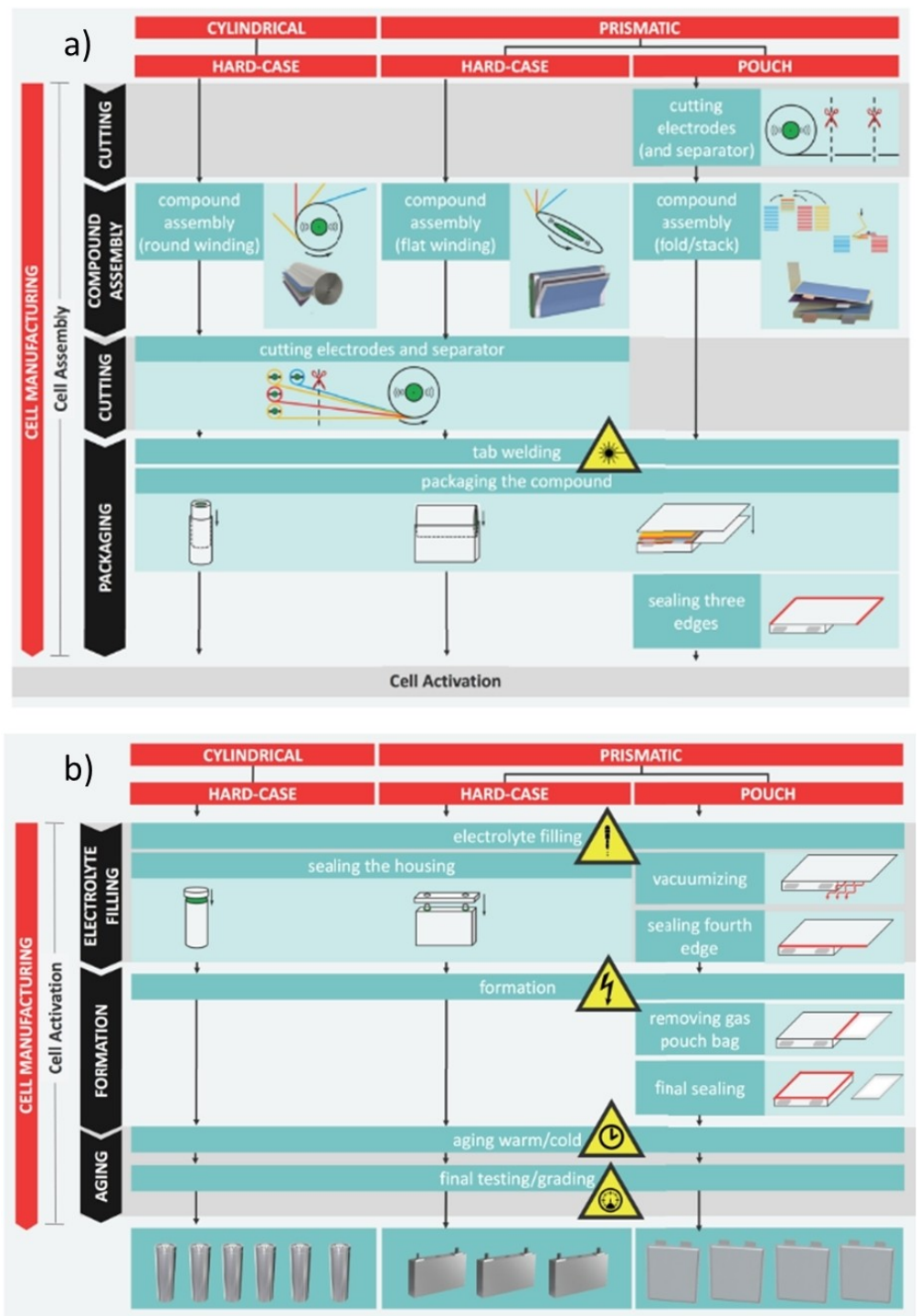


Figure 28. a) Schematic of the cell assembly procedure for different cell formats; b) A schematic of the cell activation procedure for different formats. Reprinted with permission from [247]. Copyright © Elsevier, 2017.

their nature depends on the electrolyte constituents, the remnant solvent in the electrodes, and the electrode/electrolyte interactions. It is essential to complete the formation process by eliminating the gases formed before the cell is resealed (in the case of pouch cells) or the gas outlets are closed (in the case of prismatic hard case or cylindrical cells). The specifics of the formation step, including presodiation and aging procedures,

are industrial trade secrets today, and consequently, limited public information is available on the chosen procedures. However, each formation step is characterized by specially adapted charging procedures, including constant current and constant voltage charging steps at specified voltages. After the formation step, the typical testing procedures commence to

characterize the capacity and performance of the developed cells.

In summary, similar processes are expected when manufacturing sodium-ion capacitors compared to sodium-ion or lithium-ion batteries. However, several critical steps, such as electrode drying and formation procedures, may pose challenges in terms of cost, equipment limitations, and process optimization. The high surface area of activated carbon must be effectively studied to guarantee optimal handling and smooth drying and formation processes. The highest surface area sample may not necessarily be the best choice, as it may cause process issues, as mentioned previously. Energy consumption during capacitor manufacturing is much higher than batteries due to the drying conditions for the electrodes and stacks arising from the high surface area of activated carbon. This is eventually reflected in the unit cost per F of a capacitor. Therefore, more emphasis must be placed on evaluating potential cost reduction strategies such as eliminating solvent use, alternative drying techniques, and correlating the properties of the activated carbon with the ease of drying.

5. Applications and Management System

Despite SICs not having reached the market yet, their performance is expected to be on par with that of LICs, with anticipated improvements in power performance and sustainability due to the inherent nature of the carbon materials used in SIC technology. Therefore, the applications section is covered by the existing LIC technology, with high expectations that SICs will replace LICs in the future. Compared to conventional lithium-ion or sodium-ion batteries, LICs offer several advantages in applications requiring:

- i) high-power density
- ii) very short charge and discharge times ranging from seconds to minutes,
- iii) thousands of charge/discharge cycles or/and floating hours
- iv) low-self discharge
- v) wide operating temperature

Compared to EDLCs, which can meet most of the above-mentioned requirements (except for self-discharge, which can be the limiting factor in many applications), LICs offer 3 to 4 times higher energy density. Table 4 compares LICs and SICs with the other two major electrochemical energy storage devices (excluding Pb-Acid), which are currently used in many target applications for SIC technology.

Moreover, SICs will allow energy storage in applications where it was previously not possible and can be hybridized with other technologies, such as metal-ion batteries (LIBs or SIBs) and fuel cells. These strategies increase the efficiency and life expectancy of storage systems, directly reducing environmental impact and improving sustainability. In the following sections, a description is provided of the various applications in which SICs can be implemented after LICs or SCs have demonstrated their value, as well as considerations regarding the MIC-based energy storage management system.

Table 4. Characteristics of different electrochemical energy storage systems.

	EDLC	LIB	LIC	SIC
Negative Elec.	AC	Graphite	Graphite	HC
Positive Elec.	AC	LFP, NMC	AC	AC
Energy Density	—	+++	++	++
Power Density	+++	—	++	+++
Charge – discharge	In seconds	Hours/minutes	In seconds	In seconds
Internal resistance	+++	—	+	++
Low T performance	+++	—	+	++
Self-discharge	—	+++	++	++
Cycle Life	1 M	1–5 k	1 k–1 M	1 k–1 M
Safety	+++	—	++	+++
CRM	No	Yes	Yes	No
Applications	High power	High energy	High power medium energy	High power medium energy

Applications

This section reviews different applications where SICs can have an impact (see Figure 29a), including integration with renewable energy, mobility, and industrial applications. As shown in Figure 29b, energy storage systems can provide various services depending on the response time needed. SICs may be suitable when long discharge duration times are required, such as in primary and secondary response services, black start, and power quality.^[250] Figure 29c summarizes the suitability of different energy storage technologies for a wide range of stationary applications.

Stationary Sector

In recent years, the focus on climate change and sustainability has led to a reduction in dependence on fossil fuels like coal and oil, with the introduction of renewable energy sources such as wind and solar energy. This shift has resulted in a less centralized energy system, potentially reducing grid stability. Additionally, renewable energy sources like wind and solar are intermittent, making energy storage vital, where MICs have already demonstrated their benefits. Wind energy, for instance, experiences large voltage oscillations due to power generation fluctuations under different wind conditions, which can harm connected electronic systems. SICs offer a solution for stabilizing power transmission and storing excess energy. For solar energy, SICs present a promising way to bridge the gap between the specific energy, power, and service life of batteries and supercapacitors.^[252] For low-power wide-area network (LPWAN) applications, LICs are already being used with solar panels.^[253] Beyond renewables, backup power generators are

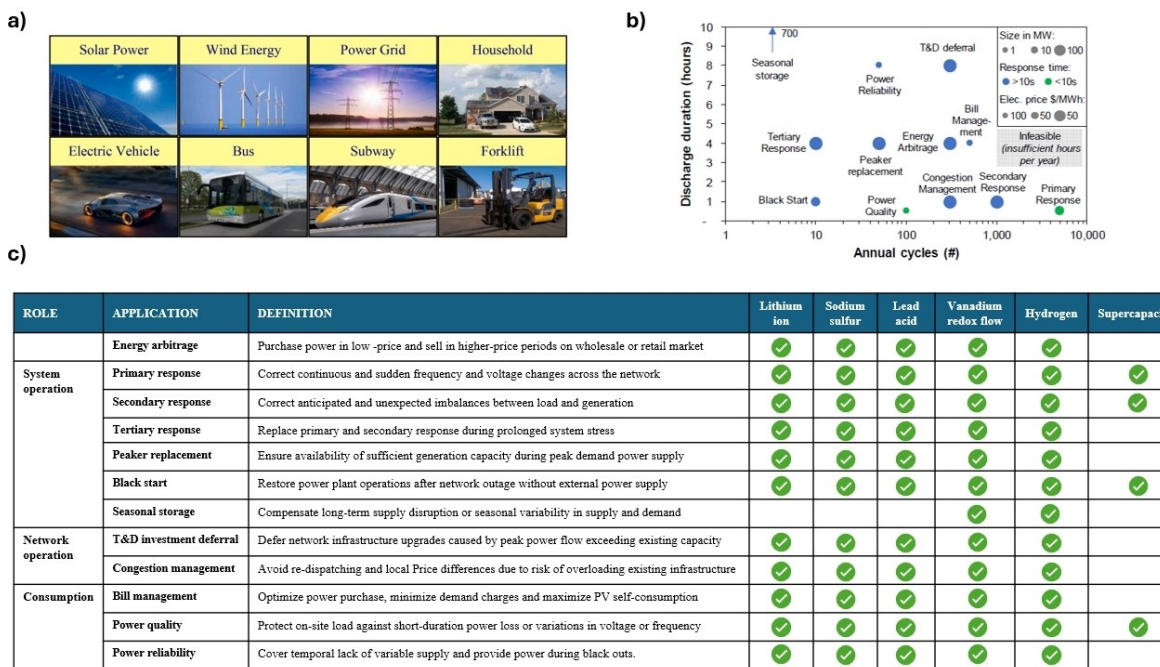


Figure 29. a) Applications. Reproduced with permission from [251]. Copyright © Elsevier, 2021; b) Application with technical requirements^[250]; c) Description of electricity energy storage applications and technology suitability^[250]. Reproduced with permission. Copyright © Cell Press (2019)

employed to ramp up power after a network outage. Due to their quick response time, some companies already commercialize power supply systems based on LICs.^[254–256]

Mobility Sector

The need to create a green, sustainable society free of CO₂ emissions drives the electrification of transportation. Electric vehicles for both public and private transport are becoming an integral part of modern transport systems, enhanced by hybridization solutions combining different storage elements. Hybridization arises from the need for both high energy and high specific power.^[257] In mobility applications, SICs could stabilize the electrical system's power during regenerative braking energy recovery and acceleration boosts, protect batteries and fuel cells from peak loads, and reduce H₂ consumption in fuel cell-based systems. Compared to existing EDLC-based solutions, SICs could achieve this with half the weight and volume, thanks to their higher energy density.

In^[258,259] the concepts, topologies, and advantages of external hybridization of batteries and supercapacitors in electric vehicle applications are discussed, while^[260] discusses the dynamic and thermal behaviors of supercapacitors. Recent studies address the modeling of commercial SCs and hybrid systems. The first hybrid bus in Europe with SCs was the so-called "Ultracap Bus" tested in Nuremberg, Germany, in 2001. Then, the electric bus fleet was tested in Luzern, Switzerland, in 2002. After every transportation cycle, the SCs could be recharged within 3 to 4 min with a high-speed power charger. After LICs reached the market, 15 buses in Manchester were equipped with LIC modules in 2015.^[263] The LIC modules installed by JM Energy could provide the same service as the

EDLC modules, at less than half the weight and saving quite an amount of space. The comparison of specifications of both LIC and EDLC modules can be seen in Figure 30b.^[264] Currently, manufacturers such as Toyota, Peugeot, and Lamborghini that use an SC to increase vehicle performance^[265,266] could benefit from using SICs to save volume and weight, thus, obtaining cars with less consumption.

The hybridization of high-energy fuel cell-based systems with a power device was also pioneered by supercaps.^[267] The impact of the hybridization of SC with fuel cells in terms of efficiency, high performance, low size, and light system is evidenced.^[268] The hybrid fuel cell/battery/SC configuration still provides the most extended lifetime for batteries.^[269,270] However, in recent times, the replacement of EDLCs with LICs, and ultimately with SICs, holds promise for more efficient hybridization strategy.^[271]

Studies in the railway sector address the advantages of SCs in terms of efficiency for braking energy recovery and as an energy storage element both in railway substations and the train's own 750 V DC bus.^[272,273] On the other hand, in,^[274] the effectiveness of implementing a hybrid energy storage system in terms of efficiency in railway systems is demonstrated.^[275] Again, SCs pioneered the field, but after years of research, LICs have now entered the market and can potentially replace EDLCs. Similarly to some commercial hybrid solutions already existing for SCs, like the Paris T3 tram line and Geneva Public Transport tram,^[276] it is expected that the use of LICs and SICs will soon become widespread.

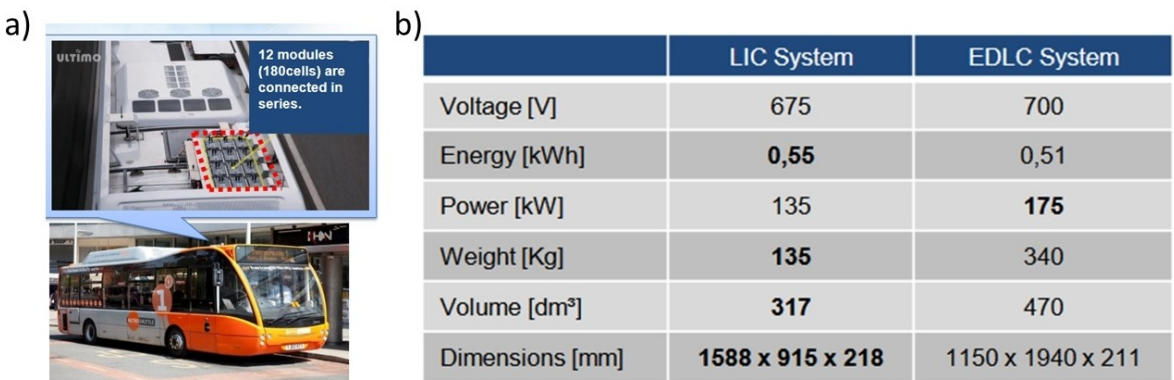


Figure 30. a) Bus equipped with LIC modules. b) Specification comparison for LICs and EDLCs for bus application.

Industrial Sector

In recent decades, industries have been moving towards more autonomous operations, leading to a high energy demand to operate various equipment. Additionally, some sectors cannot afford power downtimes, making reliable energy storage solutions essential. SICs could be well-suited for several applications, such as logistics equipment, medical devices, and the Internet of Things (IoT).

For example, logistics equipment like forklifts are traditionally powered by gasoline engines, which contribute to gas emissions and noise. They have been increasingly replaced by LIBs. Similarly, Automatic Guided Vehicles (AGVs) are currently powered by LIBs. However, both require long charging times—often several hours—which limits their efficiency in industrial settings. In contrast, LICs provide sufficient energy density and high-rate current performance, allowing for rapid starts and stops in forklifts and enabling fast charging within minutes. This significantly reduces downtime due to charging. Moreover, LICs have a longer cycle life compared to LIBs, leading to reduced replacement and battery costs, as well as savings in space and weight. For instance, Zhang et al. demonstrated the integration of LICs into an AGV, achieving a maintenance-free AGV capable of charging in just 2 minutes and operating 24/7.^[277]

Medical equipment is critical and cannot afford any energy downtime. Thus, the installation of energy backup systems is crucial. In this sense, these systems must provide high power in a short time. The weight of this backup system is also important. Here, SICs can provide high power in a short period (in the range of seconds), offer long cycle life, and are lighter than lithium-ion batteries. In addition, safety is much improved compared to LIBs since no thermal runaway can occur. For medical devices like wheelchairs, the implementation of SICs could also be beneficial. Hussain et al. analyzed the benefits of using SCs in a wheelchair that also contained LIBs.^[278] They found that the proposed system required less charging time and was more efficient for high-power demands. SICs could potentially offer even better performance by providing a lighter solution with the same energy and power characteristics as SCs.

The use of IoT devices has significantly increased in recent years, driven by the digitalization of industries. In 2020, the European Institute of Innovation & Technology identified IoT as

a key segment for capacitor development due to the need for energy storage systems capable of delivering high periodic pulses of current to transmit data, having long cycle life to minimize replacements, and operating effectively over a wide temperature range. Hybrid cells like SICs can also be considered as they enable miniaturization of the devices, potentially keeping the benefits provided by SCs.

Sodium Ion Capacitor Management System (SMS)

As discussed in the previous section, SICs can be utilized in a wide variety of applications. However, to integrate these cells into a real-world system and achieve the desired power, voltage, and energy levels, multiple cells must be connected in series and/or parallel to form a module. It is important to note that when a cell or module operates outside its specified voltage range, above the maximum allowable charge/discharge current values, or beyond its temperature limits, it experiences accelerated degradation and an increased risk of failure.

To mitigate these risks, the Sodium Ion Capacitor Management System (SMS) continuously monitors cell and module parameters in real time and protects the module under various operating conditions. This monitoring enhances performance and safety while extending the module's lifespan. The following sections will outline the main functionalities and structure of the SMS (Figure 31a).

Similar to a Battery Management System (BMS), the SMS can be defined as the system responsible for managing the SIC module. As can be seen in Figure 31a, it presents voltage, current and temperature inputs corresponding to the data achieved by sensoring the pack, and as outputs different commands such as protections, state of the SIC, and signals about thermal management of the system. In the following sections, an explanation of the SMS structure will be given.

Protections

In general, cell operating conditions are specified by the manufacturer based on the materials used in their construction. The manufacturer provides key parameters in the datasheet, such as the recommended voltage range, maximum allowable charging and discharging currents, and the acceptable temperature range. These parameters are essential for defining SMS

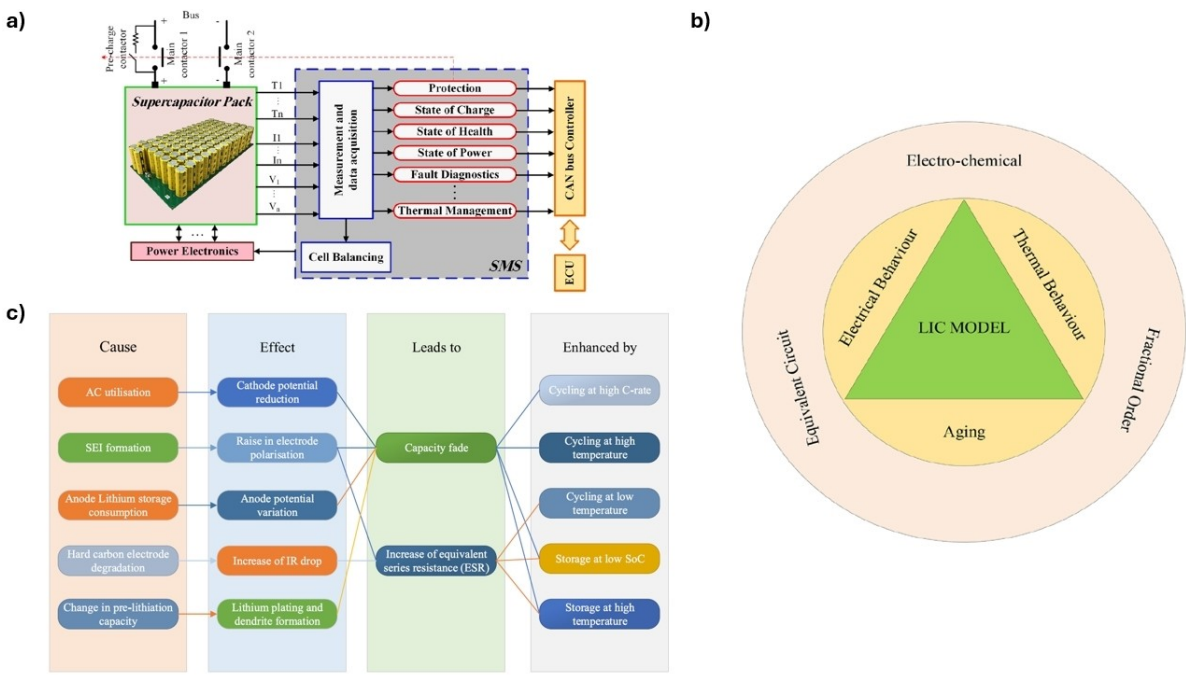


Figure 31. a) a block diagram of the SMS ; b) a LIC model transferrable to SICs; c) SIC aging mechanisms inferred using LIC as a model. Reproduced from [279] under the CC BY 4.0 license. Copyright © Elsevier, 2022.

protections, which ensure that cells operate within safe limits, preventing unsafe conditions that could lead to cell failure.

Common SMS protections include safeguards against over-voltage and under-voltage, over-current and short-circuit, and over-temperature and under-temperature. In 2019, Oca et al. analyzed potential responses to extreme conditions by studying the safety performance of several commercial cells subjected to electrical abuse tests.^[280] The study found that under over-charge and deep discharge conditions, the internal resistance of the cells increased significantly (up to 234 mΩ), accompanied by gas formation and cell swelling. Although no severe hazards like fire or explosion were observed, the cells did suffer irreversible damage.

Additionally, it is important to consider that the high currents used by SICs can lead to overheating. As Soltani et al. analyzed, a thermal management system is crucial to maintaining thermal stability and prolonging the lifespan of the modules.^[281] Their study demonstrated that an air-cooling system is an effective solution to keep the system within an optimal temperature range.

Performance Management

The performance management of the SMS is responsible for analyzing data related to the system's voltage, temperature, and current. By processing this information, the SMS can estimate key state variables such as State of Health (SoH), State of Charge (SoC), and State of Power (SoP). It also manages cell balancing within the module to ensure optimal performance. The following sections provide a brief overview of parameter estimators, control methods, and cell balancing techniques. Since SICs are still in the early stages of development, most

available data and performance benchmarks are derived from LICs, which serve as a foundational reference for advancing SIC technology.

Parameter estimation: the optimal control of a SIC system requires a precise state estimation. To this end, it is essential to study the electrical and thermal behavior of the system, as well as aging mechanisms (see Figure 31b). Electrical performance depends significantly on the temperature, current, and SoC of the system. Moreover, parameters such as impedance and stored capacity vary during the system's lifetime. Different equivalent circuit models have been presented in the literature by combining resistances and capacitors, which reflect the charge transfer of lithium ions and diffusion mechanisms occurring inside LICs.^[282,283]

To achieve more accurate modeling, fractional-order models are often employed. These models utilize constant-phase elements (CPEs) and the Warburg element, which better reflect the dynamics of LICs. The thermal behavior of the system is equally crucial since high currents can generate significant amounts of heat during operation. In terms of aging mechanisms, capacity fade and internal resistance increase during cycling indicate degradation, which is further accelerated by calendar aging. Various factors, including negative electrode and positive electrode materials, as well as prelithiation agents, can affect electrochemical stability. Figure 31c summarizes the primary mechanisms responsible for SIC degradation.

Thus, having a comprehensive understanding of the operating mechanisms, alongside monitoring various variables, is essential for the reliable estimation of SoC, SoH, and SoP. The work already done on LICs provides a foundation for SIC

technology, helping to shorten the adaptation period from one technology to the other.

Cell balancing: Cell balancing is performed to equalize the voltages of individual cells within a module. Even when cells are produced by the same manufacturer and follow the same production process, they can still exhibit differences in capacity and internal resistance. When assembled into a module, these differences can lead to cell imbalances. Therefore, implementing a balancing system is crucial to equilibrate the cell voltages and minimize these variations. There are generally two types of balancing methods:

- **Passive Balancing:** This method involves a resistive circuit and a switch for each cell, allowing the circuit to open and close as needed. Passive balancing is simple and cost-effective, but it dissipates excess energy as heat, which can be less efficient.
- **Active Balancing:** In this method, energy is transferred from cells with higher voltage to those with lower voltage. Although active balancing is more efficient and helps maintain a longer overall battery life, it is also more complex and expensive to implement.

To summarize, this section highlights the potential use of SICs in various applications, including stationary storage, mobility, and other industries. SICs can combine with other energy storage technologies like LIBs and fuel cells, extend the lifespan of storage systems, enhance efficiency, and reduce size and weight. A well-developed SMS is crucial for the safe and efficient utilization of SICs. Continuous monitoring, advanced algorithms, and real-time estimations of SIC state of charge, state of health, and state of power are essential. These tools facilitate fault diagnosis, prevent premature aging, and provide valuable performance data. This, in turn, supports optimized energy management, improves efficiency and longevity, and contributes to reduced environmental impact and overall cost.

6. Life Cycle Assessment

Sustainability Considerations

Within the context of the energy transition and the decarbonization of industry and transport sectors, energy storage technologies such as electrochemical capacitors are expected to display competitive performance from both a technical and sustainability point of view. Lithium-based systems are widely popular but notions about potential effects on the environment and the criticality of resources (which may also determine cost) can trigger the development of technologies such as SICs. These systems have displayed promising performance while making use of a more abundant and widely distributed resource such as sodium, reducing concerns associated with resource scarcity.^[165] A lower risk of detrimental effects such as water or soil pollution can also be attributed to the extraction and processing of sodium, in contrast to that of other metals like lithium. In addition, due to the incompatibility between graphite and sodium, sodium-based systems employ hard carbon as negative electrode active material instead.^[284] The previous considerations mean that these technologies can

be characterized with lesser resource criticality, given the critical nature of materials such as graphite and cobalt commonly employed in other types of storage systems (LIBs). However, despite the technological maturity of this technology, little is known about its environmental and economic implications from a life cycle perspective. The sustainability character of SICs, and any technology for that matter, should be assessed in a comprehensive manner that allows for the quantification of their environmental and cost performance throughout the different stages of their life cycle. To do so, commonly employed methods such as the Life Cycle Assessment (LCA) and Life Cycle Costing (LCC) measure the associated mass and energy flows along the supply chain, manufacture, use, and End-of-Life management of a product. These flows are subsequently translated into impacts and costs, which can be used to describe the sustainability profile of the system. Although SCs have already been introduced to the market, a review of the available literature reveals a knowledge gap in environmental and cost analyses, let alone LICs or SICs. Cost assessments dating back to 2016 and environmental assessments more prominent since 2019 can be found via typical search engines such as Google Scholar, Science Direct, Scopus, and CORDIS when using keyword strings such as 'supercapacitor/hybrid capacitor /ultracapacitor/Sodium ion capacitor/Lithium ion capacitor AND (LCA OR environmental impacts)', or 'supercapacitor/hybrid capacitor /ultracapacitor/Sodium ion capacitor/Lithium ion capacitor AND (LCC OR cost OR CAPEX)'. A total number of 32 LCA and 33 LCC scientific research articles, as well as a total of 13 and 7 European projects for LCA and LCC, respectively, were found (Figure 32).

Life Cycle Assessments for Sodium-Ion Capacitors

While there exists a robust body of research dedicated to understanding the environmental footprint of LIBs across their entire life cycle, encompassing the extraction of raw materials, manufacturing, use, and final disposal, the exploration of LCAs for SCs lags due to their limited market. Most studies are limited to specific aspects of the production phase, such as the manufacture of electrode materials. Furthermore, LCA analysis for LIC technology is limited to 1 or 2 studies while there are no works dedicated to SICs. However, some estimations can be made since the SIC positive electrode is composed of AC whose production routes stay the same as for its application in SCs. Similarly, the production route for the negative electrode composed of HC can be extracted from studies on SIBs. For instance, Glogic et al.^[285] conducted an LCA on producing high-performance AC electrodes from coconut shells for supercapacitors. The study highlighted the environmental benefits of using a steam activation process. It showed that producing 1 kg of AC emits 5.68 kg of CO₂ and consumes 34.4 MJ of energy, with AC production accounting for 60% of the environmental impacts of supercapacitor electrodes. The findings pointed to environmental advantages and areas for improvement. Additionally, Wang et al.^[286] examined the environmental impacts of producing AC from lignocellulosic biomass. Their LCA revealed that the in-plant production stage had the highest impact, particularly in carcinogenic, ecotoxicity, and non-carcinogenic

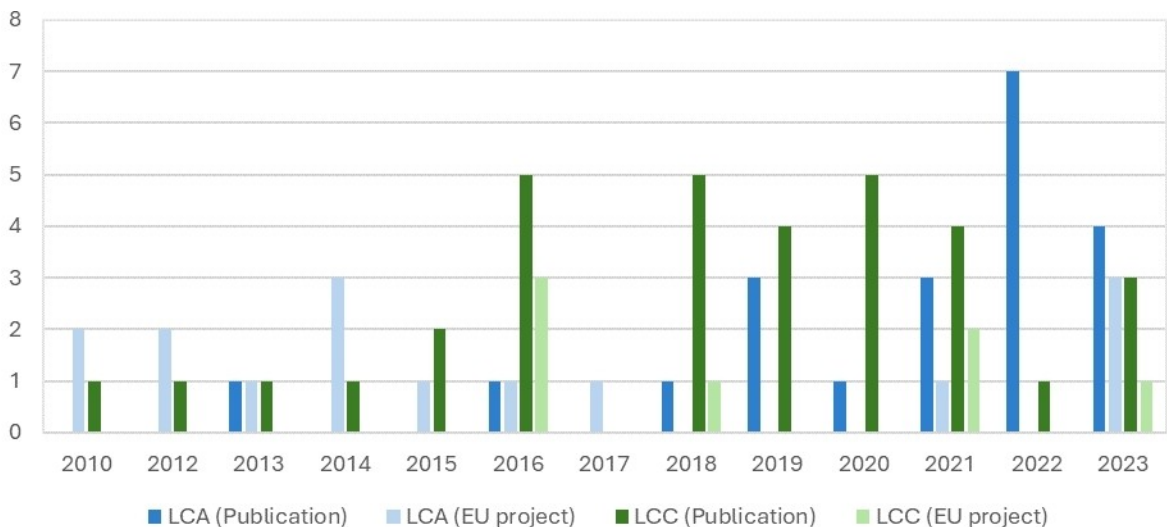


Figure 32. Number of LCA and LCC publications and EU projects per year between 2010 and 2023

categories. The “feedstock establishment” phase contributed 50.3%–85.2% of the total impacts. They compared KOH-reuse and steam processes, finding greenhouse gas emissions of 15.4 kg and 10.2 kg CO₂ equivalent per kilogram of activated carbon, respectively.

With regards to the negative electrode, not only is graphite unsuitable for use in sodium-based systems, but is also listed as a critical material by the EU,^[287] making its substitution in other systems highly desirable. Hard carbon is considered a promising alternative due to its abundance, potential low costs, and advantageous physical properties,^[288] with some studies already evaluating its environmental profile. For instance, Peters et al.^[289] conducted an LCA of an SIB with sugar-derived HC in the negative electrode. The results identified the production of sugar as a hotspot of environmental impacts. Alternative precursors such as starch, cellulose, organic waste, and petroleum coke were also explored, concluding that using starch or cellulose increased the environmental impacts, whereas organic waste and petroleum coke significantly reduced them. Other precursors such as waste apple pomace, waste tires, and synthetic resin were studied by [290]. The results highlighted the potential of organic waste, especially apple pomace, in reducing the carbon footprint. Liu et al.^[291] found that coconut shell-derived hard carbon bears low environmental impacts due to simpler processing and lower carbonization temperatures.

Aside from the study of HC precursors, Liu et al.^[291] compared different routes to produce HC, concluding that using any of these in the synthesis of cellulose-based HC is already more environmentally benign than producing commercial graphite. A combined process of hydrothermal carbonization with pyrolysis was found to be the most sustainable alternative while also enabling better electrochemical performance of the material. The use of various sources of biomass as precursors can be a key strategy to reduce production costs, but also requires the identification of adequate methods capable of meeting the specific production needs for each

material.^[292] By integrating the results from these component-specific LCAs, we propose that SICs can offer a highly sustainable energy storage solution. The exclusion of lithium and graphite, materials commonly linked to substantial environmental and economic burdens, highlights the potential advantages of SICs. Regarding the methodological aspects of LCA studies for SCs and SIBs (given the lack of SIC-specific literature), large variability in the definition of goals, system boundaries, and functional units (FUs), has been identified across different sources. While some studies adopt a cradle-to-gate perspective, considering impacts from raw materials extraction to product manufacturing, others consider only the production phase (gate-to-gate perspective). Few studies contemplate the use and final disposal phase in their assessments (cradle-to-grave perspective). The selection of FUs also varies based on the goals, scope, and application field of the technology. Commonly found FUs include capacitance expressed in F [Cossutta et al.,^[293] Glogic et al.,^[294] Glogic et al.,^[285] and Kamali et al.^[295]] and mass of electrode material produced.^[296] Additional discrepancies in system boundaries include the use of different manufacturing conditions such as electricity mix and the scale of production (e.g., laboratory, pilot, or industrial), which may pose a large influence on the results further challenging their comparability. Figure 33 illustrates the different geographies found in the literature on LCAs for SCs based on the electricity supply chain, which were used in these studies. As a reference, studies focused on SIBs have employed FUs like 1 Wh^[289,297,298] and one cell^[299] to estimate the environmental footprint of their systems, given that they analyze the entire production of a whole battery. To address some of the previously mentioned challenges, a unified approach to life cycle inventories is recommended. This would involve homogenizing system boundaries and functional units to allow for fair and accurate comparisons between different studies, thereby facilitating a more comprehensive understanding of the environmental implications of supercapacitor technologies.

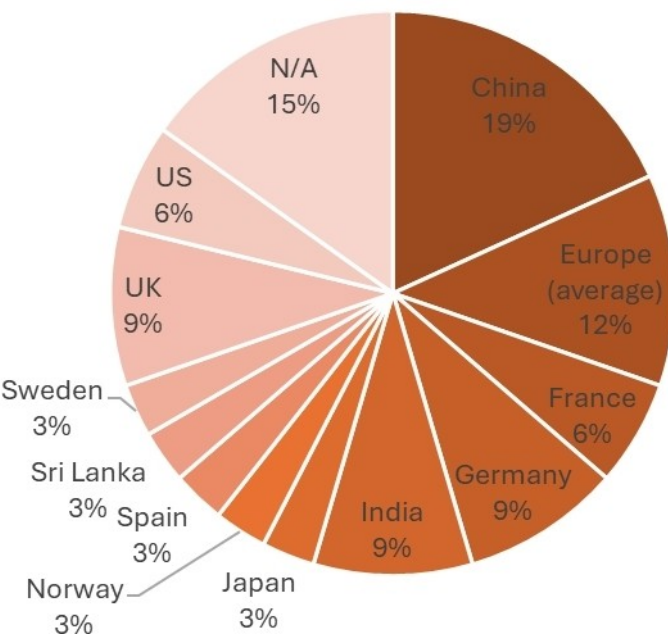


Figure 33. Geographic distribution of studies on LCAs based on the electricity supply chain.

Many existing assessments focus solely on electrode material production, with few studies analyzing full energy storage system components. Additionally, little attention is given to the use phase, where technical performance aspects such as energy density and life cycle are crucial for the calculation of environmental impacts. The use of sodium and the absence of critical materials, such as lithium and graphite, can be the most significant factor in the assessment of sustainable materials in LCA studies for SICs. This approach highlights the need for comprehensive analyses that encompass the entire life cycle of energy storage systems. On the other hand, within the available literature, a trend to conduct a detailed analysis of climate change potential can be identified, whereas mineral resource criticality issues related to energy storage systems are often overlooked.

Literature on Costing for Sodium Ion Capacitors

As in the case of Life Cycle Analysis, due to the early stage of SIC technology, no literature on costing has been found. However, the same approach as for LCA can be followed for the LCC analysis.

In terms of activated carbon, Wang et al.^[286] performed a comprehensive assessment of the economic feasibility as well as the LCA of lignocellulosic-based activated carbon employed in supercapacitors. They studied the annual operating costs for an AC plant, considering costs associated with electricity, raw materials, operating labor, maintenance and repair, and depreciation, among others and they concluded that the required selling price of the activated carbon production of the study was USD 16.79 per kg, which, as they compared, was in the range of commercial activated carbons (USD 15 to 50 per kg). In fact, in terms of commercial AC products, Weinstein et al.^[300] declared in 2013 that all supercapacitor manufacturers of

that time used coconut shell activated carbon as their active material. As they stated, Kuraray activated carbon price dropped significantly from 150–200 \$ kg⁻¹ to 15 \$ kg⁻¹ within the years.

In terms of hard carbon, the active material widely employed in sodium-ion batteries, in 2019 Peters et al.^[301] explored the economic potential of sodium-ion batteries by comparing the cell costs per kWh of storage capacity broken down to battery components and materials, comparing SIB, NMC, and LFP technologies. In terms of the hard carbon market prices, no results were found. However, three different hard carbon production costs were studied, depending on the materials used: hard carbon from sugar, coconut shell, and petroleum coke. Analyzing the different elements needed for the production of 1 kg of each hard carbon, they found the petroleum coke to be the cheapest (3.65 € kg⁻¹), followed by coconut shell hard carbon (6.30 € kg⁻¹), and finally, the hard carbon derived from sugar (17.28 € kg⁻¹), which is, in fact, a similar cost to the activated carbon cost but without considering the activation. Compared to the synthetic graphite price declared in the study (13.73 € kg⁻¹), they concluded the possibility of producing hard carbon at prices below the battery-grade graphite.

Another key element of sodium-ion capacitors is the electrolyte. Due to the lack of cost information about the different electrolytes employed in SICs, the cost of electrolytes for sodium-ion batteries has been taken as a reference. In this way, Peters et al.^[301] analyzed the cost of 1 M NaPF₆ EC:DMC 4:1 wt. % electrolyte, considering the available market prices for the precursors. They obtained an electrolyte cost of 15.84 € L⁻¹, slightly lower than the corresponding LIB electrolyte (16.06 € L⁻¹).

Thus, by integrating the results from the activated carbon from supercapacitors and the hard carbon and electrolyte from

sodium-ion batteries, we propose that SICs could offer a more economical energy storage solution considering the active material prices. In addition, the SIC electrolyte cost could also be reduced compared to the similar SIB electrolyte when an aqueous-based electrolyte is employed.

However, when broadening the system boundaries to the use phase, most of the articles do not consider LIC or SIC technology but examine the costs of integration of SCs in electromobility and renewable energy systems, due to the higher TRL of the technology. A deep analysis of the several applications that they can cover can be found in the “application section”. In terms of cost analysis, examples of the integration of supercapacitors in the transport sector,^[302,303] as well as their integration as support for renewable energy systems demonstrate the potential cost savings and performance benefits of this technology compared to traditional solutions.^[304,305] Figure 34 illustrates the distribution of different SC applications found in the literature. The overall conclusion was that SICs overcome SCs in performance since they can offer, for the same application, the same solution, with a smaller number of cell units as well as less space, volume, and weight.

Just as in the case of SCs, operating conditions such as temperature and depth of discharge influence the degradation rate of SIC systems. This would have a direct impact on its technical performance and lifetime, which is reflected in costs of Operation and Maintenance (O&M). Due to the lack of information about the economic aspects of SIC, in terms of supercapacitors, Song *et al.*^[306] analyzed the economic effects of degradation in a hybrid energy storage system (HESS) finding a correlation between operating temperature and costs. Similarly, Gbadegesin *et al.*^[307] found potentially high overestimations of energy outputs when the degradation mechanisms are neglected, leading to an underestimation of investment and operation costs. Another aspect worth pointing out is the focus on investment costs while overlooking the costs of disposal and waste management. Furthermore, the point in time for which the analysis is made can significantly influence the results due

to rapid technology development, changing user demand, market volatility, and global socioeconomic events, which would also hamper comparability across studies.

Outlook of Literature on Environmental and Cost Assessments

Overall, due to the limited number of detailed analyses and the heterogeneous system boundaries among them, estimating the average environmental and cost performance for SICs is currently unfeasible. However, some available studies provide disclosed life cycle inventories of the materials composing the technology, which may facilitate the reproducibility and traceability of results. This would enable potential reconstruction, homogenization, and comparison between different systems, leading to clearer insights into SICs' environmental and economic impacts. In general, with the available information, SIC technology could become more sustainable and cost-effective compared to related supercapacitors and sodium-ion batteries. However, a more comprehensive understanding of the sustainability and economic viability of SIC technology needs to be developed.

7. Outlook: Key Design Rules for Sodium-Ion Capacitors

Sodium-ion capacitors represent a promising advancement in electrochemical energy storage technologies, offering a unique combination of high energy and power densities with environmental sustainability. However, their path to market readiness requires addressing several interconnected challenges in materials development, manufacturing, and application-specific optimization.

Advancing Material Innovation

The performance of SICs hinges on the development of advanced electrode materials. Hard carbons, derived from biomass, have emerged as leading candidates for negative electrodes due to their high capacity, good rate capability, durability, and potential for scalability at low cost. Further research is needed to optimize their microstructure, balancing sloping and plateau regions to maximize energy and power outputs. Additionally, tailored pyrolysis conditions and the careful selection of precursors can enhance sodium storage properties while aligning with sustainability goals. For positive electrodes, porous carbons with high surface areas and tailored nanoscale pores are essential. Advanced activation techniques and heteroatom doping strategies can improve ionic interactions, enhancing energy density and charge storage efficiency. Furthermore, pseudocapacitive materials such as transition metal oxides or hybrid nanocomposites, present promising avenues to further enhance SICs' energy storage capabilities. These materials can introduce additional faradaic reactions that complement capacitive storage mechanisms, potentially boosting energy density while maintaining fast charge/discharge capabilities. To achieve practical implementation, sustainable,

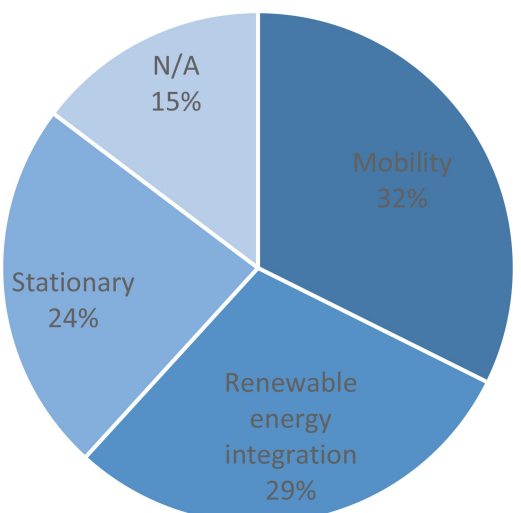


Figure 34. Distribution of various SC applications.

scalable and environmentally friendly production methods must be prioritized to meet industrial demands.

Tackling Presodiation Challenges

Presodiation remains a critical step in SIC assembly, ensuring sodium-rich negative electrodes for optimal operation. However, current methods face limitations, including uneven sodium distribution and the challenges of handling reactive sodium. Future advancements should focus on developing in-situ presodiation techniques integrated into manufacturing processes, simplifying production and improving consistency. Insights from computational modeling and real-time monitoring can further optimize presodiation dynamics, reducing side reactions and improving the longevity of SICs.

Enhancing Scalability and Manufacturing

The industrialization of SICs requires robust, cost-effective, and environmentally compliant production processes. Transitioning biomass-derived carbons from lab-scale synthesis to large-scale manufacturing is a critical priority. Scalable methods must ensure high yield and reproducibility without compromising material performance. Innovations such as water based roll-to-roll electrode production or dry processing can enhance throughput, minimizing chemical waste will lower costs and environmental impact. Improving and reducing activation or formation process is key to increase productivity and reduce cost.

Bridging the Performance Gap

While SICs excel in bridging the gap between batteries and supercapacitors, further optimization is needed to fully realize their potential. Increasing energy density requires material innovations that expand voltage windows and improve electrode compatibility. Simultaneously, advanced electrode architectures and electrolyte formulations can enhance power density and rate capabilities by improving reaction kinetics and ion transport. Addressing degradation mechanisms, such as electrolyte breakdown and SEI instability, will ensure long-term cycling stability, making SICs more competitive with other energy storage technologies.

Prioritizing Sustainability

Sustainability is central to the SIC value proposition. A comprehensive life cycle analysis (LCA) must guide every stage of development, from material sourcing and production to disposal and recycling. Compared to lithium-based systems, SICs do not rely on critical raw materials and offer advantages in reducing water usage, carbon emissions, and material toxicity. However, efforts must continue to close the loop on material use through efficient recycling methods and the integration of circular economy principles.

Driving Market Adoption

The market potential for sodium-ion capacitors (SICs) lies in their ability to fill critical gaps between traditional batteries and supercapacitors, addressing applications that demand both energy density and rapid power delivery. However, achieving

widespread market adoption requires strategic alignment with application-specific needs, cost competitiveness, and the development of supportive ecosystems. The versatility of SICs makes them suitable for a wide range of applications, including renewable energy storage, electric mobility, and portable electronics. Their ability to stabilize renewable energy systems and provide peak shaving or voltage support makes them valuable for grid applications. In electric vehicles, SICs can serve as auxiliary power units or energy buffers in hybrid systems. For portable devices, the balance of energy and power densities positions SICs as strong candidates for next-generation electronics. However, market adoption relies on SICs achieving cost parity with competing technologies. While economies of scale will help, their manufacturing costs must be addressed.

8. Conclusions

The development of sodium-ion capacitors presents both challenges and opportunities. By addressing material and manufacturing barriers, optimizing performance, and embedding sustainability into the design process, SICs can emerge as a transformative energy storage solution. Collaborative efforts among researchers, industry leaders, and policymakers will be critical to realizing the potential of SICs. Through continued innovation and strategic alignment with global sustainability goals, SICs can achieve widespread adoption, serving as a vital component of the transition to cleaner, more sustainable energy systems. As a hybrid solution bridging the strengths of batteries and supercapacitors, SICs have the potential to meet the demands of diverse energy storage applications while fostering a more sustainable future.

Acknowledgements

Authors would like to acknowledge the MUSIC project, funded by the European Union's Horizon Europe Research and Innovation program under grant agreement number 101092080

Conflict of Interests

The authors declare no conflict of interest.

Data Availability Statement

Data sharing is not applicable to this article as no new data were created or analyzed in this study.

Keywords: Sodium ion capacitors • Sustainability • Hard carbon • Activated carbon • Presodiation • Life cycle assessment

- [1] Sustainable, <https://dictionary.cambridge.org/dictionary/english/sustainable>.
- [2] M. Daniel Thomas, *What is Sustainability? How Sustainable Work, Benefits, and Example.*
- [3] Report of the World Commission on Environment and Development: Our Common Future.
- [4] D. B. Agusdinata, W. Liu, H. Eakin, H. Romero, *Environ. Res. Lett.* **2018**, *13*, 123001.
- [5] Y. Zhang, J. Jiang, Y. An, L. Wu, H. Dou, J. Zhang, Y. Zhang, S. Wu, M. Dong, X. Zhang, Z. Guo, *ChemSusChem* **2020**, *13*, 2522.
- [6] G. G. Amatucci, F. Badway, A. D. Pasquier, T. Zheng, *J. Electrochem. Soc.* **2001**, *148*, A930.
- [7] Z. Chen, V. Augustyn, X. Jia, Q. Xiao, B. Dunn, Y. Lu, *ACS Nano* **2012**, *6*, 4319.
- [8] K. Kuratani, M. Yao, H. Senoh, N. Takeichi, T. Sakai, T. Kiyobayashi, *Electrochim. Acta* **2012**, *76*, 320.
- [9] P. W. Ruch, D. Cericola, A. Foelske, R. Kötz, A. Wokaun, *Electrochim. Acta* **2010**, *55*, 2352.
- [10] Z. Tian, Y. Zou, G. Liu, Y. Wang, J. Yin, J. Ming, H. N. Alshareef, *Adv. Sci. (Weinh)* **2022**, *9*, 2201207.
- [11] H. Moon, A. Innocenti, H. Liu, H. Zhang, M. Weil, M. Zarrabeitia, S. Passerini, *ChemSusChem* **2023**, *16*, e202201713.
- [12] N. Sun, J. Qiu, B. Xu, *Adv. Energy Mater.* **2022**, *12*, 2200715.
- [13] L. Xie, C. Tang, Z. Bi, M. Song, Y. Fan, C. Yan, X. Li, F. Su, Q. Zhang, C. Chen, *Adv. Energy Mater.* **2021**, *11*, 2101650.
- [14] K. Hong, L. Qie, R. Zeng, Z. Yi, W. Zhang, D. Wang, W. Yin, C. Wu, Q. Fan, W. Zhang, *J. Mater. Chem. A* **2014**, *2*, 12733.
- [15] P. Liu, Y. Li, Y.-S. Hu, H. Li, L. Chen, X. Huang, *J. Mater. Chem. A* **2016**, *4*, 13046.
- [16] A. Björlin, A. Hansson, Y. L. Zhou, *Waste-derived hard carbon anode materials for sodium-ion batteries: The potential of using cardboard as precursor material in sodium-ion batteries for hard carbon production in Sweden*, **2023**.
- [17] D. Chen, W. Zhang, K. Luo, Y. Song, Y. Zhong, Y. Liu, G. Wang, B. Zhong, Z. Wu, X. Guo, *Energy Environ. Sci.* **2021**, *14*, 2244.
- [18] D. Saurel, B. Orayech, B. Xiao, D. Carriazo, X. Li, T. Rojo, *Adv. Energy Mater.* **2018**, *8*, 1703268.
- [19] R. Morita, K. Gotoh, M. Fukunishi, K. Kubota, S. Komaba, N. Nishimura, T. Yumura, K. Deguchi, S. Ohki, T. Shimizu, *J. Mater. Chem. A* **2016**, *4*, 13183.
- [20] D. A. Stevens, J. R. Dahn, *J. Electrochem. Soc.* **2000**, *147*, 1271.
- [21] D. A. Stevens, J. R. Dahn, *J. Electrochem. Soc.* **2000**, *147*, 4428.
- [22] D. A. Stevens, J. R. Dahn, *J. Electrochem. Soc.* **2001**, *148*, A803.
- [23] A. Beda, C. Villevieille, P.-L. Taberna, P. Simon, C. M. Ghimbeu, *J. Mater. Chem. A* **2020**, *8*, 5558.
- [24] J. S. Weaving, A. Lim, J. Millichamp, T. P. Neville, D. Ledwoch, E. Kendrick, P. F. McMillan, P. R. Shearing, C. A. Howard, D. J. Brett, *ACS Appl. Energy Mater.* **2020**, *3*, 7474.
- [25] Y. Li, A. Vasileiadis, Q. Zhou, Y. Lu, Q. Meng, Y. Li, P. Ombrini, J. Zhao, Z. Chen, Y. Niu, *Nature Energy* **2024**, *1*.
- [26] A. P. Cohn, K. Share, R. Carter, L. Oakes, C. L. Pint, *Nano Lett.* **2016**, *16*, 543.
- [27] P. Bai, Y. He, X. Zou, X. Zhao, P. Xiong, Y. Xu, *Adv. Energy Mater.* **2018**, *8*, 1703217.
- [28] C. Bommier, T. W. Surta, M. Dolgos, X. Ji, *Nano Lett.* **2015**, *15*, 5888.
- [29] H. Au, H. Alptekin, A. C. Jensen, E. Olsson, C. A. O'Keefe, T. Smith, M. Crespo-Ribadeneyra, T. F. Headen, C. P. Grey, Q. Cai, *Energy Environ. Sci.* **2020**, *13*, 3469.
- [30] J. M. Stratford, A. K. Kleppe, D. S. Keeble, P. A. Chater, S. S. Meysami, C. J. Wright, J. Barker, M.-M. Titirici, P. K. Allan, C. P. Grey, *J. Am. Chem. Soc.* **2021**, *143*, 14274.
- [31] S. Qiu, L. Xiao, M. L. Sushko, K. S. Han, Y. Shao, M. Yan, X. Liang, L. Mai, J. Feng, Y. Cao, *Adv. Energy Mater.* **2017**, *7*, 1700403.
- [32] K. Wang, Y. Xu, Y. Li, V. Dravid, J. Wu, Y. Huang, *J. Mater. Chem. A* **2019**, *7*, 3327.
- [33] N. Sun, Z. Guan, Y. Liu, Y. Cao, Q. Zhu, H. Liu, Z. Wang, P. Zhang, B. Xu, *Adv. Energy Mater.* **2019**, *9*, 1901351.
- [34] B.-H. Hou, Y.-Y. Wang, Q.-L. Ning, W.-H. Li, X.-T. Xi, X. Yang, H.-J. Liang, X. Feng, X.-L. Wu, *Adv. Mater.* **2019**, *31*, 1903125.
- [35] S. Alvin, D. Yoon, C. Chandra, H. S. Cahyadi, J.-H. Park, W. Chang, K. Y. Chung, J. Kim, *Carbon* **2019**, *145*, 67.
- [36] Y. Jin, S. Sun, M. Ou, Y. Liu, C. Fan, X. Sun, J. Peng, Y. Li, Y. Qiu, P. Wei, *ACS Appl. Energy Mater.* **2018**, *1*, 2295.
- [37] Y. Morikawa, S. Nishimura, R. Hashimoto, M. Ohnuma, A. Yamada, *Adv. Energy Mater.* **2020**, *10*, 1903176.
- [38] Z. Wang, X. Feng, Y. Bai, H. Yang, R. Dong, X. Wang, H. Xu, Q. Wang, H. Li, H. Gao, *Adv. Energy Mater.* **2021**, *11*, 2003854.
- [39] M. Yuan, B. Cao, H. Liu, C. Meng, J. Wu, S. Zhang, A. Li, X. Chen, H. Song, *Chem. Mater.* **2022**, *34*, 3489.
- [40] Y. Huang, X. Zhong, X. Hu, Y. Li, K. Wang, H. Tu, W. Deng, G. Zou, H. Hou, X. Ji, *Adv. Funct. Mater.* **2024**, *34*, 2308392.
- [41] C. Qiu, A. Li, D. Qiu, Y. Wu, Z. Jiang, J. Zhang, J. Xiao, R. Yuan, Z. Jiang, X. Liu, *ACS Nano* **2024**, *18*, 11941.
- [42] S. Fleischmann, Y. Zhang, X. Wang, P. T. Cummings, J. Wu, P. Simon, Y. Gogotsi, V. Presser, V. Augustyn, *Nat. Energy* **2022**, *7*, 222.
- [43] C. Merlet, C. Péan, B. Rotenberg, P. A. Madden, B. Daffos, P.-L. Taberna, P. Simon, M. Salanne, *Nat Commun* **2013**, *4*, 2701.
- [44] Z. Liu, Z. Lu, S. Guo, Q.-H. Yang, H. Zhou, *ACS Cent Sci.* **2023**, *9*, 1076.
- [45] J. Meng, G. Jia, H. Yang, M. Wang, *Front Chem* **2022**, *10*, 986541.
- [46] F. A. Soto, A. Marzouk, F. El-Mellouhi, P. B. Balbuena, *Chem. Mater.* **2018**, *30*, 3315.
- [47] Y. Ji, J. Qiu, W. Zhao, T. Liu, Z. Dong, K. Yang, G. Zheng, G. Qian, M. Yang, Q. Chen, *Chem* **2023**, *9*, 2943.
- [48] Q. Li, X. Liu, Y. Tao, J. Huang, J. Zhang, C. Yang, Y. Zhang, S. Zhang, Y. Jia, Q. Lin, *Natl. Sci. Rev.* **2022**, *9*, nwac084.
- [49] D. Saurel, J. Segalini, M. Jauregui, A. Pendashteh, B. Daffos, P. Simon, M. Casas-Cabanás, *Energy Storage Materials* **2019**.
- [50] X. Chen, J. Tian, P. Li, Y. Fang, Y. Fang, X. Liang, J. Feng, J. Dong, X. Ai, H. Yang, *Adv. Energy Mater.* **2022**, *12*, 2200886.
- [51] J. Yang, X. Wang, W. Dai, X. Lian, X. Cui, W. Zhang, K. Zhang, M. Lin, R. Zou, K. P. Loh, *Nano-micro Lett.* **2021**, *13*, 1.
- [52] M. Salanne, B. Rotenberg, K. Naoi, K. Kaneko, P.-L. Taberna, C. P. Grey, B. Dunn, P. Simon, *Nat. Energy* **2016**, *1*, 1.
- [53] H. Guo, M. Elmanzalawy, P. Sivakumar, S. Fleischmann, *Energy Environ. Sci.* **2024**, *17*, 2100.
- [54] Z. Lu, C. Geng, H. Yang, P. He, S. Wu, Q.-H. Yang, H. Zhou, *Proceedings of the Natl. Acad. Sci.* **2022**, *119*, e2210203119.
- [55] J. Chmiola, G. Yushin, Y. Gogotsi, C. Portet, P. Simon, P.-L. Taberna, *Science* **2006**, *313*, 1760.
- [56] K. Ge, H. Shao, E. Raymundo-Piñero, P.-L. Taberna, P. Simon, *Nat Commun* **2024**, *15*, 1935.
- [57] S.-J. Jang, J. H. Lee, S. H. Kang, Y. C. Kang, K. C. Roh, *Energies* **2021**, *14*, 7629.
- [58] M. Sevilla, R. Mokaya, *Energy Environ. Sci.* **2014**, *7*, 1250.
- [59] J. Wang, S. Kaskel, *J. Mater. Chem.* **2012**, *22*, 23710.
- [60] D. Lozano-Castello, M. A. Lillo-Rodénas, D. Cazorla-Amorós, A. Linares-Solano, *Carbon* **2001**, *39*, 741.
- [61] N. Jackel, P. Simon, Y. Gogotsi, V. Presser, *ACS Energy Lett.* **2016**, *1*, 1262.
- [62] C. Largeot, C. Portet, J. Chmiola, P.-L. Taberna, Y. Gogotsi, P. Simon, *J. Am. Chem. Soc.* **2008**, *130*, 2730.
- [63] S. Liu, C. Song, W. Zhang, T. Zhang, W. Shao, Z. Weng, M. Yao, H. Huang, X. Jian, F. Hu, *Chem. Eng. J.* **2022**, *450*, 138103.
- [64] E. Zhang, Y.-C. Wu, H. Shao, V. Klimavicius, H. Zhang, P.-L. Taberna, J. Grothe, G. Buntkowsky, F. Xu, P. Simon, *J. Am. Chem. Soc.* **2022**, *144*, 14217.
- [65] H. Yin, H. Shao, B. Daffos, P.-L. Taberna, P. Simon, *Electrochim. Commun.* **2022**, *137*, 107258.
- [66] X. Liu, D. Lyu, C. Merlet, M. J. Leesmith, X. Hua, Z. Xu, C. P. Grey, A. C. Forse, *Science* **2024**, *384*, 321.
- [67] Z. Weng, F. Li, D.-W. Wang, L. Wen, H.-M. Cheng, *Angew. Chem. Int. Ed.* **2013**, *52*, 3722.
- [68] K. Breitsprecher, M. Janssen, P. Srimuk, B. L. Mehdi, V. Presser, C. Holm, S. Kondrat, *Nat Commun* **2020**, *11*, 6085.
- [69] A. Hagopian, M.-L. Doublet, J.-S. Filhol, *Energy Environ. Sci.* **2020**, *13*, 5186.
- [70] B. Li, H. Zhang, D. Wang, H. Lv, C. Zhang, *RSC Adv.* **2017**, *7*, 37923.
- [71] J. J. Lamb, O. S. Burheim, *Energies* **2021**, *14*.
- [72] O. Barbieri, M. Hahn, A. Herzog, R. Kötz, *Carbon* **2005**, *43*, 1303.
- [73] S. Shiraishi, *Key Eng. Mater.* **2012**, *497*, 80.
- [74] P. González-García, *Renewable Sustainable Energy Rev.* **2018**, *82*, 1393.
- [75] M. A. Yahya, Z. Al-Qodah, C. W. Z. Ngah, *Renewable Sustainable Energy Rev.* **2015**, *46*, 218.
- [76] A. M. Abioye, F. N. Ani, *Renewable Sustainable Energy Rev.* **2015**, *52*, 1282.
- [77] H. Zabed, J. N. Sahu, A. N. Boyce, G. Faruq, *Renewable Sustainable Energy Rev.* **2016**, *66*, 751.
- [78] X. Dou, I. Hasa, D. Saurel, C. Vaalma, L. Wu, D. Buchholz, D. Bresser, S. Komaba, S. Passerini, *Mater. Today* **2019**, *23*, 87.
- [79] R. E. Franklin, *Proc. R. Soc. Lond. A* **1951**, *209*, 196.

- [80] R. E. Franklin, *Acta Crystallographica* **1951**, *4*, 253.
- [81] A. Pendashteh, B. Orayech, H. Suhard, M. Jauregui, J. Ajuria, B. Silván, S. Clarke, F. Bonilla, D. Saurel, *Energy Storage Mater.* **2022**, *46*, 417.
- [82] H. Yamamoto, S. Muratsubaki, K. Kubota, M. Fukunishi, H. Watanabe, J. Kim, S. Komaba, *J. Mater. Chem. A* **2018**, *6*, 16844.
- [83] B. Xiao, T. Rojo, X. Li, *ChemSusChem* **2019**, *12*, 133.
- [84] C. Zhao, Q. Wang, Y. Lu, B. Li, L. Chen, Y.-S. Hu, *Science Bulletin* **2018**, *63*, 1125.
- [85] A. Kamiyama, K. Kubota, D. Igarashi, Y. Youn, Y. Tateyama, H. Ando, K. Gotoh, S. Komaba, *Angew. Chem. Int. Ed.* **2021**, *60*, 5114.
- [86] W. Luo, Z. Jian, Z. Xing, W. Wang, C. Bommier, M. M. Lerner, X. Ji, *ACS Cent. Sci.* **2015**, *1*, 516.
- [87] A. Pendashteh, B. Orayech, J. Ajuria, M. Jáuregui, D. Saurel, *Energies* **2020**, *13*, 4189.
- [88] M. Schroeder, S. Menne, J. Ségalini, D. Saurel, M. Casas-Cabanas, S. Passerini, M. Winter, A. Balducci, *J. Power Sources* **2014**, *266*, 250.
- [89] Z. Jian, C. Bommier, L. Luo, Z. Li, W. Wang, C. Wang, P. A. Greaney, X. Ji, *J. Mater. Chem.* **2017**, *29*, 2314.
- [90] H. Hou, X. Qiu, W. Wei, Y. Zhang, X. Ji, *Adv. Energy Mater.* **2017**, *7*, 1602898.
- [91] J. S. Xue, J. R. Dahn, *J. Electrochem. Soc.* **1995**, *142*, 3668.
- [92] C. Liu, F. Li, L.-P. Ma, H.-M. Cheng, *Adv. Mater.* **2010**, *22*, E28.
- [93] R. Fong, U. von Sacken, J. R. Dahn, *J. Electrochem. Soc.* **1990**, *137*, 2009.
- [94] W. Xing, J. S. Xue, J. R. Dahn, *J. Electrochem. Soc.* **1996**, *143*, 3046.
- [95] E. Buiel, J. R. Dahn, *J. Electrochem. Soc.* **1998**, *145*, 1977.
- [96] C. Bommier, W. Luo, W.-Y. Gao, A. Greaney, S. Ma, X. Ji, *Carbon* **2014**, *76*, 165.
- [97] Y.-X. Wang, S.-L. Chou, H.-K. Liu, S.-X. Dou, *Carbon* **2013**, *57*, 202.
- [98] B. Zhang, C. M. Ghimbeu, C. Laberty, C. Vix-Guterl, J.-M. Tarascon, *Adv. Energy Mater.* **2016**, *6*, 1501588.
- [99] Y. Li, S. Xu, X. Wu, J. Yu, Y. Wang, Y.-S. Hu, H. Li, L. Chen, X. Huang, *J. Mater. Chem. A* **2015**, *3*, 71.
- [100] J. J. Kipling, J. N. Sherwood, P. V. Shooter, N. R. Thompson, *Carbon* **1964**, *1*, 315.
- [101] T. Matsumoto, *1985*, *57*, 1553.
- [102] S. Ōtani, *Carbon* **1965**, *3*, 31.
- [103] J. Mittal, R. B. Mathur, O. P. Bahl, M. Inagaki, *Carbon* **1998**, *36*, 893.
- [104] A. Nagap, M. Ishikawa, J. Masuko, N. Sonobe, H. Chuman, T. Iwasaki, *MRS Online Proc. Library* **1995**, *393*, 339.
- [105] J.-P. Pirard, C. Bossuet, P. Kreit, *Method and installation for making carbon nanotubes*, **2004**.
- [106] H. Y. Teah, T. Sato, K. Namiki, M. Asaka, K. Feng, S. Noda, *ACS Sustainable Chem. Eng.* **2020**, *8*, 1730.
- [107] W. Weng, L. Tang, W. Xiao, *J. Energy Chem.* **2019**, *28*, 128.
- [108] P. Srinivasan, *Carbon Budget and Cost Analysis of C2CNT: A Carbon Dioxide to Solid Carbon Conversion Process*, **2018**.
- [109] M. Johnson, J. Ren, M. Lefler, G. Licht, J. Vicini, X. Liu, S. Licht, *Mater. Today Energy* **2017**, *5*, 230.
- [110] S. Licht, A. Douglas, J. Ren, R. Carter, M. Lefler, C. L. Pint, *ACS Cent Sci* **2016**, *2*, 162.
- [111] A. Douglas, R. Carter, M. Li, C. L. Pint, *ACS Appl. Mater. Interfaces* **2018**, *10*, 19010.
- [112] X. Liu, G. Licht, X. Wang, S. Licht, *Catalysts* **2022**, *12*, 137.
- [113] R. Yu, J. Xiang, K. Du, B. Deng, D. Chen, H. Yin, Z. Liu, D. Wang, *Nano Lett.* **2022**, *22*, 97.
- [114] K. Moyer, M. Zohair, J. Eaves-Rathert, A. Douglas, C. L. Pint, *Carbon* **2020**, *165*, 90.
- [115] Z. Yang, B. Deng, K. Du, H. Yin, D. Wang, *Green Energy Environ.* **2022**.
- [116] S. Alaei, W. Jiao, S. Ghazvini, K. Moyer-Vanderburgh, R. Bardhan, A. Douglas, C. L. Pint, *ACS Appl. Nano Mater.* **2023**, *6*, 17792.
- [117] Z.-Y. Sui, Q.-H. Meng, J.-T. Li, J.-H. Zhu, Y. Cui, B.-H. Han, *J. Mater. Chem. A* **2014**, *2*, 9891.
- [118] F. Rodríguez-Reinoso, M. Molina-Sabio, *Adv. Colloid Interface Sci.* **1998**, *76*–*77*, 271.
- [119] J. Li, J. Kossmann, K. Zeng, K. Zhang, B. Wang, C. Weinberger, M. Antonietti, M. Odziomek, N. López-Salas, *Angew. Chem.* **2023**, *135*, 202217808.
- [120] J. Li, Y. Xu, P. Li, A. Völkel, F. I. Saldaña, M. Antonietti, N. López-Salas, M. Odziomek, *Creating Porosity Without Etching Using Cesium Effect. Advanced Materials* **2024**, *23*11655.
- [121] J. Li, J. Kossmann, K. Zeng, K. Zhang, B. Wang, C. Weinberger, M. Antonietti, M. Odziomek, N. López-Salas, *Angew. Chem.* **2023**, *135*, e202217808.
- [122] J. Li, Y. Xu, P. Li, A. Völkel, F. I. Saldaña, M. Antonietti, N. López-Salas, M. Odziomek, *Adv. Mater.* **2024**, *23*11655.
- [123] J. Ajuria, E. Redondo, M. Arnaiz, R. Mysyk, T. Rojo, E. Goikolea, *J. Power Sources* **2017**, *359*, 17.
- [124] H. Liu, X. Liu, H. Wang, Y. Zheng, H. Zhang, J. Shi, W. Liu, M. Huang, J. Kan, X. Zhao, D. Li, *ACS Sustainable Chem. Eng.* **2019**.
- [125] M. D. Casal, N. Díez, S. Payá, M. Sevilla, *ACS Appl. Energy Mater.* **2023**, *6*, 8120.
- [126] P. Cai, R. Momen, M. Li, Y. Tian, L. Yang, K. Zou, X. Deng, B. Wang, H. Hou, G. Zou, X. Ji, *Chem. Eng. J.* **2021**, *420*, 129647.
- [127] N. Diez, M. Sevilla, A. B. Fuertes, *Carbon* **2023**, *201*, 1126.
- [128] T. N. Phan, M. K. Gong, R. Thangavel, Y. S. Lee, C. H. Ko, *J. Alloys Compd.* **2018**, *743*, 639.
- [129] H. Huang, D. Kundu, R. Yan, E. Tervoort, X. Chen, L. Pan, M. Oschatz, M. Antonietti, M. Niederberger, *Adv. Energy Mater.* **2018**, *8*, 1802800.
- [130] J. Li, B. Wang, T. Hu, Y. Wang, Z. Sun, C. Wang, D. Zhang, Z. Wang, F. Li, *J. Mater. Chem. A* **2021**, *9*, 3360.
- [131] R. Yan, E. Josef, H. Huang, K. Leus, M. Niederberger, J. P. Hofmann, R. Walczak, M. Antonietti, M. Oschatz, *Adv. Funct. Mater.* **2019**, *29*, 1902858.
- [132] A. Fombona-Pascual, N. Díez, A. B. Fuertes, M. Sevilla, *ChemSusChem* **2022**, *15*, e202201046.
- [133] H. Li, J. Lang, S. Lei, J. Chen, K. Wang, L. Liu, T. Zhang, W. Liu, X. Yan, *Adv. Funct. Mater.* **2018**, *28*, 1800757.
- [134] R. Yan, M. Antonietti, M. Oschatz, *Adv. Energy Mater.* **2018**, *8*, 1800026.
- [135] P. Ruschhaupt, A. Varzi, S. Passerini, *ChemSusChem* **2020**, *13*, 763.
- [136] D. Bresser, D. Buchholz, A. Moretti, A. Varzi, S. Passerini, *Energy Environ. Sci.* **2018**, *11*, 3096.
- [137] W. Dou, M. Zheng, W. Zhang, T. Liu, F. Wang, G. Wan, Y. Liu, X. Tao, *Adv. Funct. Mater.* **2023**, *33*, 2305161.
- [138] R.-R. Li, Z. Yang, X.-X. He, X.-H. Liu, H. Zhang, Y. Gao, Y. Qiao, L. Li, S.-L. Chou, *Chem. Commun.* **2021**, *57*, 12406.
- [139] A. Rensmo, E. K. Savvidou, I. T. Cousins, X. Hu, S. Schellenberger, J. P. Benskin, *Environ. Sci.: Processes Impacts* **2023**, *25*, 1015.
- [140] Y. Lu, C.-Z. Zhao, H. Yuan, J.-K. Hu, J.-Q. Huang, Q. Zhang, *Matter* **2022**, *5*, 876.
- [141] N. Hayagan, I. Gaalich, P. Loubet, L. Croguennec, C. Aymonier, G. Philippot, J. Olchowka, *Batteries Supercaps* **2024**, *7*, e202400120.
- [142] N. Yabuuchi, K. Kubota, M. Dahbi, S. Komaba, *Chem. Rev.* **2014**, *114*, 11636.
- [143] L. O. Vogt, M. El Kazzi, E. Jämstorp Berg, S. Pérez Villar, P. Novák, C. Villevieille, *Chem. Mater.* **2015**, *27*, 1210.
- [144] S. Komaba, Y. Matsuura, T. Ishikawa, N. Yabuuchi, W. Murata, S. Kuze, *Electrochem. Commun.* **2012**, *21*, 65.
- [145] J.-Y. Hwang, S.-T. Myung, Y.-K. Sun, *Chem. Soc. Rev.* **2017**, *46*, 3529.
- [146] B. Dyatkin, V. Presser, M. Heon, M. R. Lukatskaya, M. Beidagi, Y. Gogotsi, *ChemSusChem* **2013**, *6*, 2269.
- [147] H. Y. Tran, M. Wohlfahrt-Mehrens, S. Dsoke, *J. Power Sources* **2017**, *342*, 301.
- [148] M. Aslan, D. Weingarth, P. Herbeck-Engel, I. Grobelsek, V. Presser, *J. Power Sources* **2015**, *279*, 323.
- [149] A. Varzi, S. Passerini, *J. Power Sources* **2015**, *300*, 216.
- [150] P. Kulkarni, H. Jung, D. Ghosh, M. Jalalah, M. Alsaiari, F. A. Harraz, R. G. Balakrishna, *J. Energy Chem.* **2023**, *76*, 479.
- [151] C. Zhang, H. Zhao, Y. Lei, *Sodium- and potassium-ion batteries: cost-effective and sustainable successors to lithium-ion batteries in the future.*
- [152] Soda Ash Trading Economics.
- [153] LithiumTrading Economics.
- [154] S. K. Alva, Manufacturing & Regional Cost Competitiveness of Commercial Sodium Ion Cells. Degree Project In Sustainable Energy Engineering, KTH Royal Institute of Technology, Stockholm, **2023**.
- [155] P. Cai, K. Zou, X. Deng, B. Wang, M. Zheng, L. Li, H. Hou, G. Zou, X. Ji, *Adv. Energy Mater.* **2021**, *11*.
- [156] J. Ding, W. Hu, E. Paek, D. Mitlin, *Chem. Rev.* **2018**, *118*, 6457.
- [157] A. Hainthaler, A. S. Sidharthan, D. Leistenschneider, A. Balducci, *J. Power Sources Adv.* **2024**, *30*, 100158.
- [158] D. Morales, L. G. Chagas, D. Paterno, S. Greenbaum, S. Passerini, S. Suarez, *Electrochim. Acta* **2021**, *377*, 138062.
- [159] N. Phattharasupakun, J. Wuttiprom, N. Ma, N. Chanlek, M. Sawangphrak, *Electrochim. Acta* **2018**, *286*, 55.
- [160] X. Wang, S. Kajiyama, H. Inuma, E. Hosono, S. Oro, I. Moriguchi, M. Okubo, A. Yamada, *Nat Commun.* **2015**, *6*, 6544.
- [161] D. S. Lutsenko, E. V. Belova, M. V. Zakharkin, O. A. Drozhzhin, E. V. Antipov, *Chemistry* **2023**, *5*, 1588.
- [162] K. Wang, N. Wang, J. He, Z. Yang, X. Shen, C. Huang, *ACS Appl. Mater. Interfaces* **2017**, *9*, 40604.

- [163] J. Tang, X. Huang, T. Lin, T. Qiu, H. Huang, X. Zhu, Q. Gu, B. Luo, L. Wang, *Energy Storage Mater.* **2020**, *26*, 550.
- [164] P. Han, X. Han, J. Yao, L. Zhang, X. Cao, C. Huang, G. Cui, *J. Power Sources* **2015**, *297*, 457.
- [165] Y. Yuan, C. Wang, K. Lei, H. Li, F. Li, J. Chen, *ACS Cent. Sci.* **2018**, *4*, 1261.
- [166] C. Wang, F. Wang, Z. Liu, Y. Zhao, Y. Liu, Q. Yue, H. Zhu, Y. Deng, Y. Wu, D. Zhao, *Nano Energy* **2017**, *41*, 674.
- [167] K. Wasiński, P. Półrolniczak, M. Walkowiak, *Electrochim. Acta* **2018**, *259*, 850.
- [168] A. Ponrouch, E. Marchante, M. Courty, J.-M. Tarascon, M. R. Palacín, *Energy Environ. Sci.* **2012**, *5*, 8572.
- [169] Y.-E. Zhu, L. Yang, J. Sheng, Y. Chen, H. Gu, J. Wei, Z. Zhou, *Adv. Energy Mater.* **2017**, *7*, 1701222.
- [170] M. Liu, J. Niu, Z. Zhang, M. Dou, Z. Li, F. Wang, *J. Power Sources* **2019**, *414*, 68.
- [171] Z. Le, F. Liu, P. Nie, X. Li, X. Liu, Z. Bian, G. Chen, H. B. Wu, Y. Lu, *ACS Nano* **2017**, *11*, 2952.
- [172] S. Li, J. Chen, J. Xiong, X. Gong, J. Ciou, P. S. Lee, *Nanomicro Lett.* **2020**, *12*, 34.
- [173] S. K. Park, S. H. Kwon, S. G. Lee, M. S. Choi, D. H. Suh, P. Nakhanivej, H. Lee, H. S. Park, *ACS Energy Lett.* **2018**, *3*, 724.
- [174] P. Wang, B. Yang, G. Zhang, L. Zhang, H. Jiao, J. Chen, X. Yan, *Chem. Eng. J.* **2018**, *353*, 453.
- [175] B. Yang, J. Chen, S. Lei, R. Guo, H. Li, S. Shi, X. Yan, *Advanced Energy Materials* **2017**, *8*.
- [176] G. Dong, H. Wang, W. Liu, J. Shi, S. Sun, D. Li, H. Zhang, Y. Yang, Y. Cui, *ACS Appl. Energy Mater.* **2018**.
- [177] J. Ding, H. Wang, Z. Li, K. Cui, D. Karpuzov, X. Tan, A. Kohandehghan, D. Mitlin, *Energy Environ. Sci.* **2015**, *8*, 941.
- [178] H. Wang, D. Mitlin, J. Ding, Z. Li, K. Cui, *J. Mater. Chem. A* **2016**, *4*, 5149.
- [179] J. Ding, Z. Li, K. Cui, S. Boyer, D. Karpuzov, D. Mitlin, *Nano Energy* **2016**, *23*, 129.
- [180] J. Ding, H. Wang, Z. Li, A. Kohandehghan, K. Cui, Z. Xu, B. Zahiri, X. Tan, E. M. Lotfabad, B. C. Olsen, D. Mitlin, *ACS Nano* **2013**, *7*, 11004.
- [181] S. Wang, R. Wang, Y. Zhang, D. Jin, L. Zhang, *J. Power Sources* **2018**, *379*, 33.
- [182] J. Yin, L. Qi, H. Wang, *ACS Appl. Mater. Interfaces* **2012**, *4*, 2762.
- [183] K. Zou, P. Cai, C. Liu, J. Li, X. Gao, L. Xu, G. Zou, H. Hou, Z. Liu, X. Ji, *J. Mater. Chem. A* **2019**, *7*, 13540.
- [184] F. Wang, X. Wang, Z. Chang, X. Wu, X. Liu, L. Fu, Y. Zhu, Y. Wu, W. Huang, *Adv. Mater.* **2015**, *27*, 6962.
- [185] C. Leibing, D. Leistenschneider, C. Neumann, M. Oschatz, A. Turchanin, A. Balducci, *ChemSusChem* **2023**, *16*.
- [186] T. C. Mendes, F. Zhou, A. J. Barlow, M. Forsyth, P. C. Howlett, D. R. MacFarlane, *Sustainable Energy Fuels* **2018**, *2*, 763.
- [187] K. Krishnamoorthy, P. Pazhamalai, S. Sahoo, J. H. Lim, K. H. Choi, S. J. Kim, *ChemElectroChem* **2017**, *4*, 3302.
- [188] I. M. Abdulagatov, A. Zeinalova, N. D. Azizov, *Fluid Phase Equilib.* **2005**, *227*, 57.
- [189] W. Wu, S. Shabtag, J. Chang, A. Rutt, J. F. Whitacre, *J. Electrochem. Soc.* **2015**, *162*, A803.
- [190] B. Babu, M. Enke, S. Prykhodskaya, A. Lex-Balducci, U. S. Schubert, A. Balducci, *ChemSusChem* **2021**, *14*, 4836.
- [191] M. Park, G. K. Veerasubramani, R. Thangavel, Y. Lee, D. Kim, *ChemElectroChem* **2018**, *6*, 653.
- [192] K. Aruchamy, S. Ramasundaram, S. Divya, M. Chandran, K. Yun, T. H. Oh, *Gels* **2023**, *9*, 585.
- [193] A. Fukunaga, T. Nohira, R. Hagiwara, K. Numata, E. Itani, S. Sakai, K. Nitta, S. Inazawa, *J. Power Sources* **2014**, *246*, 387.
- [194] Y. Sun, P. Shi, H. Xiang, X. Liang, Y. Yu, *Small* **2019**, *15*.
- [195] G. G. Eshetu, S. Grignon, H. Kim, S. Jeong, L. Wu, G. Gachot, S. Laruelle, M. Armand, S. Passerini, *ChemSusChem* **2016**, *9*, 462.
- [196] C. Gong, S. D. Pu, X. Gao, S. Yang, J. Liu, Z. Ning, G. J. Rees, I. Capone, L. Pi, B. Liu, G. O. Hartley, J. Fawdon, J. Luo, M. Pasta, C. R. M. Grovenor, P. G. Bruce, A. W. Robertson, *Adv. Energy Mater.* **2021**, *11*.
- [197] C. Wang, Y. S. Meng, K. Xu, *J. Electrochem. Soc.* **2018**, *166*, A5184.
- [198] M. Dahbi, N. Yabuuchi, K. Kubota, K. Tokiwa, S. Komaba, *Phys. Chem. Chem. Phys.* **2014**, *16*, 15007.
- [199] S. Komaba, T. Ishikawa, N. Yabuuchi, W. Murata, A. Ito, Y. Ohsawa, *ACS Appl. Mater. Interfaces* **2011**, *3*, 4165.
- [200] Z. Shadike, E. Zhao, Y. Zhou, X. Yu, Y. Yang, E. Hu, S. Bak, L. Gu, X. Yang, *Advanced Energy Materials* **2018**, *8*.
- [201] A. Ponrouch, R. Dedryvère, D. Monti, A. E. Demet, J. M. Ateba Mba, L. Croguennec, C. Masquelier, P. Johansson, M. R. Palacín, *Energy Environ. Sci.* **2013**, *6*, 2361.
- [202] L. Köps, F. A. Kreth, A. Bothe, A. Balducci, *Energy Storage Mater.* **2022**, *44*, 66.
- [203] E. Paméte, L. Köps, F. A. Kreth, S. Pohlmann, A. Varzi, T. Brousse, A. Balducci, V. Presser, *Adv. Energy Mater.* **2023**, *13*.
- [204] J. Krummacher, L. Heß, A. Balducci, *ChemSusChem* **2017**, *10*, 4178.
- [205] K. Li, J. Zhang, D. Lin, D.-W. Wang, B. Li, W. Lv, S. Sun, Y.-B. He, F. Kang, Q.-H. Yang, L. Zhou, T.-Y. Zhang, *Nat. Commun.* **2019**, *10*, 725.
- [206] K. N. Wood, G. Teeter, *ACS Appl. Energy Mater.* **2018**, *1*, 4493.
- [207] Y. Pan, Y. Zhang, B. S. Parimalam, C. C. Nguyen, G. Wang, B. L. Lucht, *J. Electroanal. Chem.* **2017**, *799*, 181.
- [208] M. Carboni, J. Manzi, A. R. Armstrong, J. Billaud, S. Brutt, R. Younesi, *ChemElectroChem* **2019**, *6*, 1745.
- [209] J. E. N. Swallow, M. W. Fraser, N.-J. H. Kneusels, J. F. Charlton, C. G. Sole, C. M. E. Phelan, E. Björklund, P. Bencok, C. Escudero, V. Pérez-Dieste, C. P. Grey, R. J. Nicholls, R. S. Weatherup, *Nat. Commun.* **2022**, *13*, 6070.
- [210] L. H. Hess, L. Wittscher, A. Balducci, *Phys. Chem. Chem. Phys.* **2019**, *21*, 9089.
- [211] F. A. Kreth, L. H. Hess, A. Balducci, *Energy Storage Mater.* **2023**, *56*, 192.
- [212] L. Zhang, C. Tsolakidou, S. Mariyappan, J.-M. Tarascon, S. Trabesinger, *Energy Storage Mater.* **2021**, *42*, 12.
- [213] M. He, K. Fic, E. Fraćkowiak, P. Novák, E. J. Berg, *Energy Environ. Sci.* **2016**, *9*, 623.
- [214] J. Tan, J. Liu, *Energy Environ. Mater.* **2020**, *4*, 302.
- [215] D. Schäfer, K. Hankins, M. Allion, U. Krewer, F. Karcher, L. Derr, R. Schuster, J. Maibach, S. Mück, D. Kramer, R. Mönig, F. Jeschull, S. Daboss, T. Philipp, G. Neusser, J. Romer, K. Palanisamy, C. Kranz, F. Buchner, R. J. Behm, A. Ahmadian, C. Kübel, I. Mohammad, A. Samoson, R. Witter, B. Smarsly, M. Rohnke, *Advanced Energy Materials* **2024**, *14*.
- [216] M. Arnaiz, J. Ajuria, *Batteries Supercaps* **2021**, *4*, 733.
- [217] S. Zhang, R. Cao, X. Pu, A. Zhao, W. Chen, C. Song, Y. Fang, Y. Cao, *J. Energy Chem.* **2024**, *92*, 162.
- [218] W. Wang, Y. Gang, Z. Hu, Z. Yan, W. Li, Y. Li, Q.-F. Gu, Z. Wang, S.-L. Chou, H.-K. Liu, S.-X. Dou, *Nat. Commun.* **2020**, *11*, 980.
- [219] F. Ding, Q. Meng, P. Yu, H. Wang, Y. Niu, Y. Li, Y. Yang, X. Rong, X. Liu, Y. Lu, L. Chen, Y.-S. Hu, *Adv. Funct. Mater.* **2021**, *31*, 2101475.
- [220] Y. Liu, X. Wu, A. Moezz, Z. Peng, Y. Xia, D. Zhao, J. Liu, W. Li, *Adv. Energy Mater.* **2023**, *13*, 2203283.
- [221] J. Martínez De Ilarduya, L. Otaegui, J. M. López del Amo, M. Armand, G. Singh, *J. Power Sources* **2017**, *337*, 197.
- [222] B. Shen, R. Zhan, C. Dai, Y. Li, L. Hu, Y. Niu, J. Jiang, Q. Wang, M. Xu, *J. Colloid Interface Sci.* **2019**, *553*, 524.
- [223] J. Martínez De Ilarduya, L. Otaegui, M. Galcerán, L. Acebo, D. Shanmukaraj, T. Rojo, M. Armand, *Electrochim. Acta* **2019**, *321*, 134693.
- [224] X. Liu, Y. Tan, W. Wang, P. Wei, Z. W. Seh, Y. Sun, *ACS Appl. Mater. Interfaces* **2021**, *13*, 27057.
- [225] Q. Zhang, X.-W. Gao, Y. Shi, W.-B. Luo, Y. Li, Q.-F. Gu, H.-N. Fan, F. Li, H.-K. Liu, *Energy Storage Mater.* **2021**, *39*, 54.
- [226] J. Tang, D. K. Kye, V. G. Pol, *J. Power Sources* **2018**, *396*, 476.
- [227] Y. Cao, T. Zhang, X. Zhong, T. Zhai, H. Li, *Chem. Commun.* **2019**, *55*, 14761.
- [228] M. Liu, J. Zhang, S. Guo, B. Wang, Y. Shen, X. Ai, H. Yang, J. Qian, *ACS Appl. Mater. Interfaces* **2020**, *12*, 17620.
- [229] X. Liu, Y. Tan, T. Liu, W. Wang, C. Li, J. Lu, Y. Sun, *Adv. Funct. Mater.* **2019**, *29*, 1930795.
- [230] M. Arnaiz, J. L. Gómez-Cámera, J. Ajuria, F. Bonilla, B. Acebedo, M. Jáuregui, E. Goikolea, M. Galceran, T. Rojo, *Chem. Mater.* **2018**, *30*, 8155.
- [231] X. Pan, A. Chojnacka, P. Jeżowski, F. Béguin, *Electrochim. Acta* **2019**, *318*, 471.
- [232] M. Arnaiz, D. Shanmukaraj, D. Carriazo, D. Bhattacharjya, A. Villaverde, M. Armand, J. Ajuria, *Energy Environ. Sci.* **2020**.
- [233] X. Pan, A. Chojnacka, F. Béguin, *Energy Storage Mater.* **2021**, *40*, 22.
- [234] P. Jeżowski, A. Chojnacka, X. Pan, F. Béguin, *Electrochimica Acta* **2021**, *137980*.
- [235] P. Jeżowski, O. Crosnier, T. Brousse, *Open Chem.* **2021**, *19*, 432.
- [236] C. Sun, X. Zhang, C. Li, K. Wang, X. Sun, Y. Ma, *J. Power Sources* **2021**, *515*, 230628.
- [237] C. Sun, X. Zhang, C. Li, K. Wang, X. Sun, F. Liu, Z.-S. Wu, Y. Ma, *J. Energy Chem.* **2022**, *64*, 442.
- [238] X. Pan, A. Chojnacka, F. Béguin, *J. Energy Chem.* **2022**, *72*, 33.
- [239] A. Maćkowiak, P. Jeżowski, Y. Matsui, M. Ishikawa, K. Fic, *Energy Storage Mater.* **2024**, *65*, 103163.

- [240] B. Gorska, P. Bujewska, K. Fic, *Phys. Chem. Chem. Phys.* **2017**, *19*, 7923.
- [241] B. Vertruyen, N. Eshraghi, C. Piffet, J. Bodart, A. Mahmoud, F. Boschini, *Materials* **2018**, *11*.
- [242] V. Wenzel, H. Nirschl, D. Nötzel, *Energy Technol.* **2015**, *3*, 692.
- [243] W. B. Hawley, J. Li, *J. Storage Mater.* **2019**, *25*, 100862.
- [244] S. N. Bryntesen, A. H. Størmann, I. Tolstorebrov, P. R. Shearing, J. J. Lamb, O. Stokke Burheim, *Energies* **2021**, *14*.
- [245] M. Arnaiz, M. Canal-Rodríguez, S. Martin-Fuentes, D. Carriazo, A. Villaverde, J. Ajuria, *J. Phys.: Energy* **2023**, *6*, 015001.
- [246] P. Luis, S. Martin, M. Arnaiz, J. Ajuria, *Batteries Supercaps* **2024**, *n/a*, e202400405.
- [247] R. Mooy, M. Aydemir, G. Seliger, *Procedia Manuf.* **2017**, *8*, 104.
- [248] C. L. Campion, W. Li, B. L. Lucht, *J. Electrochem. Soc.* **2005**, *152*, A2327.
- [249] W. Cao, Y. Li, B. Fitch, J. Shih, T. Doung, J. Zheng, *J. Power Sources* **2014**, *268*, 841.
- [250] O. Schmidt, S. Melchior, A. Hawkes, I. Staffell, *Joule* **2019**, *3*, 81.
- [251] A. F. Burke, J. Zhao, *J. Storage Mater.* **2021**, *35*, 102310.
- [252] T. Ibrahim, T. Kerekes, D. Sera, A. Lashab, D.-I. Stroe, *Batteries* **2024**, *10*.
- [253] Voltaic Systems, *Lithium Ion Capacitor Based Solar Charger with e-peas*, **2019**.
- [254] Li-Ion Capacitor UPS Powerful and reliable solution for applications requiring short back-up times, SOCOMECH. Innovative power solutions, **2019**.
- [255] Energy storage total cost of ownership comparisons in critical power applications Total cost of ownership White paper, Eaton Electronics Division, **2022**.
- [256] Supercaps for uninterruptible power supplies. White paper No. 01–2020, RPS SpA – Riello Power Solutions.
- [257] W. Zuo, R. Li, C. Zhou, Y. Li, J. Xia, J. Liu, *Adv Sci (Weinh)* **2017**, *4*, 1600539.
- [258] V. Castiglia, P. Liverri, R. Miceli, F. Pellitteri, G. Schettino, F. Viola, In *2019 AEIT International Conference of Electrical and Electronic Technologies for Automotive (AEIT AUTOMOTIVE)*, **2019**, pp. 1–5.
- [259] K. Jayasawal, A. K. Karna, K. B. Thapa, *2021 International Conference on Sustainable Energy and Future Electric Transportation, SeFet 2021* **2021**.
- [260] G. Yasser, P. Theophile, M. Tedjani, D. Sylvain, *ICEVT 2019 – Proceeding: 6th International Conference on Electric Vehicular Technology 2019* **2019**, 156.
- [261] V. Castiglia, N. Campagna, A. O. D. Tommaso, R. Miceli, F. Pellitteri, C. Puccio, F. Viola, *2020 15th International Conference on Ecological Vehicles and Renewable Energies, EVER 2020* **2020**.
- [262] V. Castiglia, N. Campagna, A. O. Di Tommaso, R. Miceli, F. Pellitteri, C. Puccio, F. Viola, In *2020 Fifteenth International Conference on Ecological Vehicles and Renewable Energies (EVER)*, IEEE, Monte-Carlo, Monaco, **2020**, pp. 1–6.
- [263] K. Fleurbaey, J. Ronsmans, J.-M. Timmermans, N. Omar, P. Van Den Bosche, J. Van Mierlo, **2015**.
- [264] J. S. R. Micro, *Lithium-Ion Capacitors (LICs): "Combining Energy With Power,"* **2017**.
- [265] First One up the Drive: A New Sort of Storage Device Gives Lithium-Ion Batteries a Run for Their Money, *The Economist* **2014**.
- [266] Supercapacitor applications – E-Mobility Engineering.
- [267] J. Schiffer, O. Bohlen, R. W. D. Doncker, D. U. Sauer, K. Y. Ahn, In *2005 IEEE Vehicle Power and Propulsion Conference*, **2005**, pp. 341–348.
- [268] E. Schaltz, A. Khaligh, P. O. Rasmussen, *2008 IEEE Vehicle Power and Propulsion Conference, VPPC 2008* **2008**.
- [269] A. Castaings, H. Caron, H. Kharrat, A. Ovalle, B. Vulturescu, *2018 IEEE International Conference on Electrical Systems for Aircraft, Railway, Ship Propulsion and Road Vehicles and International Transportation Electrification Conference, ESARS-ITEC 2018* **2018**.
- [270] M. A. Sakka, J. V. Mierlo, H. Gualous, S. Soylu, *Electric Vehicles – Modelling and Simulations* **2011**.
- [271] A. Macias, N. El Ghossein, J. Trovão, A. Sari, P. Venet, L. Boulon, *Int. J. Hydrg. Energy* **2021**, *46*, 28748.
- [272] M. B. Caracciolo, M. Berrera, M. Brenna, D. Zaninelli, In *2015 AEIT International Annual Conference (AEIT)*, IEEE, Naples, Italy, **2015**, pp. 1–6.
- [273] Z. Gao, J. Fang, Y. Zhang, D. Sun, *J. Mod. Power Syst. Clean Energy* **2014**, *2*, 181.
- [274] Z. Zhang, S. Yang, R. Yang, B. Cheng, H. Sun, N. Qi, Y. Tang, P. Wang, *Proceedings – 2023 8th Asia Conference on Power and Electrical Engineering, ACPEE 2023* **2023**, 729.
- [275] M. Steiner, M. Klohr, S. Pagiela, *Energy storage system with ultraCaps on board of railway vehicles*, **2007**, p. 10.
- [276] Railway Gazette International, *Rhein-Neckar Verkehr orders more supercapacitor trams*.
- [277] X. Zhang, X. Sun, Y. An, X. Zhang, C. Li, K. Zhang, S. Song, K. Wang, Y. Ma, *J. Storage Mater.* **2022**, *48*, 104045.
- [278] S. Hussain, M. U. Ali, S. H. Nengroo, I. Khan, M. Ishfaq, H.-J. Kim, *Electronics* **2019**, 8.
- [279] F. Naseri, S. Karimi, E. Farjah, E. Schaltz, *Renewable Sustainable Energy Rev.* **2022**, *155*, 111913.
- [280] L. Oca, N. Guillet, R. Tessard, U. Iraola, *J. Storage Mater.* **2019**, *23*, 29.
- [281] M. Soltani, G. Berckmans, J. Jaguemont, J. Ronsmans, S. Kakihara, O. Hegazy, J. Van Mierlo, N. Omar, *Appl. Therm. Eng.* **2019**, *153*, 264.
- [282] S. Barcellona, F. Ciccarelli, D. Iannuzzi, L. Piegarì, *Sustainable Energy, IEEE Transactions on* **2014**, *5*, 785.
- [283] L. Zhang, X. Hu, Z. Wang, F. Sun, D. G. Dorrell, *Renewable Sustainable Energy Rev.* **2018**, *81*, 1868.
- [284] Q. Meng, B. Chen, W. Jian, X. Zhang, S. Sun, T. Wang, W. Zhang, *J. Power Sources* **2023**, *581*, 233475.
- [285] E. Glogic, A. K. Kamali, N. M. Keppetipola, B. Alonge, G. R. A. Kumara, G. Sonnemann, T. Toupance, L. Cojocaru, *ACS Sustainable Chem. Eng.* **2022**, *10*, 15025.
- [286] Y. Wang, J. Wang, X. Zhang, D. Bhattacharyya, E. M. Sabolsky, *Energies* **2022**, *15*.
- [287] H. Liu, Z. Xu, Z. Guo, J. Feng, H. Li, T. Qiu, M. Titirici, *Philosophical Transactions of the Royal Society A: Mathematical, Physical and Engineering Sciences* **2021**, *379*, 20200340.
- [288] S. K. Saju, S. Chattopadhyay, J. Xu, S. Alhashim, A. Pramanik, P. M. Ajayan, *Cell Rep. Phys. Sci.* **2024**, 5.
- [289] J. Peters, D. Buchholz, S. Passerini, M. Weil, *Energy Environ. Sci.* **2016**, *9*, 1744.
- [290] J. F. Peters, M. Abdelbaky, M. Baumann, M. Weil, *Matériaux & Techniques* **2019**, 107.
- [291] H. Liu, C. R. Tomasini, L. Lan, J. Li, X. Zhang, N. Aßen, M. Weil, In *Waste-to-Resources 2021: 9th International Symposium Circular Economy, MBT, MRF and Recycling*. Ed.: M. Kühle-Weidemeier, Cuvillier Verlag, Online, **2021**, pp. 319–332.
- [292] F. N. Shafiee, S. A. Mohd Noor, M. A. A. Mohd Abdah, S. H. Jamal, A. Samsuri, *Helyon* **2024**, 10.
- [293] M. Cossutta, V. Vretenar, T. A. Centeno, P. Kotrusz, J. McKechnie, S. J. Pickering, *J. Cleaner Prod.* **2020**, *242*, 118468.
- [294] E. Glogic, A. Adán-Más, G. Sonnemann, M. de F. Montemor, L. Guerlou-Demouragues, S. B. Young, *RSC Adv.* **2019**, *9*, 18853.
- [295] A. K. Kamali, E. Glogic, N. M. Keppetipola, G. Sonnemann, T. Toupance, L. Cojocaru, *ACS Sustainable Chem. Eng.* **2023**, *11*, 15898.
- [296] P. De, D. Mandal, S. Biswas, A. Kumar, S. Priya, B. K. Dubey, A. K. Srivastava, A. Chandra, *Energy Fuels* **2023**, *37*, 5595.
- [297] S. Wickerts, R. Arvidsson, A. Nordelöf, M. Svanström, P. Johansson, *J. Ind. Ecol.* **2024**, *28*, 116.
- [298] W. Guo, T. Feng, W. Li, L. Hua, Z. Meng, K. Li, *J. Storage Mater.* **2023**, *72*, 108589.
- [299] E. Batuecas, C. S. Martínez-Cisneros, D. Serrano, A. Várez, *J. Storage Mater.* **2024**, *80*, 110355.
- [300] L. Weinstein, R. Dash, *Mater. Today* **2013**, *16*, 356.
- [301] J. F. Peters, A. Peña Cruz, M. Weil, *Batteries* **2019**, 5.
- [302] A. Khaligh, Z. Li, *Vehicular Technology, IEEE Transactions on* **2010**, *59*, 2806.
- [303] M. Wieczorek, M. Lewandowski, W. Jefimowski, *Bulletin of the Polish Academy of Sciences Technical Sciences* **2023**.
- [304] P. K. Roy, H. Karayaka, J. He, Y.-H. Yu, *Economic Comparison between Battery and Supercapacitor for Hourly Dispatching Wave Energy Converter Power*, **2021**.
- [305] T. R. Ayodele, A. S. O. Ogunjuyigbe, B. E. Olateju, *J. Renewable Sustainable Energy* **2018**, *10*, 013503.
- [306] Z. Song, J. Li, J. Hou, H. Hofmann, M. Ouyang, J. Du, *Energy* **2018**, *154*, 433.
- [307] A. O. Gbadegesin, Y. Sun, N. I. Nwulu, *Sustainable Energy Technol. Assess.* **2019**, *36*, 100536.

Manuscript received: December 20, 2024
 Revised manuscript received: January 28, 2025
 Accepted manuscript online: January 30, 2025
 Version of record online: February 26, 2025